In Situ Product Recovery of Antibodies with a Reverse-flow Diafiltration Membrane Bioreactor

Von der Fakultät für Maschinenwesen der Rheinisch-Westfälischen Technischen Hochschule Aachen zur Erlangung des akademischen Grades einer Doktorin der Ingenieurwissenschaften genehmigte Dissertation

vorgelegt von

Kristina Meier

Berichter: Universitätsprofessor Dr.-Ing. Jochen Büchs
Universitätsprofessor em. Dr.-Ing. Thomas Melin

Tag der mündlichen Prüfung: 04. Februar 2015

Vorwort

Die vorliegende Dissertation entstand während meiner Tätigkeit als wissenschaftliche Mitarbeiterin am Lehrstuhl für Bioverfahrenstechnik innerhalb der Aachener Verfahrenstechnik an der RWTH Aachen. Die Arbeit wurde ihm Rahmen des Projekts „Modulare Bioproduktion – Disposable und Kontinuierlich (MoBiDiK)“ angefertigt, welches von der Europäischen Union (Europäsicher Fond für die regionale Entwicklung – Investition in Ihre Zukunft) und dem Land Nordrhein-Westfalen gefördert worden ist. Die Projektleitung erfolgte durch Bayer Technology Services.

Mein besonderer Dank gilt Professor Jochen Büchs für die Betreuung der vorliegenden Arbeit sowie für die Möglichkeit, am Lehrstuhl für Bioverfahrenstechnik zu promovieren. Seine Unterstützung und Anregungen sowie seine Offenheit und Neugier gegenüber neuen Ideen waren stets wertvoll und haben diese Arbeit erst ermöglicht. Ganz herzlich bedanke ich mich bei Professor Thomas Melin, der sowohl den Grundstein dieses Forschungsprojekts gelegt hat als auch die Grundlagen meiner verfahrenstechnischen Laufbahn entscheidend begleitet hat. Bei Professor Andreas Schuppert und Professor Klaus Radermacher möchte ich mich für die Übernahme des Prüfungsvorsitzes bzw. Prüfungsbeisitzes recht herzlich bedanken.

Weiterhin möchte ich mich für die gute Zusammenarbeit innerhalb des Projekts MoBiDiK bedanken. Für die konstruktiven und offenen Diskussionen danke ich vor allem Frederike Carstensen (Aachener Verfahrenstechnik - Chemische Verfahrenstechnik) und Tobias Klement (Aachener Verfahrenstechnik – Bioverfahrenstechnik). Mein weiter Dank gilt Burkhard Schmidt (Institut für Umweltforschung), Tanja Holland und Nicole Raven (Fraunhofer IME) für ihre experimentelle Unterstützung sowie Andrea Vester und Kai Temming (Bayer Technology Services) für die Leitung und Organisation des Projekts MoBiDiK.

Bei den Kollegen der BioVT möchte ich für die Zeit am Lehrstuhl bedanken, für viele anregende fachliche und private Diskussionen. Besonders zu nennen sind hier meine Bürokollegen Simon Roth und Jens Begemann sowie Elena Herweg. Lars Regestein gilt mein Dank für die Betreuung und Unterstützung im Rahmen der Fermentergruppe.

Meine ehemaligen Studenten haben einen wichtigen inhaltlichen Beitrag zu meiner Dissertation und einen ebenso großen Beitrag zu meiner persönlichen Entwicklung geleistet. Dafür danke ich Suzana, Anne, Christoph, Sarah, Elena, Jonas, Effi, Tamara, Michael, Kai, Andrei, Andreas sowie Niklas und Friderike.

Meiner Familie möchte ich dafür danken, dass sie mich immer unterstützt und mich nie zu etwas gedrängt haben. Sie haben mir vieles mit auf den Weg gegeben, von dem ich heute profitieren kann. Zuletzt möchte ich Clemens für sein Vertrauen, seine Ermutigungen und seine bedingungslose Begleitung in den letzten Jahren danken.

Publications

This work was performed as part of the project “MoBiDiK”, which is co-funded by the European Union (European Regional Development Fund - Investing in your future) and the German federal state North Rhine-Westphalia (NRW).

Aspects of this thesis have been published previously or are submitted for publication:

- Meier K, Herweg E, Schmidt B, Klement T, Regestein L, Büchs J. 2013. Quantifying the release of polymer additives from single-use materials by respiration activity monitoring. Polymer Testing 32:1064-1071.

- Meier K°, Carstensen F°, Scheeren C, Regestein L, Wessling M, Büchs J. 2014a. *In situ* product recovery of single-chain antibodies in a membrane bioreactor. Biotechnology and Bioengineering: DOI: 10.1002/bit.25220.

- Meier K, Carstensen F, Wessling M, Regestein L, Büchs J. 2014b. Quasi-continuous reverse-flow diafiltration. Journal of Biochemical Engineering, submitted in May 2014.

- Meier K, Carstensen F, Djeljadini S, Wessling M, Regestein L, Büchs J. 2014c. *In situ* product recovery of antibodies in a membrane bioreactor. Biotechnology Progress, submitted in June 2014.

° Both authors contributed equally to the publication.

Kurzfassung

Die industrielle Herstellung von Massenprodukten erfolgt in vielen Branchen, wie beispielweise der Stahl-, Lebensmittel- oder petrochemischen Industrie, durch kontinuierliche Produktionsprozesse. Obwohl sie durch hohe Raum-Zeit-Ausbeuten, konstante Produktqualitäten sowie geringere Rüstzeiten überzeugen, konnten sich kontinuierliche Prozesse für die biotechnologische Produktion von Pharmazeutika bislang nur sehr vereinzelt durchsetzen. Dies ist vor allem in einer erhöhten Komplexität der Verfahrensführung, einer gesteigerten Kontaminationsgefahr sowie strikten Regularien begründet. Zudem wird in biotechnologischen Prozessen meistens eine zusätzliche Apparatur zum Rückhalt von Zellen benötigt, um die Produktausbeute zu steigern und somit wirtschaftlich kompetitiv zu sein. Eine Verfahrensausführung zur kontinuierlichen biotechnologischen Produktion mit integrierter Produktabtrennung ist die gepulste Diafiltration. Bei diesem membran-basierten Zellrückhaltesystem wird das Membranmodul in die Kultivierungsflüssigkeit des Bioreaktors getaucht. Folglich verbleiben die Zellen in ihrer optimalen Umgebung und sind daher nur minimalen Scherkräften und keinen zusätzlichen Limitationen ausgesetzt. Über die getauchte Membran wird abwechselnd Produktlösung gewonnen und Medium zugeführt, so dass die mögliche Bildung einer Deckschicht auf der Membran reduziert wird. Die Etablierung der gepulsten Diafiltration sowie ihre Modifikation für verschiedene Anwendungsbereiche ist Gegenstand dieser Arbeit.

Zunächst wurde das Membranmodul der gepulsten Diafiltration bezüglich seiner Biokompatibilität untersucht. Da in der Literatur keine standardisierten Verfahren zur Untersuchung der Biokompatibilität von Kunststoffen beschrieben sind, wurde im Rahmen dieser Arbeit ein solches Testverfahren entwickelt. Die Atmungsaktivität von Mikroorganismen wird bei diesem Biokompatibilitätstest in Abhängigkeit der Konzentration

der verwendeten Kunststoffteile mittels der RAMOS Technologie (Respiration Activity Monitoring System) untersucht. Es konnte festgestellt werden, dass 40 g L^{-1} Kabelbinder bzw. 4 – 10 g L^{-1} Polyamidschlauch inhibierend auf die Hefe *Hansenula polymorpha* wirken, da das toxische Monomer 1,8-Diazacyclo-tetradecane-2,7-dione bzw. der Weichmacher N-Butylbenzolsulfonamid aus den verwenden Kunststoffen auswäscht.

Nach Gewährleistung der Biokompatibilität des Membranmoduls wurde die gepulste Diafiltration mit Fokus auf eine maximale Raum-Zeit-Ausbeute des Produktes sowie Langzeitstabilität des Filtrationsprozesses ausgelegt. Der gepulsten Diafiltration liegt eine Vier-Takt-Betriebsweise zugrunde, bei der zwischen Mediumszufuhr und Gewinnung der Produktlösung jeweils ein Zwischentakt zur Entleerung der Membran eingeführt worden ist. Durch gezielte Modifikation der Zwischentakte konnte verhindert werden, dass unverbrauchtes Medium in die Produktlösung gelangt. Das Resultat ist eine Steigerung der Raum-Zeit-Ausbeute sowie die Einsparung von Medium.

Der Prozess gilt als langzeitstabil, wenn der kritische Flux, der zu einem Anstieg des Transmembrandrucks von 45 Pa min^{-1} führt, nicht überschritten wird. Mittels der Flux-Step Methode wurde der kritische Flux für die Kultivierung der Hefe *H. polymorpha* mit Syn6-Medium bzw. der tierischen Zelllinie CHO DG44 mit Power CHO 2 Medium zu 21 L m^{-2} h^{-1} bzw. 9 L m^{-2} h^{-1} bestimmt. Basierend auf diesen Daten wurde die benötige Membranfläche für eine langzeitstabile Anwendung beider Systeme abgeleitet.

Eine erfolgreiche Demonstration der gepulsten Diafiltration ist sowohl für *H. polymorpha*, welche ein Antikörperfragment sezerniert, als auch für CHO Zellen, welche einen vollständigen Antikörper produzieren, in einen großen Durchflussratenbereich erfolgt. Im Vergleich zu einem konventionellen kontinuierlichen Prozess konnte die Antikörper-produktion mittels *H. polymorpha* verdreifacht werden. In diesem Versuch hat die Antikörpertransmission über 80% betragen und die Vitalität aller Zellen ist konstant größer als 85% gewesen. Die Anwendung der gepulsten Diafiltration für CHO Zellen erzielte Antikörpertransmissionen von 40 – 60%. Dies ist ein in der Literatur üblicher Wert für membranbasierte Zellrückhaltesysteme. Über 90% der CHO Zellen waren während der gesamten Anwendung der gepulsten Diafiltration vital. In beiden Fermentationen war der

Transmembrandruck über einen Zeitraum von mehr als drei Wochen unkritisch, so dass die gepulste Diafiltration als langzeitstabiler, kontinuierlicher Prozesse betrachtet werden kann.

Die Betriebsweise der gepulsten Diafiltration verursacht zeitlich heterogene Bedingungen, da Überschuss und Limitation der C-Quelle abwechselnd vorliegen. Dieser kurzzeitige Überschuss kann insbesondere bei Mikroorganismen im höheren Durchflussratenbereich zu kurzzeitigen Sauerstofflimitationen führen. Unter diesen Bedingungen produziert *H. polymorpha* Ethanol und die Produktausbeute wird verringert. Für die in dieser Arbeit untersuchten künstlich induzierten kurzzeitigen Sauerstofflimitationen hat die Konzentration des Antikörpers um 25% abgenommen. Eine sequentielle Verwendung von drei Membranen ermöglicht eine quasi kontinuierliche Medienzufuhr, so dass konstante und nahezu homogene Kultivierungsbedingungen ohne Bildung von Ethanol bei gleichbleibender Produkt-konzentration realisiert werden konnten.

In dieser Arbeit hat sich die gepulste Diafiltration als robuster, langzeitstabiler und einfach umzusetzender Prozess zur *in situ* Produktgewinnung mit geringen Investmentkosten und minimalen Geräteaufwand erwiesen. Die Raum-Zeit-Ausbeute konnte deutlich gesteigert werden. Besonders vorteilhaft zeigte sich der Prozess bei scherempfindlichen Zellen und Organismen, welche Sauerstoff schnell verbrauchen.

Abstract

Continuous processes are established in many industrial sectors such as steel, food or petrochemistry due to their cost effectiveness. Though they are characterized by their high space-time-yields, constant product quality as well as low downtimes, only a few continuous processes were implemented in the biotechnological pharmaceutical industry. This is caused by an increased complexity, a higher contamination risk and extensive regulations. Furthermore, in continuous biochemical engineered processes an additional cell retention system is required to achieve high product yields and to be economical competitive. In this regard, one option is the reverse-flow diafiltration, a membrane-based cell retention system. The membrane module is submerged in the bioreactor broth. Thus, cells are retained in their optimal environment minimizing shear stress and avoiding limitations such as oxygen. Over the submerged membrane product withdrawal and supply of fresh medium is alternated reducing a potential fouling layer. The objective of this work is to establish the reverse-flow diafiltration and modify its settings for different applications.

At first, the membrane module was investigated regarding its biocompatibility. As there is no standardized analytical device or method to test biocompatibility, such a test method was developed within this work. The metabolic activity of various microorganisms was determined with the Respiration Activity MOnitoring Systems (RAMOS) as a function of the added amount of polymers commonly applied in biotechnology. Nylon and Polyamide 12, used in cable ties and tubing respectively, were found to delay and inhibit microbial growth. This is caused due to leaching of the plasticizer N-butylbenzenesulfonamide and the monomer 1,8-Diazacyclotetradecane-2,7-dione, respectively, from the polymers. A metabolic activity inhibition threshold concentration between 4 – 10 g L^{-1} Polyamide 12 tubing and approximately 40 g L^{-1} Nylon was determined for the cultivation of the yeast *Hansenula polymorpha*, respectively.

After the membrane module was proven to be biocompatible, a configuration of reverse-flow diafiltration was conducted with focus on maximization of space-time-yield and long-term filtration stability. Maximization resulted in an improved 4-step mode of operation. Between each alternation of product solution withdrawal and supply of fresh medium one intermediate step empties the membrane. The two intermediate steps were adjusted and, thus, mixing of permeate and fresh medium could be prevented. Hence, fresh medium was saved while simultaneously dilution of the product solution was avoided.

Long-term stability is achieved if the critical flux is not exceeded which is reached at a critical transmembrane pressure increase of 45 Pa min^{-1}. Optimal flux ranges for this process could be identified by a systematic flux step method: The critical flux for the yeast *Hansenula polymorpha* cultured in minimal Syn6 medium and the mammalian cell line CHO DG44 cultured in Power CHO 2 medium is 21 L m^{-2} h^{-1} and 9 L m^{-2} h^{-1}, respectively. The required membrane area for long-term stable processes is determined based on this data.

Reverse-flow diafiltration was successfully applied over a broad range of dilution rates for both, the yeast *H. polymorpha* secreting a single-chain antibody and the mammalian cell line CHO DG44 secreting a full length antibody. The space-time-yield for *H. polymorpha* could be tripled in comparison to conventional continuous processes. Antibody transmission was above 80% and viability was constantly above 85% for this experiment. Application of reverse-flow diafiltration for CHO cells yields an antibody transmission between 40 and 60%, which is a typical value for membrane-based cell retention systems in literature. Viability was constantly above 90%. The transmembrane pressure was below the critical value for the culture time of over three weeks in both experiments indicating long-term stability. Thus, reverse-flow diafiltration proved to be an *in situ* cell retention device appropriate for cultivation of yeast and CHO cells.

Conventional reverse-flow diafiltration pulses medium resulting in temporal heterogeneities. In microbial cultures especially the C-source alternates between depletion and excess, which leads to oscillations of the DOT signal. This effect is enforced at increased dilution rates. Artificially induced short-term oxygen limitations for *H. polymorpha* result in the formation of ethanol and a reduced product concentration of 25%. To overcome this cyclic problem, sequential operation of three membranes is introduced. Thus, quasi-continuous feeding is

achieved reducing the oscillation of the DOT signal providing a nearly homogenous culture over time.

In this thesis, reverse-flow diafiltration proved to be a fail-safe, long-term stable, easy applicable *in situ* product recovery process with low investment costs and minimal equipment requirements. Space-time-yields could be enhanced remarkably. RFD proved to be especially suitable for shear sensitive cells or organism prone to oxygen limitation.

Contents

Nomenclature

Abbreviations

1,8-DACTD-2,7-D	1,8-Diazacyclotetradecane-2,7-dione
2,6-DTBP	2,6-Di-tert-butylphenol
ATF	Alternating tangential flow system
BCA	Bicinchoninic acid
BSA	Bovine serum albumin
C	Constant
CHO	Chinese hamster ovary
CFU	Colony forming units
CSPR	Cell specific perfusion rate
CTR	Carbon transfer rate [mmol L^{-1} h^{-1}]
DCW	Dry cell weight [g L^{-1}]
DHPS	Dihydropteroate Synthetase
DOT	Dissolved oxygen tension [%]
DTT	Dithiothreitol

EDTA	Ethylenediaminetetraacetic acid
F	Free
Fab	Fragment antigen binding
Fc	Fragment crystallizable
FPLC	Fast protein liquid chromatography
GC-MS	Gas chromatography-mass spectrometry
GMP	Good manufacturing practice
H	Heavy
H	Sample Harvest
HC	Heavy chain
HPLC	High performance liquid chromatography
IgG	Immunoglobulin of type G
L	Light
LC	Light chain
M	Marker
MES	2-(N-morpholino)ethanesulfonic acid
MF	Microfiltration
MoBiDiK	Modulare Bioproduktion – Disposable und Kontinuierlich

MOPS	3-(N-morpholino)propanesulfonic acid
NBBS	N-Butylbenzenesulfonamide
Nylon	Polyamide 6.6
OTR	Oxygen transfer rate [mmol L^{-1} h^{-1}]
OD_{600}	Optical density measured at 600 nm
PA	Polyamide 12
PBS	Phosphate buffered saline
PBST	Phosphate buffered saline tween 20
PEEK	Polyether ether ketone
PES	Polyethersulfone
PI	Propidiumiodid
PP	Polyproplyene
PUR	Polyurethane
R	Sample Reactor
RAMOS	Respiration Activity Monitoring System
RFD	Reverse-flow Diafiltration
RQ	Respiration quotient [-]
SDS	Sodium dodecyl sulfate polyacrylamide

Teflon	Polytetrafluoroethylene
TMP	Transmembrane pressure
UV	Ultraviolet
V	Variable
YPG	Yeast extract peptone dextrose

Roman Symbols

a	Acceleration rate [h^{-2}]
a_E	Emptying constant [-]
a_F	Flushing constant [-]
A_M	Outer membrane area [m²]
A_Q	Area of cross section [m²]
BP_A	Byproduct ammonium [g L^{-1}]
BP_L	Byproduct lactate [g L^{-1}]
$c_{Ab,P}$	Antibody concentration in the permeate stream [g L^{-1}]
$c_{Ab,NF}$	Antibody concentration in the non-filtered product stream [g L^{-1}]
c_{cells}	Concentration of cells [cells mL^{-1}]

c_S	Concentration of dye solution [g L^{-1}]
$c_{S,f}$	Equilibrium dye concentration [g L^{-1}]
$c_{S,i}$	Initial dye concentration [g L^{-1}]
c_Ψ	Concentration of Ψ [g L^{-1}]
D	Dilution rate [h^{-1} or d^{-1} for microbial or cell culture, respectively]
d_{Glut}	Degradation rate of glutamine [h^{-1}]
d_i	Inner diameter polymer tubing or membrane [mm]
D_{max}	Wash out point [h^{-1} or d^{-1} for microbial or cell culture, respectively]
D_0	Initial dilution rate for acceleration-stat mode [h^{-1}]
d_o	Outer diameter polymer tubing or membrane [mm]
$F_{F,E}$	Flux / specific feed flow rate at emptying step [L m^{-2} h^{-1}]
$F_{F,F}$	Flux / specific feed flow rate at flushing step [L m^{-2} h^{-1}]
$F_{F,Feed}$	Flux / specific feed flow rate at feed step [L m^{-2} h^{-1}]
$F_{F,P}$	Flux / specific feed flow rate at permeate step [L m^{-2} h^{-1}]
$F_{P,E}$	Flux / specific permeate flow rate at emptying step [L m^{-2} h^{-1}]
$F_{P,F}$	Flux / specific permeate flow rate at flushing step [L m^{-2} h^{-1}]
$F_{P,Feed}$	Flux / specific permeate flow rate at feed step [L m^{-2} h^{-1}]
$F_{P,P}$	Flux / specific permeate flow rate at permeate step [L m^{-2} h^{-1}]

k	Constant for determination of viable cell density [-]
k_d	Constant for cell dying [h^{-1}]
$k_{d,A}$	Half-maximum concentration of ammonium for cell death [g L^{-1}]
$k_{d,L}$	Half-maximum concentration of lactate for cell death [g L^{-1}]
$k_{M,A}$	Half-maximum concentration (Monod) constant ammonium [g L^{-1}]
$k_{M,Gluc}$	Half-maximum concentration (Monod) constant glucose [g L^{-1}]
$k_{M,Glut}$	Half-maximum concentration (Monod) constant glutamine [g L^{-1}]
$k_{M,L}$	Half-maximum concentration (Monod) constant lactate [g L^{-1}]
L	Membrane length [m]
m_{Gluc}	Maintenance coefficient glucose [10^{-12} mg L $cells^{-1}$ h^{-1}]
m_{Glut}	Maintenance coefficient glutamine [10^{-12} mg L $cells^{-1}$ h^{-1}]
m_M	Mass of absorbing mass [g]
m_X	Mass of biomass [g]
n	Constant for determination of viable cell density [-]
n_{cells}	Number of cells [-]
n_{square}	Number of squares [-]
NF	Non-filtered ratio [-]
P	Product concentration [g L^{-1}]

P_X	Percentage of dead yeast cells [%]
p_{max}	Maximal parameter for parameter estimation [-]
p_{min}	Minimal parameter for parameter estimation [-]
r	Randomly chosen value [-]
r_A	Removal rate of ammonium [h^{-1}]
$S_{F,Gluc}$	Concentration of fed glucose [g L^{-1}]
$S_{F,Glut}$	Concentration of fed glutamine [g L^{-1}]
S_{Gluc}	Concentration of substrate glucose [g L^{-1}]
S_{Glut}	Concentration of substrate glutamine [g L^{-1}]
t	Time [h]
t_C	Cycle time [s]
t_E	Emptying step time [s]
t_F	Flushing step time [s]
t_{Feed}	Feeding step time [s]
t_P	Permeate steü time [s]
v	Feed flow velocity [m s^{-1}]
$\bar{v}$	Average feed flow velocity [m s^{-1}]
$\dot{V}$	Volume flow through the reactor [L s^{-1}]

v_{max}	Tip feed flow velocity [m s^{-1}]
V_E	Emptying volume [m^3]
V_F	Flushing volume [m^3]
$\dot{V}_F$	Feed flow into the reactor [L s^{-1}]
V_L	Filling volume reactor [m^3]
V_M	Volume of the membrane [m^3]
$\dot{V}_{NF}$	Non-filtered product stream flow out of the reactor [L s^{-1}]
V_{Lu}	Volume of the lumen [m^3]
V_P	Volume of the pores [m^3]
$\dot{V}_P$	Permeate flow out of the reactor [m^3 s^{-1}]
$V_{P,g}$	Gained permeate [L]
X	Biomass [g L^{-1} or 10^6 cells mL^{-1} for microbial or CHO cells, respectively]
$x_{cells,P}$	Number of cells in permeate [-]
$x_{cells,R}$	Number of cells in reactor [-]
$Y_{XS_{Gluc}}$	Yield coefficient biomass / glucose [10^6 cells mL^{-1} mg^{-1}]
$Y_{XS_{Glut}}$	Yield coefficient biomass / glutamine [10^6 cells mL^{-1} mg^{-1}]
$Y_{BP_LS_{Gluc}}$	Yield coefficient lactate / glucose [g g^{-1}]

$Y_{BP_A S_{Glut}}$	Yield coefficient ammonium / glutamine [g g^{-1}]
z	Control variable for membrane length [m]

Greek Symbols

α	Luedking Piret constant for growth associated production [10^{-12} L $cells^{-1}$ h^{-1}]
α_1	Constant for glutamine maintenance [10^{-12} mg L $cells^{-1}$ h^{-1}]
α_2	Constant for glutamine maintenance [g L^{-1}]
β	Luedking Piret constant for non-growth associated production [10^{-12} L $cells^{-1}$ h^{-2}]
θ	Estimated parameter [-]
$\theta_{i,exp}$	Experimental value for parameter to estimate [-]
$\theta_{i,sim}$	Simulated value for parameter to estimate [-]
μ	Growth rate [h^{-1}]
μ_d	Death rate [h^{-1}]
μ_{max}	Maximum growth rate [h^{-1}]
Σ_Ψ	Conversion of Ψ
τ	Residence time [s]

$\dot{\Psi}_{in}$	Flow of Ψ into a system
$\dot{\Psi}_{out}$	Flow of Ψ out of a system
Ψ	Extensive property

List of Figures

List of Tables

Chapter 1

Introduction

1.1 Biotechnological Production of Antibodies

The demand for biopharmaceuticals has grown significantly over the last years. With a market share of 40%, monoclonal antibodies represent the most important product class of biopharmaceuticals (Walsh, 2010). Traditionally, antibodies are expressed in mammalian cell lines due to quality characteristics such as glycosylation and folding (Jostock, 2011). Especially Chinese hamster ovary cells (CHO cells) are often the production system of choice as they can be grown in suspensions suitable for high density cultures (Wurm, 2004). Genetic engineering tools for CHO cells are established and the risk of human virus transition is low (Cacciatore et al., 2010). However, cultivation of mammalian cells is time-consuming and accident-sensitive (Melmer et al., 2011). Furthermore, the medium is highly complex, expensive and often based on serum which is prone to contamination (Brunner et al., 2010).

In the past years microbial expression systems for antibody production were investigated as they can grow faster, are more cost-efficient and can yield higher product concentrations (Zha et al., 2011). Recently, Ihssen et al. (2010) demonstrated an *Escherichia coli* (*E.coli*) strain expressing a suitable glycoprotein for vaccination. However, correct folding and glycosylation of antibodies produced in prokaryotes such as *E. coli* require a high degree of optimization if it is possible at all (Jostock, 2011). Eukaryotes such as yeast combine advantages of microbial and mammalian cells. They are capable of expressing correct folded proteins, are fast growing and robust. Furthermore, genetic engineering of yeasts is

established and proteins can be secreted into the medium, which simplifies purification (Melmer et al., 2011). Li et al. (2006) engineered a *Pichia pastoris* strain expressing a functional full length antibody. Though, these examples of functional expression of antibodies exist, glycosylation is limited in eukaryotes in comparison to mammalian cells (Ghaderi et al., 2012).

As discussed in this chapter, each organism has its advantages and drawbacks. Thus, depending on the application, the different organisms have to be traded against each other. A suitable cultivation system is capable of applying both. Hence, the cultivation system established in this work, a membrane bioreactor, should be adapted and put to test for both organisms, microbial and mammalian cells.

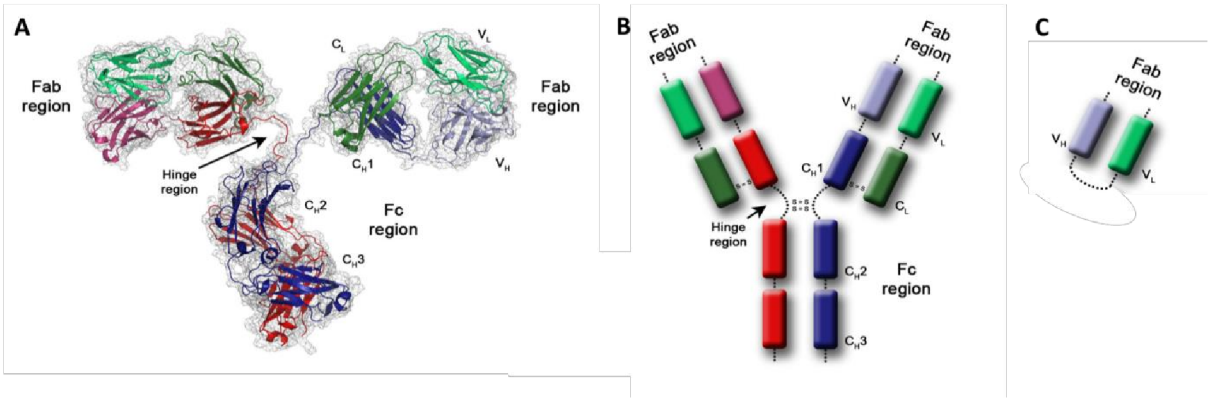

Figure 1-1: (Single-chain) antibodies. A) Ribbon model of a full length antibody, B) Schematic drawing of a full length antibody C) Schematic drawing of a single-chain antibody. Fab: Fragment antigen binding Fc: Fragment crystallizable, C: Constant, V: Variable, L: Light, H: Heavy. Picture modified from Badrilla Ltd. (2014)

1.2 Continuous and Perfusion Processes

Industrial production of antibodies is mostly performed in batch or fed-batch mode. These established processes are particularly known for their reliable performance. However, continuous processes provide several advantages such as constant product quality, smaller equipment size, higher space-time-yields, lower downtime and faster adaption of cells to changing environments (Kuystermans and Al-Rubeai, 2011; Liang et al., 2013; Rodrigues et al., 2010; Su, 2010; Warikoo et al., 2012). In addition, integrated continuous processes applying cell retention are characterized by a higher product yield because the catalyst does have to be produced only once. Thus, continuous cell retention processes have been extensively studied in the last years (Bleckwenn et al., 2005; Carstensen et al., 2013; Clincke et al., 2013a; Clincke et al., 2013b; Johnson et al., 1996; Meier et al., 2014; Trampler et al., 1994), being economical and promising for production of monoclonal antibodies (Carstensen et al., 2012a; Castilho and Medronho, 2002; Konstantinov et al., 2006; Pollock et al., 2013; Warikoo et al., 2012). These processes were referred to as "perfusion processes" in mammalian cell technology and thus, also in this study if CHO cells are applied (Zeng and Sun, 2010). Apart from that, the term "continuous process applying cell retention" is used.

In general, cell retention devices can be arranged external or internal. External devices can easily be connected to all kinds of bioreactors and exchanged if necessary. However, supply of nutrients such as oxygen is difficult and, thus, most often not conducted. Furthermore, shear stress in external devices is high, especially if cells are directed through pumps. Internal devices are characterized by their gentle treatment of cells. In internal devices cells are retained in the bioreactor and thus, in their optimal environment, which is advantageous for shear sensitive cells and microbial cultures prone to oxygen limitation. Recently, Carstensen et al. (2012a) and Jain et al. (2008) discussed the drawbacks and advantages of external and internal devices intensively in review publications.

The main applied separation criteria in cell retention devices are size and density (Voisard et al., 2003). Cell retention devices based on density are for example hydrocyclones (Elsayed et al., 2006; Jockwer et al., 2001) and centrifuges (Johnson et al., 1996; Kim et al., 2007;

Takamatsu et al., 1996), both working with centrifugal forces, settlers (Choo et al., 2007; Hülscher et al., 1992; Pohlscheidt et al., 2013; Searles et al., 1994) using sedimentation properties and acoustic filters (Baptista et al., 2013; Dalm et al., 2005; Ryll et al., 2000), where an ultrasonic field enhances the sedimentation. Separation by means of size exclusion is conducted most often using filtration. State of the art implies hollow-fiber modules (Banik and Heath, 1995; Büntemeyer et al., 1987), cross-flow filtration devices (Caron et al., 1994; Delabroise et al., 1991; Kawahara et al., 1994) and rotating or spin-filters (Avgerinos et al., 1990; Deo et al., 1996). Recent studies in literature often apply the ATF module (Alternating Tangential Flow, Refine Technology, New Jersey, USA) which is commercially available in several scales (Bleckwenn et al., 2005; Clincke et al., 2013b). The ATF process is based on the so-called "starling flow". It works similarly to cross-flow operation and consists of two steps: In the first step suspension from the reactor is drawn through the inside of a hollow-fiber membrane module into a diaphragm pump (Furey, 2000). In the next step the pump pushes the suspension back into the reactor. Hereby, an overpressure in the membrane leads to inside-out filtration. Backflush (outside-in) is induced by a temporary overpressure on the shell side. However, this overpressure exists only partly along the membrane length leading to a non-uniform reduction of the fouling layer. In addition, the module is externally located. Consequently, drawbacks of externally located modules occur for this device.

Recently, reverse-flow diafiltration (RFD) was introduced as an internal or so called *in situ* membrane based product recovery and cell retention process for continuous and perfusion cultures (Carstensen et al., 2013; Carstensen et al., 2012b; Meier et al., 2014; Meier et al., May 2014). RFD alternates harvesting of product and feeding of fresh medium over the same submerged membrane enabling gentle cell retention while the formation of a fouling layer is minimized. However, alternation of harvesting and feeding results in a pulsed feeding of substrate. Therefore, concentrations of substrates fluctuate over time causing heterogeneous fermentation conditions.

Heterogeneities in bioreactors were examined extensively in literature (Delafosse et al., 2010; Enfors et al., 2001; Hewitt and Nienow, 2007; Lara et al., 2006; Nienow, 2006; Xu et al., 1999). The main focus of these studies was on large-scale bioreactors, where spatial heterogeneities of e.g. nutrients or the pH value occur due to poor mixing conditions at large scale. Hence, regions with high C-source concentrations and C-source-limited regions exist

simultaneously within the same bioreactor. Studies investigating heterogeneities of nutrients by applying glucose pulse experiments or bioreactors with poor mixed regions were conducted with *Saccharomyces cerevisiae* (Delvigne et al., 2006; George et al., 1993; Lejeune et al., 2013; Reijenga et al., 2005), *Escherichia coli* (Delvigne et al., 2009; Hewitt et al., 2007; Lara et al., 2009; Sunya et al., 2013) and other bacteria (Brooks and Meers, 1973; da Silva et al., 2008; Junne et al., 2011; Korneli et al., 2011; Schroeter et al., 2013) and yeast (Liang et al., 2013; Lorantfy et al., 2013). In these studies, it could be shown that overflow metabolites occur due to locally high substrate concentrations. Furthermore, short-term oxygen limitations of the microorganisms could be detected, causing a reduction of biomass and product concentration or the formation of overflow metabolites (Brooks and Meers, 1973; Enfors et al., 2001; George et al., 1993; Hewitt et al., 2007; Junne et al., 2011; Korneli et al., 2011; Lara et al., 2009; Lejeune et al., 2013; Lorantfy et al., 2013). However, also positive effects of short-term oxygen limitation could be noticed as the number of dead cells decreased (Enfors et al., 2001; Hewitt et al., 2007).

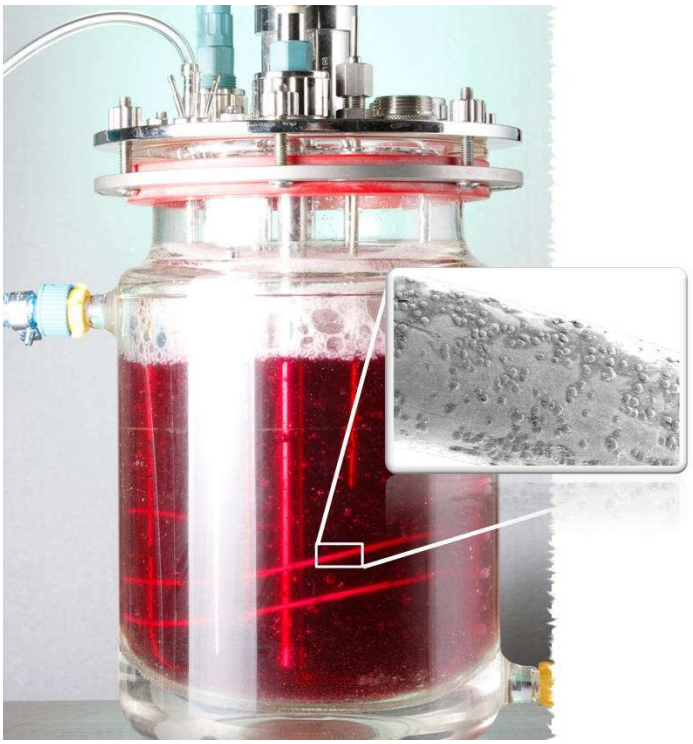

Figure 1-2: Membrane bioreactor for Reverse-flow diafiltration with an integrated hollow-fiber microfiltration membrane.

Continuous and perfusion cultures with externally arranged cell retention devices are prone to spatial heterogeneities as microorganisms are exposed to changing environmental conditions during passage through the device (Carstensen et al., 2012a). In contrast, cells are generally retained in their optimal environment in internally arranged cell retention devices.

1.3 Qualification of Single-Use Materials in Bioreactors

In the past fifty years, single-use technologies have become increasingly relevant in biomanufacturing (Ott, 2011; Sinclair and Monge, 2005). They are attractive, because they are more flexible in their applications, they minimize the risk of batch-to-batch contamination and they are cost-effective as a clean in place procedure is not necessary. Moreover, single-use technologies can contribute to a reduction of the carbon footprint (Haxthausen, 2012). Composed of polymers as well as various processing aids and additives (McMillin, 1996), these single-use materials have raised concerns among scientists and manufactures of bioproducts. In particular, leaching of additives has been discussed as a major issue (Jenke, 2007a; Skjevrak et al., 2005). These additives can be toxic to humans and they may also adversely affect microorganism during culture.

Although some regulations regarding the qualification of single-use materials exist (International Conference on Harmonization, 2000; International Organization for Standardization, 2009; Pharmaceutical Inspection Co-operation Scheme, 2007; US Pharmacopeia), a standardized method is not available to test the biocompatibility of such materials. Even though, manufactures of single-use components do certify their products after extensive investigation procedures, these procedures are often not comparable (Merseburger, 2011). In addition, threshold concentrations of potentially harmful components leaching from polymer materials need to be defined as “safe”. This is highly complex, as the threshold concentrations are depending on the particular application (Jenke, 2007b). In particular, single-use polymer bags (Eibl et al., 2011) and tubing (Jenke et al., 2006) have been developed and investigated regarding their biocompatibility. However, little is known about how leaching of polymer additives may affect microbial activity and compromise Good Manufacturing Practice (GMP).

1.4 The „MoBiDiK“ Project

“Modulare Bioproduktion – Disposable und Kontinuierlich (MoBiDiK)” aims to realize a paradigm change from the established batch and fed-batch cultures to small, flexible and disposable continuous processes to meet the demand of patient- and disease-oriented biopharmaceuticals. By establishing a technology platform of continuous upstreaming and downstreaming processes the time-to market of newly developed biopharmaceuticals can be minimized and production becomes more economical. Furthermore, the shift between productions of different biopharmaceuticals can be conducted time-efficient as cleaning and down-times are reduced due to the disposable character of the equipment. Thus, patient can be treated with tailored biopharmaceuticals after a brief production time.

The vision expressed in MoBiDiK results in the following requirements for an upstreaming process: A sterile, robust and biocompatible perfusion system should be developed. Long-term stability with continuous high cell retention and antibody transmission must be proven. Antibody transmission is defined by the concentration of antibodies in the harvest dived by the concentration of antibodies in the bioreactor. Furthermore, the perfusion system should be small and producible as single-use system. Within the MoBiDiK project reverse-flow diafiltration was examined as one potential perfusion system. As the mention requirements were the basis of evaluation, they were also the main criteria considered within this thesis.

1.5 Objectives and Overview

Reverse-flow diafiltration (RFD) was first basically described by Carstensen et al. (2012b) applying model fluids. The potential of RFD in bioprocesses was exemplarily demonstrated for the recovery of itaconic acid produced by the fungus *Ustilaog maydis* (Carstensen et al., 2013). One dilution rate was successfully applied. However, a broader range of dilution rates and long-term stability of the filtration process could not be shown yet. Furthermore, the applied bioreactor set-up of RFD developed within a cooperation project of Carstensen (2013)

and Klement (2013) was very basic. Thus, robust cultivations could not be performed. Moreover, in Carstensen et al. (2013) the product tank was diluted with unreacted substrate, leading to a loss of substrate, lower space-time-yields and more complicated purification.

This thesis describes the efforts to establish RFD by improving the experimental set-up as well as settings and to broaden the scope of application through required modifications. Previous to the investigation of RFD, three analytical assays had to be established: First, single-use materials needed to be qualified for application in bioreactors. As the Respiration Activity MOnitoring Systems (RAMOS) has been proven to be a sensitive device to observe growth behavior as well as metabolic activities in general (Stöckmann et al., 2003), it was investigated whether biocompatibility tests for single-use materials can be conducted with the RAMOS device. Second and third, various methods to determine the concentration of the desired product, a single-chain antibody, as well as the viable cell density are investigated.

In the subsequent chapter, optimizations of RFD settings are conducted based on mathematical calculations and experimental data. The target of this optimization step is to enhance space-time-yield significantly, prevent a loss of substrate and enable stable long term operation conditions. Furthermore, application and modification of RFD for the production of single-chain antibodies secreted by yeast as well as antibodies produced by mammalian cells is intended. Experiments applying conventional RFD with optimized settings are discussed for yeasts and mammalian cells in chapter 5.

As experiments with mammalian cells are time-consuming and expensive, application of RFD for CHO cells is simulated. On the basis of the two experiments conducted and discussed in chapter 5, parameters of the CHO culture are estimated and a promising operation strategy is investigated in chapter 6.

Conventional RFD is improved by realizing a quasi-continuous RFD in chapter 7. Temporally constant concentrations in the bioreactor were achieved by the sequential operation of three membranes. In the first part of the chapter, the pulsed feeding of RFD and its impact on the yeast *H. polymorpha* is investigated. In particular, fermentation conditions which result in repeated short-term oxygen limitations due to pulsed feeding were examined and compared to oxygen unlimited conditions. In the second part, a process scheme for sequential operation of

three membranes is introduced. The sequential operation is experimentally investigated for several dilution and stirring rates.

Upon completion of this thesis RFD shall have a robust set-up with complete cell retention and constantly high antibody transmission. Long-term stable filtration performance shall be guaranteed and a broad spectrum of applications shall be established particularly with regard to MoBiDiK.

Chapter 2

Materials and Methods

2.1 Membrane

Hollow fiber membranes made from polyethersulfone (Pentair, Enschede, Netherlands) were used with the smallest pore size on the inside, which is less prone to fouling. The nominal pore size on the inside was 0.2 µm, and the porosity was 40%. On the outside surface the pore size was of approximately 1 to 2 µm. The inner and outer diameters were 1.5 mm and 2.35 mm, respectively. This membrane was selected based on prior membrane screening performed by Frederike Carstensen (AVT.CVT, RWTH Aachen University). Prior to each experiment the membrane was flushed with deionized water to remove preservatives. The integrity of the membrane was checked using pressurized air at 1.5 bar.

2.2 Polymers

The following polymers were analyzed in this study regarding their leaching behavior: Polyamide 12 (PA) (outer diameter 6 mm, inner diameter 4 mm, Art. No. 259.11 S, Riegler & Co. KG, Bad Urach, Germany), polyurethane tubing (PUR) (Art. No. 259.16 S, Riegler & Co. KG, Bad Urach, Germany), polypropylene pipette tips (PP) (Art. No. 0030 000.919, Eppendorf AG, Hamburg, Germany), polytetrafluoroethylene tubing (Teflon) (Art. No. TFL 6X4 NATUR, Landefeld Druckluft und Hydraulik GmbH, Kassel, Germany), polyether ether ketone bloc (PEEK) (PPEK Natur, Horbach, Langerwehe, Germany) and polyamide 6.6 cable

tie (Nylon) (Art. No. 541665 – 62, Conrad Electronic SE, Hirschau, Germany) (Figure 2-1). Further a hollow fiber membrane made from polyethersulfone (PES) (Pentair, Enschede, Netherlands) was investigated regarding its leaching behavior.

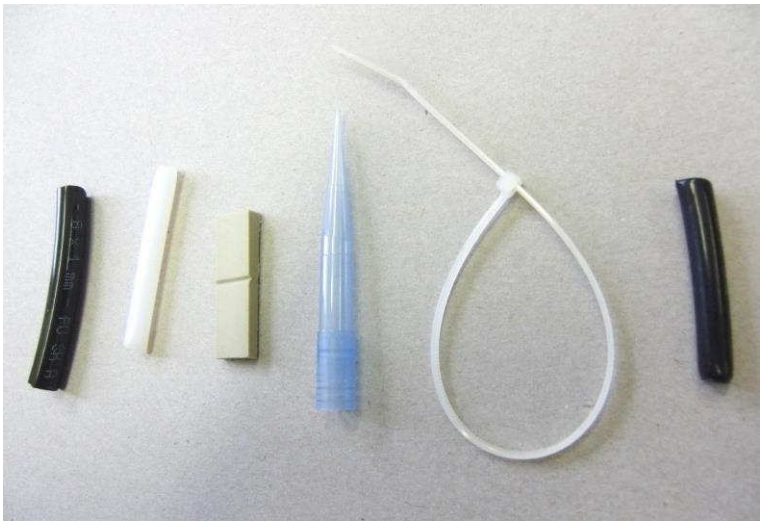

Figure 2-1: Analyzed polymers from left to right: Polyurethane tubing (PUR), polytetrafluoroethylene tubing (Teflon), polyether ether ketone bloc (PEEK), polypropylene pipette tips (PP), polyamide 6.6 cable tie (Nylon) and polyamide 12 tubing (PA).

2.3 Cultures and Media

2.3.1 *Hansenula polymorpha* pCoM11sc3625

The yeast *Hansenula polymorpha* was used in this study for assay qualification as well as in reverse-flow diafiltration experiments. *H. polymorpha* pCoM11sc3625 is an engineered strain, which was kindly provided by PharmedArtis GmbH (Aachen, Germany) (Melmer et al., 2011). This strain constitutively secrets a single-chain antibody. *H. polymorpha* was stored as cryo stock solution at -80 °C. Experiments with *H. polymorpha* were conducted in Syn6 medium (Stöckmann et al., 2003). All chemicals used were of analytical grade.

Syn 6 MES Medium for *Hansenula polymorpha*

Main solution		960 mL
$(NH_4)_2SO_4$	15.3 g L^{-1}	
KH_2PO_4	2.0 g L^{-1}	
KCl	6.6 g L^{-1}	
$MgSO_4 \cdot 7H_2O$	6.0 g L^{-1}	
NaCl	0.7 g L^{-1}	
2-morpholinoethanesulfonic acid (MES)	27.3 g L^{-1}	
Glucose (autoclaved separately) or Glycerol	20 g L^{-1}	
Calcium chloride stock solution (autoclaved)		10 mL
$CaCl_2 \cdot 2H_2O$	100 g L^{-1}	
Microelements stock solution (sterile filtered)		10 mL
Titriplex III	6.65 g L^{-1}	
$(NH_4)_2Fe(SO_4)_2 \cdot 6H_2O$	6.65 g L^{-1}	
$CuSO_4 \cdot 5H_2O$	0.55 g L^{-1}	
$ZnSO_4 \cdot 7H_2O$	2 g L^{-1}	
$MnSO_4 \cdot H_2O$	2.65 g L^{-1}	
Vitamins stock solution (sterile filtered)		10 mL
Biotin	0.04 g L^{-1}	
dissolved in Isopropanol	5 mL	
and deionized water	5 mL	
Thiamine	13.35 g L^{-1}	
dissolved in deionized water	90 mL	
Trace elements stock solution (sterile filtered)		10 mL
$NiSO_4 \cdot 6H_2O$	0.065 g L^{-1}	
$CoCl_2 \cdot 6H_2O$	0.065 g L^{-1}	
H_3BO_3	0.065 g L^{-1}	
KI	0.065 g L^{-1}	
$Na_2MoO_4 \cdot 2H_2O$	0.065 g L^{-1}	

2.3.2 *Eschericha coli* BL21

The bacterium *Eschericha coli* BL21 (DE3) piRhotHi-2-EcFbFP was kindly provided by T. Drepper (Institute of Molecular Enzyme Technology, Heinrich-Heine-University Düsseldorf) and investigated in polymer material qualification experiments and stored as cryo stock solution at -80 °C.

The *E. coli* strain was cultivated in Wilms-MOPS medium at a pH value of 7.5 according to Scheidle et al. (2007). All chemicals used were of analytical grade.

Wilms-Mops Medium for *Eschericha coli*

Main solution		977 mL
$(NH_4)_2SO_4$	7.0 g L^{-1}	
KH_2PO_4	3.0 g L^{-1}	
Na_2SO_4	2.0 g L^{-1}	
3-(N-morpholino)propanesulfonic acid (MOPS)	41.9 g L^{-1}	
Glucose (autoclaved separately)	20 g L^{-1}	
Magnesium sulfate stock solution (autoclaved)		10 mL
$MgSO_4 \cdot 7H_2O$	50 g L^{-1}	
Trace elements stock solution (sterile filtered)		1 mL
$ZnSO_4 \cdot 7H_2O$	0.54 g L^{-1}	
$CuSO_4 \cdot 5H_2O$	0.48 g L^{-1}	
$MnSO_4 \cdot H_2O$	0.30 g L^{-1}	
$CoCl_2 \cdot 6H_2O$	0.54 g L^{-1}	
$FeCl_3 \cdot 6H_2O$	41.7 g L^{-1}	
$CaCl_2 \cdot 2H_2O$	1.98 g L^{-1}	
Titriplex III	33.4 g L^{-1}	
Thiamine stock solution (sterile filtered)		1 mL
Thiamine	10.0 g L^{-1}	
Ampicillin stock solution (sterile filtered)		1 mL
Ampicillin sodium salt	100 g L^{-1}	

2.3.3 *Ustilago maydis* MB215

Ustilago maydis MB215 was used in polymer material qualification experiments. This fungus was kindly provided by M. Bölker (Philipps-Universität Marburg) and stored as cryo stock solution at -80 °C.

Experiments with the fungus *U. maydis* were conducted in a modified medium at a pH value of 6 according to Verduyn et al. (1992). All chemicals used were of analytical grade.

Verdyn Medium for *Ustilago mydis*

Main solution		979 mL
$(NH_4)_2SO_4$	5.0 g L^{-1}	
KH_2PO_4	0.5 g L^{-1}	
2-morpholinoethanesulfonic acid (MES)	0.1 g L^{-1}	
Glucose (autoclaved separately)	50.0 g L^{-1}	
Magnesium sulfate stock solution (autoclaved)		10 mL
$MgSO_4 \cdot 7H_2O$	20 g L^{-1}	
Iron sulfate stock solution (autoclaved)		10 mL
$FeSO_4 \cdot 7H_2O$	1 g L^{-1}	
Trace elements stock solution (sterile filtered)		1 mL
$ZnSO_4 \cdot 7H_2O$	4.5 g L^{-1}	
$CuSO_4 \cdot 5H_2O$	0.30 g L^{-1}	
$MnCl_2 \cdot 2H_2O$	0.84 g L^{-1}	
$CoCl_2 \cdot 6H_2O$	0.30 g L^{-1}	
$Na_2MoO_4 \cdot 2H_2O$	0.4 g L^{-1}	
$CaCl_2 \cdot 2H_2O$	4.5 g L^{-1}	
$FeSO_4 \cdot 7H_2O$	3 g L^{-1}	
H_3BO_3	1.0 g L^{-1}	
KI	0.1 g L^{-1}	

2.3.4 CHO DG44

In this study the mammalian cell line CHO DG44 producing the human IgG antibody H10 was used (Peuscher et al., 2014). This cell line was kindly provided by Fraunhofer Institute for Molecular Biology and Applied Ecology (IME, Aachen, Germany).

Twice weekly the CHO-DG44 cells were passaged 1:20 in commercially available PowerCHO 2 medium (Lonza Group Ltd, Basel, Switzerland) supplemented with 4 mM L-glutamine (Life Technologies, Darmstadt, Germany). Cultures were incubated in 50 mL disposable bioreactors (TPP, Trasadingen, Switzerland) with a working volume of 10 mL at 180 rpm, 37 °C, 5% CO_2 in a Kühner ISF1-C-CO_2 incubator (Kühner AG, Basel, Switzerland).

2.4 Culture Conditions

2.4.1 Pre-cultures

Pre-cultures of the microbial cells, namely *H. polymorpha, E. coli* and *U. maydis* were cultivated in the respective medium according to Table 2-1. Every pre-culture was inoculated with 0.5 mL cryo stock solution per flask and harvested during its exponential growth phase.

CHO DG44 pre-cultures used for inoculation of the perfusion bioreactor were cultivated in PowerCHO 2 medium (Lonza Group Ltd, Basel, Switzerland) supplemented with 4 mM L-glutamine (Life Technologies, Darmstadt, Germany). Cultures were incubated in disposable 500 mL Erlenmeyer shake flasks (Sigma Aldrich Chemie GmbH, Steinheim, Germany) with a working volume of 100 mL at 180 rpm, 37 °C, 5% CO_2 in a Kühner ISF1-C-CO_2 incubator (Kühner AG, Basel, Switzerland). Typically cell densities of $1 \cdot 10^6$ cells mL^{-1} were reached.

Table 2-1: Culture conditions of the various applied microbial culture strains

Culture parameters	***E. coli* BL21**	***U. maydis* MB215**	***H. polymorpha* pCoM11sc3625**
Temperature	37 °C	30 °C	37 °C
Shaking diameter	50 mm	50 mm	50 mm
Shaking frequency	350 rpm	350 rpm	350 rpm
Filling volume	12.5 mL	20 mL	12.5 mL

2.4.2 RAMOS Experiments

Cultures conducted in shake flasks were monitored online via the Respiration Activity MOnitoring System (RAMOS). This device measures the Oxygen Transfer Rate (OTR) and the Carbon dioxide Transfer Rate (CTR) of eight shake flasks simultaneously. The respiration Quotient (RQ) is calculated from these values. The OTR is a commonly used parameter to characterize aerobic cultures, as it reflects all oxygen converting metabolic activities such as microbial growth (Anderlei and Büchs, 2001; Anderlei et al., 2004).

The material qualification assay was conducted in shakes flasks. Main cultures in these experiments were inoculated at $OD_{600} = 0.1$ (Spectrophotometer Genesys 20, Thermo Fisher Scientific, Bonn, Germany) if not stated otherwise. For offline analysis, main cultures were conducted in parallel in conventional 250 mL Erlenmeyer flasks under identical culture conditions.

2.4.3 Biocompatibility test for CHO cells

A biocompatibility test was carried out by addition of the testing material (membrane and tubing) to a CHO DG44 culture conducted in T75 cell culture flasks (Sigma Aldrich, St. Louis, MO, USA) filled with 20 mL supplemented Power CHO 2 medium. The T75 cell culture flasks were incubated at 37 °C and 5% CO_2 in a Kühner ISF1-C-CO_2 incubator for 96 h without shaking. Viable cell densities of cultures in presence and absence of testing material were compared. The testing material had been sterilized by autoclaving prior to examination.

2.4.4 Bioreactor Experiments with Yeast Cells

Pre-cultures of *H. polymorpha* were cultivated in MES-buffered Syn6 medium in 250 mL RAMOS flasks filled with 10 mL. Cultures were incubated at 37 °C on a shaker set to 350 rpm and a shaking diameter of 50 mm. All pre-cultures were harvested during the exponential growth phase.

Continuous *H. polymorpha* cultures were grown in a 3 L fermenter (Applikon Biotechnology, Schiedam, Netherlands) filled with 1.5 L. All cultures were performed in Syn6 medium at 37 °C without buffer. The pH value was adjusted to 5.5 with 5 M NaOH. To maintain a dissolved oxygen tension above 30% air saturation, the stirring and aeration rates were adjusted in the range of 500 – 1800 rpm and 1.5 – 4.5 L min^{-1}, respectively as specified in the graphs if not stated otherwise. To prevent foam formation, Plurofac LF1200 (BASF, Ludwigshafen, Germany) was used as necessary.

In continuous cultures without cell retention, the dilution rate (D) was increased (Equation 2.1) with an acceleration rate (a) of 0.001 h^{-2}, based on the acceleration-stat mode described by Paalme et al. (1995) until the wash out point (D_{max}). The initial dilution rate (D_0) was set to 0.08 h^{-1}:

$$D = D_0 + a \cdot t \qquad (2.1)$$

In experiments with *H. polymorpha* and cell retention, *D* was raised in a stepwise fashion. To achieve stable conditions, each dilution rate was kept constant for five retention times.

2.4.5 Bioreactor Experiments with CHO cells

Batch cultures were conducted in a 3 L bioreactor (Applikon Biotechnology, Schiedam, Netherlands) filled with 1 L supplemented PowerCHO 2 medium at 37 °C. A marine impeller with a diameter of 60 mm stirred at 125 rpm. The pH was adjusted to 6.8 with autoclaved 0.2 M NaOH. The set point of the dissolved oxygen tension (DOT) was 40% and maintained by pulsed aeration. The bioreactor was inoculated with a cell density of $1 \cdot 10^5$ cells mL^{-1}.

Perfusion cultures were started in batch mode until a viable cell density of $1.8 \cdot 10^6$ cells mL^{-1} was reached applying the same settings. The bioreactor was equipped with a membrane module necessary for reverse-flow diafiltration (RFD). Dilution rates of $D = 0.5$ d^{-1}, 1 d^{-1} and 2 d^{-1} were investigated.

2.5 Treatment of Single-use Polymers in Aqueous Culture Media

Leaching of polymer additives was analyzed mainly for black polymer tubes consisting of Polyamide 12 (PA) (outer diameter 6 mm, inner diameter 4 mm, Art. No. 259.11 S, Riegler & Co. KG, Bad Urach, Germany) in aqueous culture media. A quantity of 4 g tubing equal to a length of 250 mm and a surface area of 7854 mm² was cut in pieces of 50 mm length and added to 100 mL of the respective basic medium (40 g L^{-1} PA). The tubing was heat sterilized in the medium at 121 °C and 1 bar overpressure for 20 min and removed afterwards. In order to attain set concentrations of PA, the medium, heat sterilized with tubing, was afterwards diluted with defined volumes of standard basic medium as stated in the particular experiments.

2.6 Analytics

2.6.1 Protein Quantification

The concentration of the human IgG antibody H10 was determined by means of Biacore 2000 instrument equipped with a CM5-rg sensor chip (both GE Healthcare, Uppsala, Sweden) coupled with recombinant protein A. HBS-EP served as running buffer; 575 µg mL^{-1} H10 antibody was used as standard.

An assay for the determination of the single-chain antibody produced by *Hansenula polymorpha* is not established so far. Thus, two different methods, namely the bicinochoninic acid (BCA) Protein Assay and the Fast Protein Liquid Chromatography (FPLC) were investigated in this thesis.

The bicinochoninic acid (BCA) Protein Assay determines protein concentrations by means of color changing regencies. In this study the Pierce BCA Protein Assay kit (Thermo Scientific, Rockford, USA) was used. Samples were analyzed regarding the microtiter procedure. Bovine Serum albumin (BSA) standards of 0.125 g L^{-1}, 0.25 g L^{-1}, 0.5 g L^{-1}, 0.75 g L^{-1}, 1 g L^{-1}, 1.5 g L^{-1} and 2 g L^{-1} were used for calibration. Supernatant of a *H. polymorpha* broth was analyzed with the BCA Protein Assay kit for validation. The same sample was analyzed without dilution and dilutions of 1:1, 1:2 and 1:10 for validation.

Fast Protein Liquid Chromatography (FPLC) is a method to analyze and purify proteins. In this study, determination of proteins through size exclusion is investigated. An Äkta FPLC equipped with a HiPrep 26/10 Desalting column (both GE Healthcare Life Science, Buckinghamshire, UK) was used. A 0.1 M MES buffer served as running buffer. UV peaks measured by Monitor UPC 900 (also GE Healthcare) indicate the product concentration. Calibration were conducted five-fold with 3 mL BSA samples of 0.125 g L^{-1}, 0.25 g L^{-1}, 0.5 g L^{-1}, 0.75 g L^{-1}, 1 g L^{-1} and 1.5 g L^{-1}. Supernatant of a *H. polymorpha* broth was analyzed with FPLC for validation. The same sample was analyzed without dilution and dilutions of 1:1, 1:2 and 1:10 for validation.

Fractions obtained by FPLC were analyzed by sodium dodecyl sulfate polyacrylamide gel electrophoresis (SDS-Page). Thus, the size of the protein is determined causing the peak in the FPLC signal. A volume of 6 µL of 550 µL NuPage® Sample Buffer (Life Technologies, New York, USA) prepared with 50 µL DTT (Sigma Aldrich, St. Louis, USA) was mixed with 18 µL sample volume and incubated for 5 min at 95 °C. Prefabricated NuPage® Novex® 4-12% Bis-Tris gels (Life Technologies, New York, USA) were loaded with 7 µL Roti® Mark Standard (Carl Roth, Karlsruhe, Germany) and 20 µL of each incubated sample. Gels were installed in a SDS chamber filled with 40 mL NuPage® MES Running Buffer (Life Technologies, New York, USA) and 760 mL deionized water. Power was applied with the following settings for 50 min: 200 V, 120 mA and 25 W. Gels were stained afterwards for 15 h with Roti® Blue (Carl Roth, Karlsruhe, Germany), washed with a mixture of 25 mL methanol and 75 mL deionized water and photographed (Biorad, Hercules, USA).

Antibodies were further analyzed by a reduced western blot (Holland et al., 2010). A 4-12% Bis-Tris NuPage gel (Carlsbad, CA, USA) was loaded with 30 µL sample volumes, 8 µL pre-stained marker (Fermentas, Bulingston, ON, USA) and 6 µL of antibody standard if available. The gel was run for 45 min at 200 V in MES running buffer and afterwards transferred to a nitrocellulose membrane at 250 mA for 60 min. The membrane was blocked with 5% skim milk for 1 h at room temperature, washed with PBST, incubated in 15 mL PBS supplemented with 6 µL AP-conjugate goat anti-human antibodies (Sigma Aldrich, ST. Louis, MO, USA) for 1 h at room temperature and washed again with PBST.

2.6.2 Viable Cell Density and Biomass Determination

To quantify biomass of yeast, fungi and bacteria dry cell weight (DCW) was determined four-fold. Eppendorf-tubes were stored at 80 °C for 24 hours, cooled in an exsiccator and weighed (SBC 31, Scaltec, Göttingen, Germany). The prepared Eppendorf-tubes were filled with 2 mL culture broth and centrifuged at 14000 rpm for 10 min (Centrifuge 1 - 15, Sigma Centrifuge GmbH, Göttingen, Germany). The supernatant was discarded. The pellet was stored at 80 °C for 60 hours, cooled and weighed. The difference in weight of the filled and unfilled Eppendorf-tube divided by the 2 mL broth equals the DCW.

Cell counting of viable CHO cells was conducted three-fold by using CASI I TT (Roche Inovartis, Basel, Switzerland).

Various assays exist to determine the concentration of viable yeast cells. Within this thesis three assays were investigated and compared regarding their suitability for *Hansenula polymorpha*, namely the hemocytometer, the methylene blue assay and the *LIVE/DEAD*® Funga*Light*™ Yeast Viability Kit analyzed by flow cytometry.

A disposable hemocytometer (C-Chip; NI Neubauer Improved DHC-NO1; Montreal Biotech Inc., Dorval, PQ, Canada) was used to analyze the viability of yeasts in a suspension with a volume of 10 µL. By counting the number of cells in an optional number of squares marked on the Neubauer chamber, the concentration of cells can be extrapolated (Bastidas, 2013). Methylene blue (Sigma-Aldrich, St. Louis, MO, USA) was added to the suspension in a 1:20 dilution. Since the dye diffuses mainly through the ruptured membrane of a dead cells, vivid and dead cells can easily be distinguished by their color (Schrek, 1963). Cell concentrations were determined by counting 5 of 25 small squares of a center square with a microscope at 40-fold magnification.

The methylene blue assay can also be used for the determination of viable cells. Methylene blue is a dye, which diffuses through the ruptured membranes of dead cells. According to Borzani and Vairo (1958) the diffusion can be regarded as a quantitative adsorption. Therefore, it can be described by the Freundlich law (Equation 2.2). This equation takes the mass of absorbed substance (m_X), the mass of absorbing mass (m_M), the equilibrium concentration of the solution (c_S) and two constants (n and k) into account.

$$\frac{m_X}{m_M} = k \cdot c_S^n \qquad (2.2)$$

The mass of absorbed substance (m_X) equals the initial methylene blue concentration ($c_{S,i}$) minus the equilibrium dye concentration ($c_{S,f}$). The mass of absorbing mass (m_M) is the concentration of dead cells as methylene blue diffuses mainly through the ruptured membrane of those cells. The concentration of dead cells equals the total yeast cell concentration (X) multiplied by the percentage of dead yeast cells (P_X). Conversion of equation 2.2 leads to:

$$\frac{c_{S,i} - c_{S,f}}{c_{S,f}^{n}} = k \cdot P_X \cdot X \qquad (2.3)$$

The concentration of methylene blue can be measured spectrophotometrically at 440 nm. With set dead cell concentrations, the constants *k* and *n* can be determined experimentally. With these values the unknown dead cell concentration ($P_X \cdot X$) could be determined using equation 2.3. If the individual values of P_X and X are of interest, a sample can be split into two portions, one in which the cells are killed and one untreated. As all cells are dead in the first portion ($P_X = 1$), the total cell concentration can be determined. Hence, the percentage of dead cells in the untreated sample can be calculated out of the second portion (Borzani and Vairo, 1958).

Prior to application of this method, a calibration between the methylene blue concentration and the spectrophotometrically measured value has to be conducted. Here, a serial dilution of methylene blue in the medium was used with the following concentrations: 0.05 g L^{-1}, 0.067 g L^{-1}, 0.083 g L^{-1}, 0.100 g L^{-1}, 0.125 g L^{-1}, 0.143 g L^{-1}, 0.167 g L^{-1}, 0.200 g L^{-1} and 0.250 g L^{-1}.

The initial methylene blue concentration ($c_{S,i}$) was set to 0.15 g L^{-1}. Samples with dye added were incubated for 15 min at 1000 shakes min^{-1}. Afterwards, the samples werecentrifuged at 14000 rpm for 5 min (Sigma, Osterode am Harz, Germany). The equilibrium dye concentration ($c_{S,f}$) was spectrophotometrically determined in the supernatant.

To verify this method, yeast cell suspension of *Hansenula polymorpha* with final dead cell concentrations of 1.25 g L^{-1}, 2.5 g L^{-1}, 5 g L^{-1}, 10 g L^{-1}, 15 g L^{-1}, 20 g L^{-1}, 25 g L^{-1}, 30 g L^{-1}, 40 g L^{-1}, 50 g L^{-1} were prepared and analyzed. Furthermore, dead and vivid yeast cells were mixed in various ratios between 0 – 100% with a total yeast concentration of 30 g L^{-1}. The concentration of dead cells was examined with the methylene blue assay. Hence, the influence of vivid cells on the equilibrium dye concentration could be determined as also vivid cells adsorb methylene blue to some extent.

Flow cytometry enables the determination of physiological and physical state of single cells in high throughput by laser measurement (Endo et al., 1998). Among other features, fluorescent dye labels can be determined (Deere et al., 1998). In this study, the *LIVE/DEAD*®

Funga*Light*™ Yeast Viability Kit (Molecular Probes®, Life Technologies, Germany) was used to determine the vivid and dead yeast cell concentrations. Staining was conducted by two fluorescence dyes, namely SYTO® 9 (Ex480/Em500 nm) and Propidiumiodid (Ex490/Em635 nm). Whereas SYTO® 9 stains all yeasts cells, Propidiumiodid stains only cells with compromised membranes. First, 500 µL of a yeast cell suspension was centrifuged at 14.000 rpm for 2 min (Sigma, Germany). The supernatant was discarded, while the pellet was washed with filtered (0.2 µm Filter) 0.9% NaCl. The pellet was centrifuged and resuspended in 500 µL 0.9% NaCl another time. Dilutions of cells with NaCl were prepared to obtain final cell concentrations between 50 to 500 cells μL^{-1}. Staining with SYTO® 9 as well as SYTO® 9 and Propidiumiodid were performed. Therefore, 1 mL of the yeast cell dilution was incubated with 1 µL of the respective dye for 15 min to the exclusion of light before analysis. The following settings were used: Threshold parameter: FSC; Threshold: 2; FSC gain: x 8; Compensation: SSC 557 V, GRN 725 V, YLW 504 V, RED 682 V; Scale: Area 500, Width 500; Flow rate: medium (0.59 µL s^{-1}); Events acquired in gate: 1000.

Validation of the *LIVE/DEAD*® Funga*Light*™ Yeast Viability Kit (Molecular Probes) were conducted with dead yeast cells and known mixtures of dead and vivid yeast cells at various ratios of 0 – 100% dead cells.

Cell viability was measured in chapter 5 and 7 by flow cytometry (Guava EasyCyte Mini Flow Cytometer System; Millipore, Billerica, MA, USA) and a LIVE/DEAD® FungaLightTM Yeast Viability Kit (Life Technologies, Carlsbad, CA, USA). To determine the number of vivid cells possibly passing through the membrane, permeate was also plated on YPG agar (Sigma-Aldrich, St. Louis, USA). All plates were incubated at 37 °C for 48 h.

2.6.3 Preparation of Dead Yeast Cell Concentrations

Cell death was either achieved by treatment with heat, Isopropanol or by starvation. Plating of treated cells on YPG agar was performed to prove cell death.

Yeast cells were cultured in the RAMOS device according to chapter 2.4 until an OTR of 20 mmol L^{-1} h^{-1} was reached. The suspension was centrifuged at 4000 rpm for 10 min (Centrifuge obtained from Hettich, Germany). Pellets were resuspended in 1.5 mL of

0.9% NaCl if heat treatment or 40% Isopropanol was applied and incubated for 15 min at 95 °C or at room temperature, respectively. Afterwards cells were centrifuged at 14000 rpm for 3 min in a microcentrifuge (Sigma, Germany). While the supernatant was discarded, the pellet washed with 0.9% NaCl and centrifuged again for 5 min. Dry cell weight was determined and cells were resuspended in 0.9% NaCl to the desired concentrations.

Batch cultures for starvation experiments were performed in a bioreactor and in the RAMOS device. Several samples at distinct time points were taken for offline analysis including: flow cytometry, plating on YPG agar, determination of DCW, Coulter Counter analysis and HPLC measurements of glucose and ethanol concentrations. The OTR was determined online in both devices, the bioreactor and the RAMOS device. Permittivity was measured only in the bioreactor. Starvation experiments last at least 72 h after the OTR drop due to depletion of glucose. Starved cells were harvested and centrifuged at 4000 rpm for 10 min (Hettich, Germany). Cell pellets were resuspended in 0.9% NaCl and centrifuged again.

Table 2-2: Overview of dead cell preparation methods and examined assays

Method	**Preparation method of dead cells**		
	Heat	Isopropanol	Starvation
Hemocytometer	+	-	-
Methylene Blue Assay	+	+	+
Flow cytometry	+	+	+

Dilutions of the treated yeast suspension with sterile 0.9% NaCl were plated on YPG agar. After 48 hours of incubation at 37 °C, colony forming units (CFUs) were counted and vivid cell concentrations in the original culture were calculated. An overview of the dead cell preparation methods and the examined assays are given in Table 2-2.

2.6.4 Metabolites

Glucose, ethanol, acetate and lactate concentrations were measured offline using HPLC (Dionex, Sunnyvale, USA) equipped with an Organic Acid-Resin HPLC separation column 250 × 8 mm (CS-Chromatographie, Langerwehe, Germany) and a Shodex RI-71 detector (Techlab, Erkerode, Germany). Glutamine was determined by reverse phase HPLC (Shimadzu, Kyoto, Japan) using a Nucleodur c18 ec column (Macherey-Nagel, Düren, Germany). Ammonium concentration was determined by an ammonium test kit (Lot.: HC384800) in a Spectroquant Nova 60 (both Merck Millipore, Darmstadt, Germany)

2.6.5 Exhaust Gas Analysis

Exhaust gas was analyzed online regarding its oxygen and carbon dioxide concentration by an exhaust gas analyzer (Emerson XStream; Emerson, Weßling, Germany). Out of these values the oxygen transfer rate (OTR) and the respiratory quotient (RQ) were calculated according to Regestein et al. (2013). The OTR is commonly used to characterize aerobic cultures, as it describes oxygen consumption through metabolic activities, such as microbial growth or product formation (Anderlei and Büchs, 2001). The RQ provides information about the metabolism. RQ values close to 1.0 indicate oxidative growth on glucose, values above 1.0 imply the formation of overflow metabolites such as ethanol (Anderlei et al., 2004).

2.6.6 Gas Chromatography-Mass Spectrometry

A 100 mL sample volume of medium, prepared as described in chapter 2.5 for *H. polymorpha* medium and heat sterilized with PA, was extracted with 100 mL ethyl acetate (Duffield et al., 1994). In order to accelerate the extraction, the aqueous sample and the organic solvent were

mixed with a magnetic stir bar for 0.5 h. Subsequently, a separating funnel was used to partition the two phases. The organic phase was further dehydrated with sodium sulfate. After the solid phase was removed, the organic supernatant was analyzed by means of gas chromatography–mass spectrometry (GC-MS) (HP 5890 SERIES II Gas Chromatograph, Hewlett Packard, California, USA). According to GC-MS database, the respective additive was identified and its concentration was determined by applying a standard.

To avoid cross contamination all applied jars, flasks and pipets consist of glass and were washed with pure grade ethyl acetate beforehand.

2.7 Membrane Bioreactor for Reverse-flow Diafiltration

Reverse-flow diafiltration (RFD) was first basically described by Carstensen et al. (2012b). RFD is a membrane based *in situ* cell retention and product recovery process. Permeate withdrawal and medium supply is alternated over the same submerged hollow-fiber membrane, minimizing the fouling layer. Different membrane bioreactor set-ups were analyzed and enhanced (Carstensen et al., 2013; Meier et al., 2014). The basis set-up is depicted schematically in Figure 2-2. One membrane is coiled around baffles and fixed by attached hooks. One end of the membrane is connected to the feed tubing, the other to the permeate tubing. Pressure sensors in the feed and permeate tubing measure the transmembrane pressure. Volume flows are calculated by balances of the feed and permeate tank. The reactor balance controls the non-filtered product stream pump. The applied RFD process in lab scale can be seen in Figure 2-3. The membranes coiled around the baffles are shown in Figure 2-3 A & B. Figure 2-3 C depicts the reactor with periphery, submerged membrane and culture broth, the permeate pump, the cell free permeate and the permeate balance.

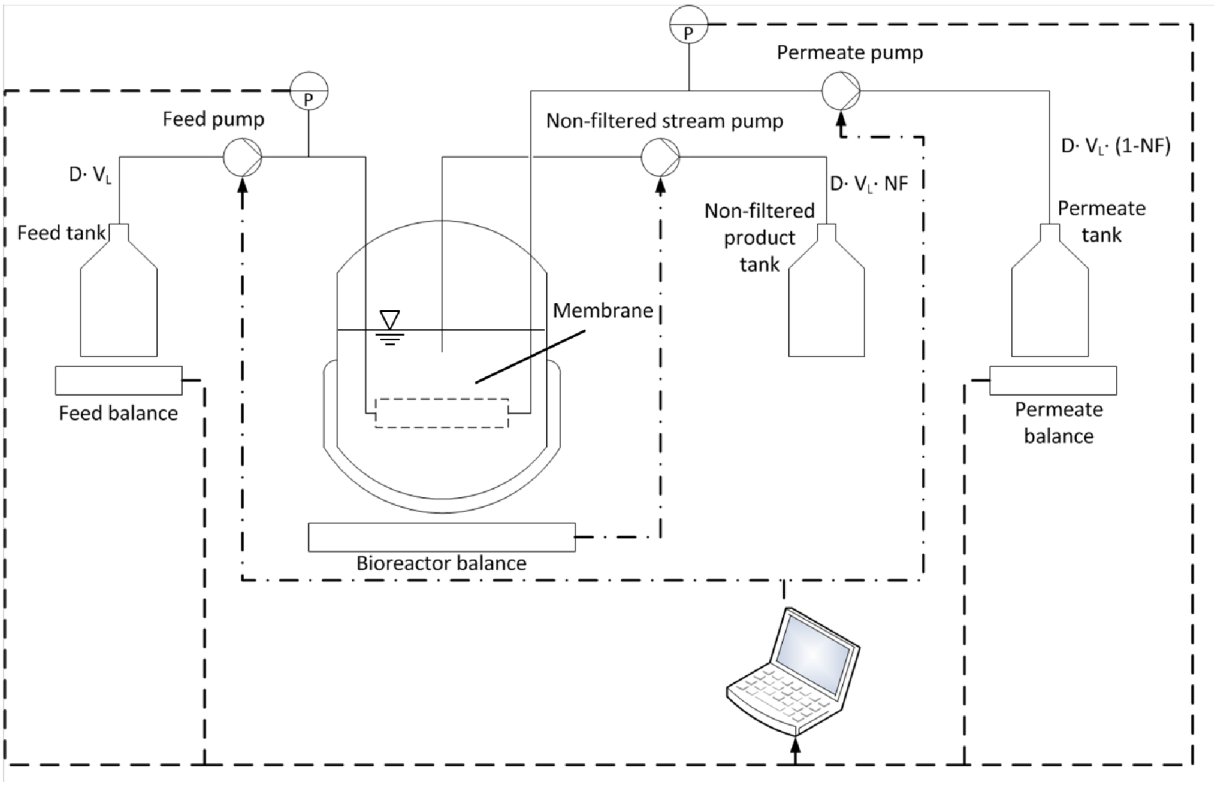

Figure 2-2: Schematic drawing of reverse-flow diafiltratoin with one submerged hollow-fiber membrane. Continuous lines represent liquid flow, dashed-dotted and dotted lines indicate control and data record, respectively. D = Dilution rate [h^{-1}], V_L = Liquid volume [L], NF = Non-filtered ratio [-].

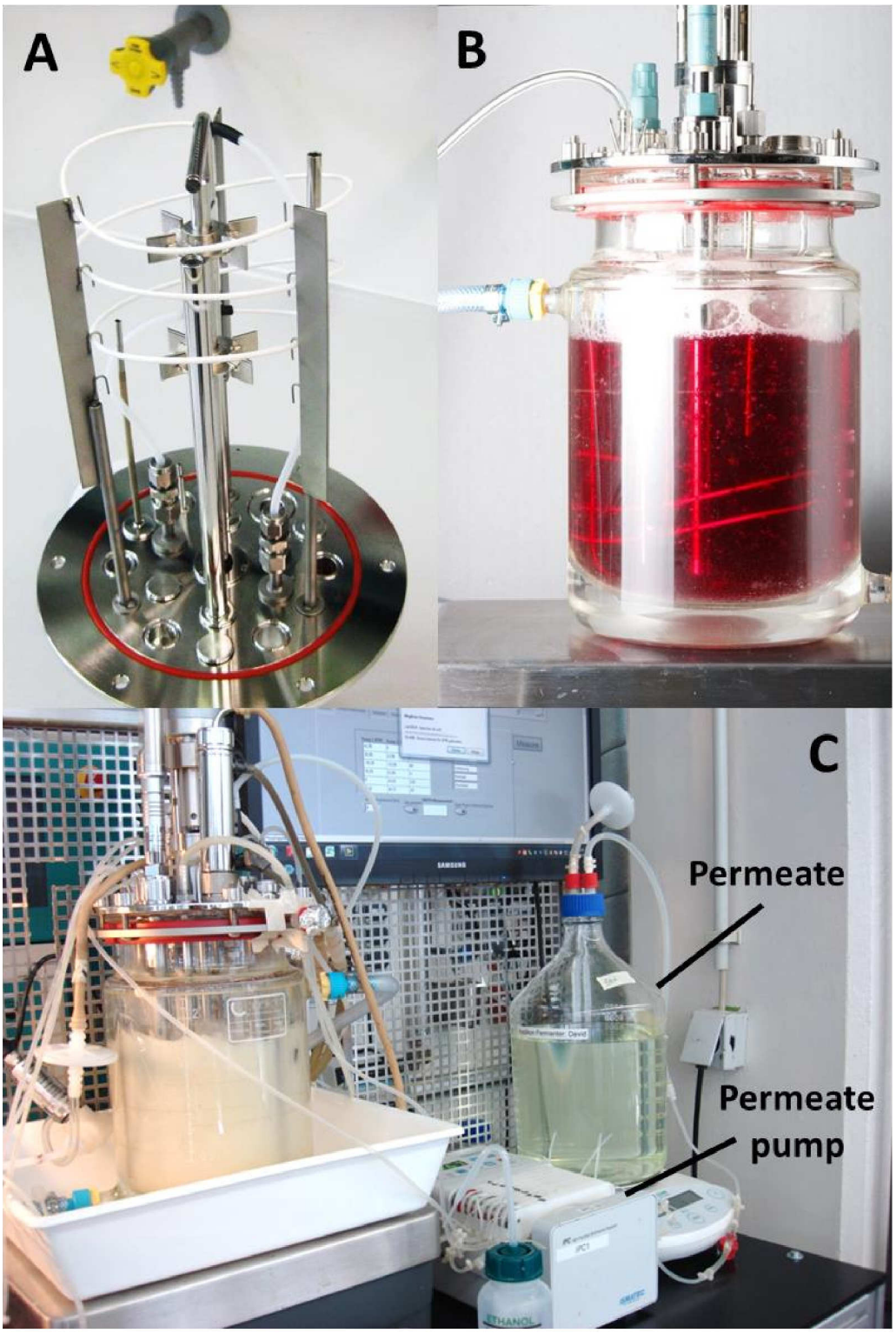

Figure 2-3: Application of reverse-flow diafiltration. A) Hollow-fiber membrane wound spirally baffels with attached hooks B) Membrane submerged in medium C) RFD applied in a culture of *Hansenula polymorpha* pCoM11sc3625. Membrane is submerged in the reactor, permeate pump extracts cell-free permeate.

As shown in Figure 2-4, RFD consists of four steps: A) Permeate step: Permeate is withdrawn from the reactor (Feed pump stops, Permeate pump works), B) Flushing step: Permeate in the membrane is replaced by medium and flushed towards the permeate tank (both pumps work), C) Feeding step: Medium is pumped into the reactor (Feed pump works, Permeate pump stops), and D) Emptying step: Medium in the membrane is replaced with permeate (both pumps work in reverse direction). Arrows in Figure 2-4 indicate the intensity gradient of the flux due to pressure loss over the membrane length. In membrane terminology, flux refers to the specific flow rate given in L m^{-2} h^{-1}.

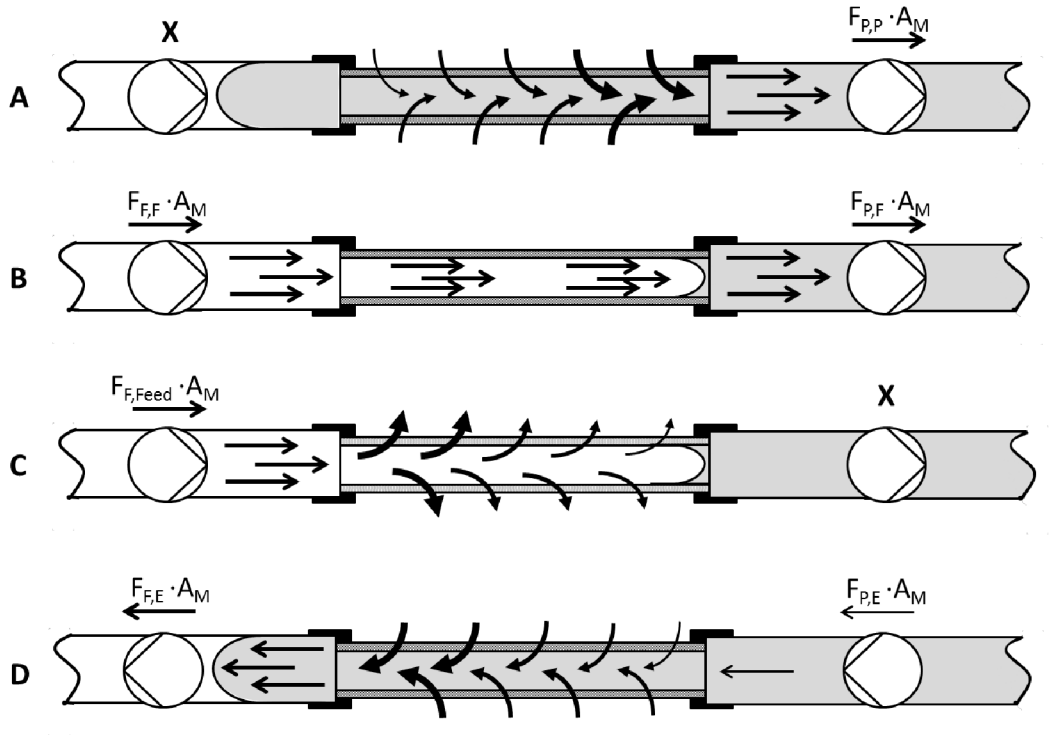

Figure 2-4: Steps of reverse-flow diafiltration: A) Permeate step, B) Flushing step, C) Feed step, D) Emptying step. **X** indicates a stop of the pump, → shows the direction of the flow. The arrow size indicates the intensity of the flux. A white filling represents fresh medium, a grey filling illustrates permeate of the culture broth. *F* is the flux generated by the pumps, the indices stand for the pump und the step, respectively. A_M is the outer membrane area.

Figure 2-5 illustrates a true to scale representation of the sequential operation of RFD using time dependent mass flows in and out of the bioreactor for three membranes operated in parallel. In addition, the non-filtered product stream is shown (Figure 2-5, dashed-dotted line), which is operated continuously due to the slow control of the bioreactor balance.

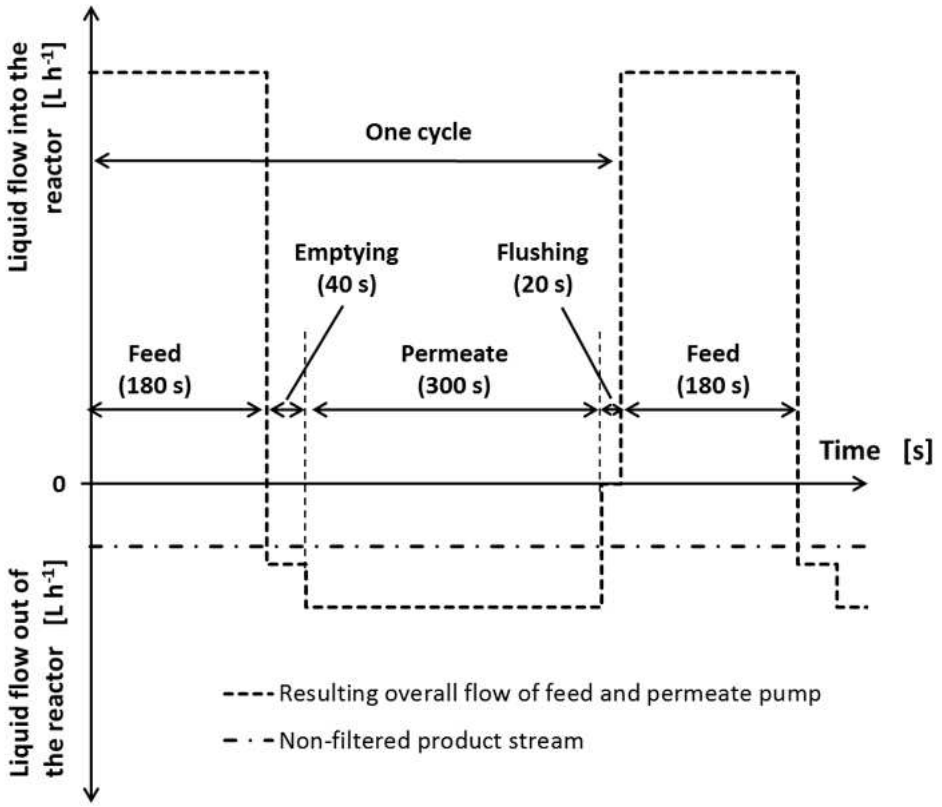

Figure 2-5: True to scale representation of the time dependent liquid flow in (positive values) and out (negative values) of the reactor in the reverse-flow diafiltration mode when membranes are operated in parallel with 50% cell retention. It should be noted that the volume pumped into (Feed) and out of the reactor (Emptying, permeate and non-filtered product stream) equals zero in every cycle.

2.7.1 Application of Yeast Cells

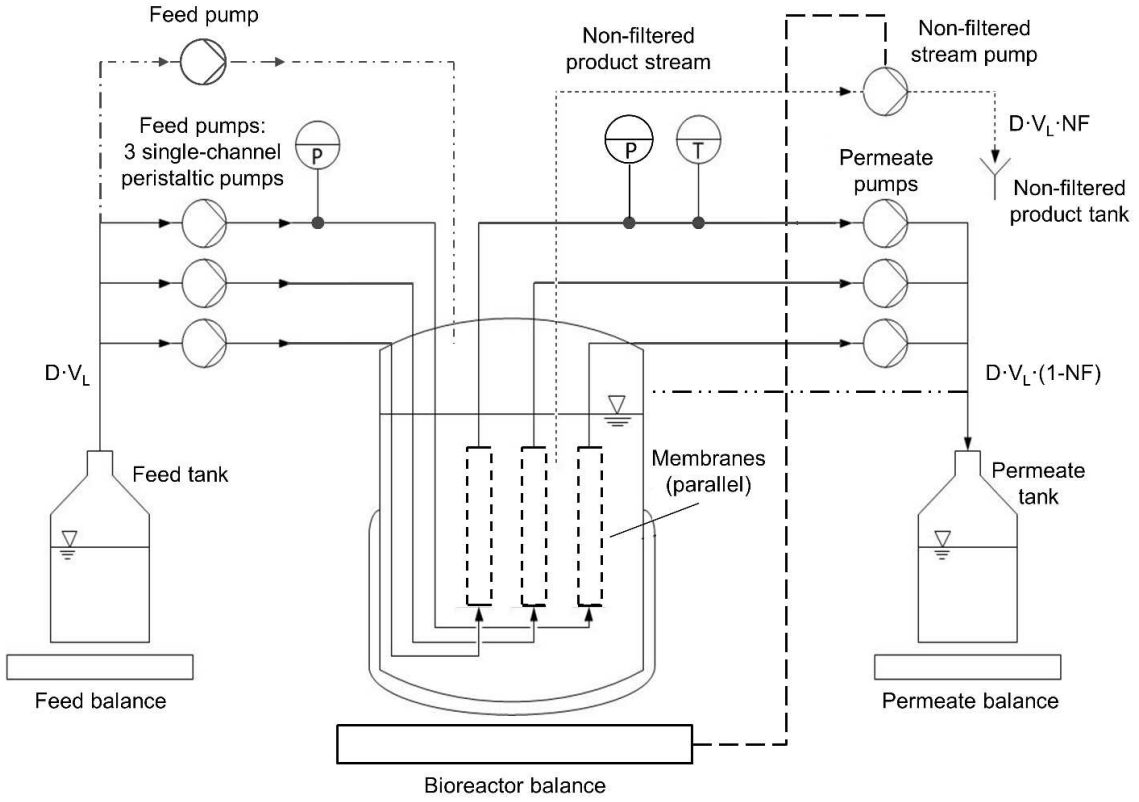

Figure 2-6**:** Schematic diagram of the reverse-flow diafiltration with three microfiltration hollow fiber membranes (nominal pore size = 0.2 µm) operating in parallel.Two pressure sensors in the feed and permeate tank monitor the transmembrane pressure for one membrane as a representative for all three membranes. Bioreactor scale controls the non-filtered product stream pump. One experiment was carried out without membranes (dashed-dotted and dotted line), in one experiment the permeate was directed back into the fermenter (continuous and dashed-dotted-dotted line). All other experiments were carried out with membranes (continuous and dotted line). D = Dilution rate [h^{-1}], V_L = Liquid volume [L], NF = Non-filtered ratio [-].The non-filtered product stream pump is controlled by the reactor weight (dashed line).

In experiments with *H. polymorpha* the reverse-flow diafiltration set-up was modified to allow operation of three membranes in parallel (pumps work simultaneously) or serial (pumps work in a time shifted sequence) as shown in Figure 2-6. Membranes operating in parallel and serial are referred to as conventional RFD and quasi-continuous RFD, respectively. Each membrane had a length of 1 m and was coiled around the baffles, where fixing hooks were attached. The ends of each membrane were individually attached to the tube system, one end to the feed tube, the other to the permeate tube. Peristaltic pumps were used to achieve an independent operation of each membrane. The non-filtered product stream (dashed line) removed cell debris among other. Its pump was regulated by a balance measuring the weight of the filled reactor (P-gain: 2000, Clycle-time: 1s). All integrated parts were tested regarding their biocompatibility before application (Meier et al., 2013).

Table 2-3: Flux generated by feed pump and permeate pump depending on the dilution rate for conventional RFD: Three MF02 membranes with 1 m length each, NF = 0.5, a_E = 1.69, a_F = 0.7, t_C = 510 s and V_L = 1.5 L

Step	**Step Times [s**	**Pump**	**Flux [L m^{-2} h^{-1}] for dilution rates [h^{-1}]**						
			0.1	**0.2**	**0.3**	**0.4**	**0.5**	**0.6**	**0.65**
Feed	150	Feed ($F_{F,Feed}$)	32.6	55.	78.	101.(	124.8	147.8	159.2
		Permeate ($F_{P,Feed}$)	0	0	0	0	0	0	0
Emptyi	40	Feed ($F_{F,E}$)	-50	-5(	-5(	-50	-50	-50	-50
		Permeate ($F_{P,E}$)	-10	-1(	-1(	-10	-10	-10	-10
Permeat	300	Feed ($F_{F,P}$)	0	0	0	0	0	0	0
		Permeate ($F_{P,P}$)	5.1	10.	16.	22.4	28.1	33.9	36.8
Flushin	20	Feed ($F_{F,F}$)	30	3(	3(	30	30	30	30
		Permeate ($F_{P,F}$)	30	3(	3(	30	30	30	30

Pressure values in one feed and permeate tube were continuously monitored as representative values for all three membranes by pressure sensors (WIKA Alexander Wiegand SE & Co. KG, Klingenberg, Germany) with a measuring range from 0 to 2.5 bar absolute. Flux of feed and permeate was calculated based on data from the two associated balances.

Cell retention experiments were carried out in conventional RFD if not stated otherwise. To examine the impact of the membrane and RFD on cell viability and product yield, an experiment was carried out in which permeate was directly pumped back into the reactor (Figure 2-6, dashed-dotted-dotted line). Consequently, the non-filtered flow rate equaled the feed flux, which was similar to a conventional continuous culture. One experiment was conducted without membranes (Figure 2-6, dashed-dotted and dotted line), but with feeding times equivalent to the settings of conventional RFD (Table 2-3).

Table 2-4: Flux generated by feed pump and permeate pump depending on the dilution rate for membranes operated in parallel: Three MF02 membranes with 1 m length each, NF = 0.5, a_E = 1.69, a_F = 0.7, t_C = 540 s and V_L = 1.5 L

Step	**Step times [s]**	**Pump**	**Flux [L m^{-2} h^{-1}] for dilution rates [h^{-1}]**	
			0.1	**0.2**
Feed	180	Feed ($F_{F,P}$)	32.6	55.7
		Permeate ($F_{P,P}$)	0	0
Emptying	40	Feed ($F_{F,F}$)	-50	-50
		Permeate ($F_{P,F}$)	-10	-10
Permeate	300	Feed ($F_{F,Feed}$)	0	0
		Permeate ($F_{P,Feed}$)	5.1	10.9
Flushing	20	Feed ($F_{F,E}$)	30	30
		Permeate ($F_{P,E}$)	30	30

The calculations of the fluxes were developed in chapter 4 and summarized in Table 4-1. The values used for conventional RFD with a feed step time of 150 s and 180 s are given in Table 2-3 and Table 2-4, respectively. Pump settings for the application of serial RFD are given in Table 2-5. Algebraic signs indicate the flow direction (compare Figure 2-4). It should be noted that fluxes in the feed and permeate step do not double for doubled dilution rates as the impact of the volume emptied (compare Figure 2-5) decreases with increasing dilution rate. Detailed information on the settings and design of RFD steps is given in chapter 4.

Table 2-5: Flux generated by feed pump and permeate pump depending on the dilution rate and step for membranes operated serial.Conditions: Three MF02 membranes with 1 m length each, NF = 0.5, a_E = 1.69, a_F = 0.7, t_C = 540 s and V_L = 1.5 L

Step	**Step Times [s]**	**Pump**	**Flux [L m^{-2} h^{-1}] for dilution rate [h^{-1}]**				
			0.1	**0.2**	**0.3**	**0.4**	**0.5**
Feed	180	Feed ($F_{F,P}$)	29.3	49.6	69.9	90.2	110.6
		Permeate ($F_{P,P}$)	0	0	0	0	0
Emptying	40	Feed ($F_{F,F}$)	-50	-50	-50	-50	-50
		Permeate ($F_{P,F}$)	-10	-10	-10	-10	-10
Permeate	300	Feed ($F_{F,Feed}$)	0	0	0	0	0
		Permeate ($F_{P,Feed}$)	6.0	12.1	18.2	24.3	30.4
Flushing	20	Feed ($F_{F,E}$)	30	30	30	30	30
		Permeate ($F_{P,E}$)	30	30	30	30	30

2.7.2 Application of CHO DG44 cells

A conventional RFD as shown in Figure 2-2 was applied for CHO DG44 cells. The membrane module was constructed as described by Carstensen et al. (2013; 2012b), but modified for an application with mammalian cell lines. One hollow fiber membrane with a length of 1 m was coiled around the sensors (pH and DOT) and the harvest tube. The ends of the membrane were attached to the feed and the permeate tube. Nine-tenth of the culture broth was gained filtered, one-tenth was pumped out non-filtered (NF = 0.1) to remove cell debris and excessive biomass. The non-filtered product stream was controlled by the bioreactor balance.

Table 2-6: Flux generated by feed pump permeate pump depending on dilution rates for a perfusion culture applying reverse-flow diafiltration: One MF02 membrane with 1 m length each, NF = 0.1, a_E = 1.69, a_F = 0.7, t_C = 510 s and V_L = 1 L

Step	**Step times [s]**	**Pump**	**Flux [L m^{-2} h^{-1}] for dilution rate [d^{-1}]**		
			0.5	**1**	**2**
Feed	150	Feed ($F_{F,P}$) Permeate ($F_{P,P}$)	20.4 0	29.9 0	49.1 0
Emptying	40	Feed ($F_{F,F}$) Permeate ($F_{P,F}$)	-50.0 -10.0	-50.0 -10.0	-50.0 -10.0
Permeate	300	Feed ($F_{F,Feed}$) Permeate ($F_{P,Feed}$)	0 4.2	0 8.6	0 18.2
Flushing	20	Feed ($F_{F,E}$) Permeate ($F_{P,E}$)	30.0 30.0	30.0 30.0	30.0 30.0

Pressure sensors in the feed and permeate tube monitored the transmembrane pressure continuously (WIKA Alexander Wiegand SE & Co. KG, Klingenberg, Germany) within a measuring range from 0 to 2.5 bar absolute. Fluxes in and out of the bioreactor were calculated based on data from a feed and a permeate balance.

The applied fluxess in this study are given in Table 2-6 for dilution rates of D = 0.5 d^{-1}, 1 d^{-1} and 2 d^{-1}. Positive and negative values indicate pumps running as shown in Figure 2-2 and in reverse direction, respectively. The ratios of volume flushed a_F (flushing step) and volume emptied a_E (emptying step) to the membrane volume were set to a_F = 0.7 and a_E = 1.69, respectively. Detailed information regarding the settings and design of RFD steps is given in chapter 4.

2.8 Flux-step Experiments

Membrane screening was performed to determine a suitable membrane for optimal cell retention and antibody recovery. Therefore, the flux-step method was applied (van der Marel et al., 2009). According to the flux-step method, a high flux phase alternates with a low flux phase. The flux during the high flux phase is increased stepwise, while the transmembrane pressure (TMP) is monitored. At low flux or the so-called relaxation phase, reversible fouling that occurs during the high flux phase is removed due to the conditions applied (e.g. generated by stirring). Each flux step, consisting of a high flux and low flux phase, yields a characteristic increase in TMP. The increase during high flux is referred to as "total TMP increase". The "irreversible TMP increase" is defined as the pressure difference before and after high flux (Figure 2-7). For stable long-term operations, the irreversible TMP increase must be subcritical to ensure only minimal fouling. The critical TMP increase depends on the membrane, the suspension as well as the process and has to be determined individually for every application. In this study, it was set to 45 Pa min^{-1} based on data obtained by Frederike Carstensen (AVT.CVT, RWTH Aachen University). Intersection of the irreversible TMP increase with the critical TMP increase determines the critical flux.

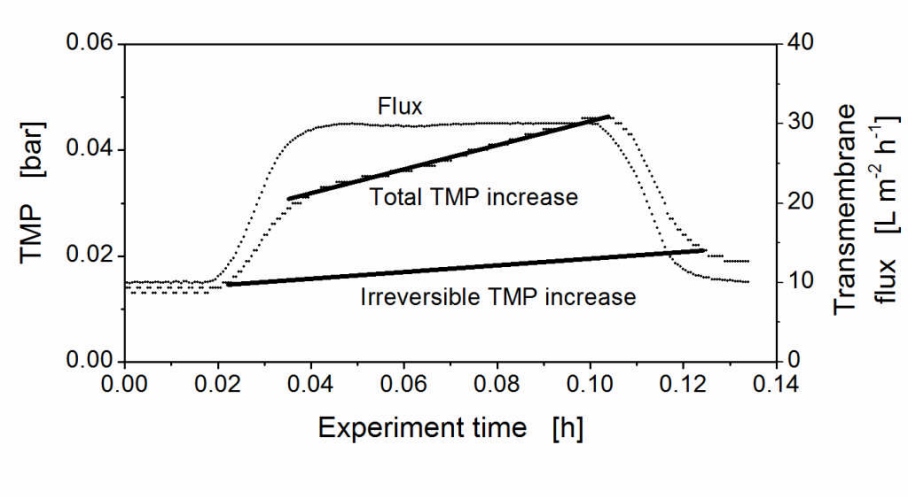

Figure 2-7: Exemplary irreversible and total TMP increase measured for a transmembrane flux of 30 L m^{-2} h^{-1}. Alternating high flux (30 L m^{-2} h^{-1}) and low flux (10 L m^{-2} h^{-1}) yield in a characteristic increase of the TMP. Increase during high flux is revered to as "Total TMP increase", increase of TMP before and after high flux is applied is revered to as "Irreversible TMP increase".

No backflushing was performed in flux step experiments with *Hansenula polymorpha* to simulate worst conditions regarding membrane fouling as settings of RFD were not fixed at that time. Since better conditions for the membrane are applied during RFD mode, the obtained data of the flux step experiments can be regarded as conservative. To a later point, experiments with CHO DG44 cells were conducted with backflushing conditions comparable to reverse-flow diafiltration as configuration of RFD was finalized by then. Hence, results are more accurate.

The specific filtration area of RFD for the chosen membrane-CHO medium combination was calculated based on the critical flux and compared to data obtained by literature for other membrane based cell retention devices (Su, 1995; Voisard et al., 2003).

Chapter 3

Material and Assay Qualification

Leaching of polymer materials can negatively influence cultivations of microorganism. As polymer materials were used in this thesis and no standardized biocompatibility test exists in literature, an analytical biocompatibility test for polymer materials is developed in the first part of this chapter. The breathing behavior of various microorganisms was determined by means of Respiration Activity MOnitoring Systems (RAMOS) as a function of the added amount of polymers commonly applied in biotechnology. This work is based on the thesis of Elena Herweg (2012) and was published in Meier et al. (2013). In the second part, an assay to determine the protein amount secreted by *Hansenula polymorpha* is established. Most of the results here were obtained by Sara Coelho (2012). Methods to determine the viable yeast cell concentration are investigated and validated in the last part of this chapter. Anne Worsch conducted the corresponding experiments (2013).

3.1 Quantifying the Release of Polymer Additives from Single-use Materials by Respiration Activity Monitoring

3.1.1 Effect of Polyamide 12 Tubing on Yeast

To investigate the effect of Polyamide 12 tubing (PA) on *H. polymorpha*, different concentrations of PA were added to the culture medium during heat sterilization. The metabolic behavior was determined via the RAMOS device. Figure 3-1 shows the online measured Oxygen Transfer Rates (OTR) as well as the offline measured Dry cell weights (DCW) and glucose concentrations.

Compared to the reference medium without PA, the cultures with PA concentrations of 0.4 – 4 g L^{-1} show no effect with regard to OTR, DCW and glucose concentration. All corresponding OTR curves reach a maximum of approx. 50 mmol L^{-1} h^{-1} after 20 h, the cultures have a DCW of 8 g L^{-1} and no glucose is left in the media. PA concentrations of 10 – 20 g L^{-1} influence and decelerate the respiration activity and the growth of *H. polymorpha*, but do not inhibit it completely. The culture with a concentration of 10 g L^{-1} PA reaches its maximal OTR value between 22 – 24 h. The maximal value of the OTR corresponding to a concentration of 20 g L^{-1} PA is not reached after 24 h. At that time, approximately 10 g L^{-1} glucose is left in the culture medium. For a PA concentration of 40 g L^{-1}, no growth can be detected, neither in the OTR nor in the DCW, nor in the glucose consumption, which remains at a constant level of 20 g L^{-1}.

Figure 3-1 demonstrates that a PA concentration of 10 g L^{-1} and above during heat sterilization influence the respiration activity of the yeast *H. polymorpha* considerably and can even inhibit its growth completely. PA concentrations of 4 g L^{-1} and below show no effect with regard to OTR, DCW and glucose concentration. Hence, a PA concentration between 4 – 10 g L^{-1} represents a threshold concentration for the inhibition of the respiration activity including the growth of this yeast. An effect of PA concentrations barely above this threshold can clearly be monitored using the RAMOS device, though they are hardly detectable offline e.g. by DCW and glucose depletion measurements (Figure 3-1, 10 g L^{-1} PA). Thus, applying

the RAMOS device generates threshold data for particular applications, in contrast to tests cited in the literature (Jenke, 2007a).

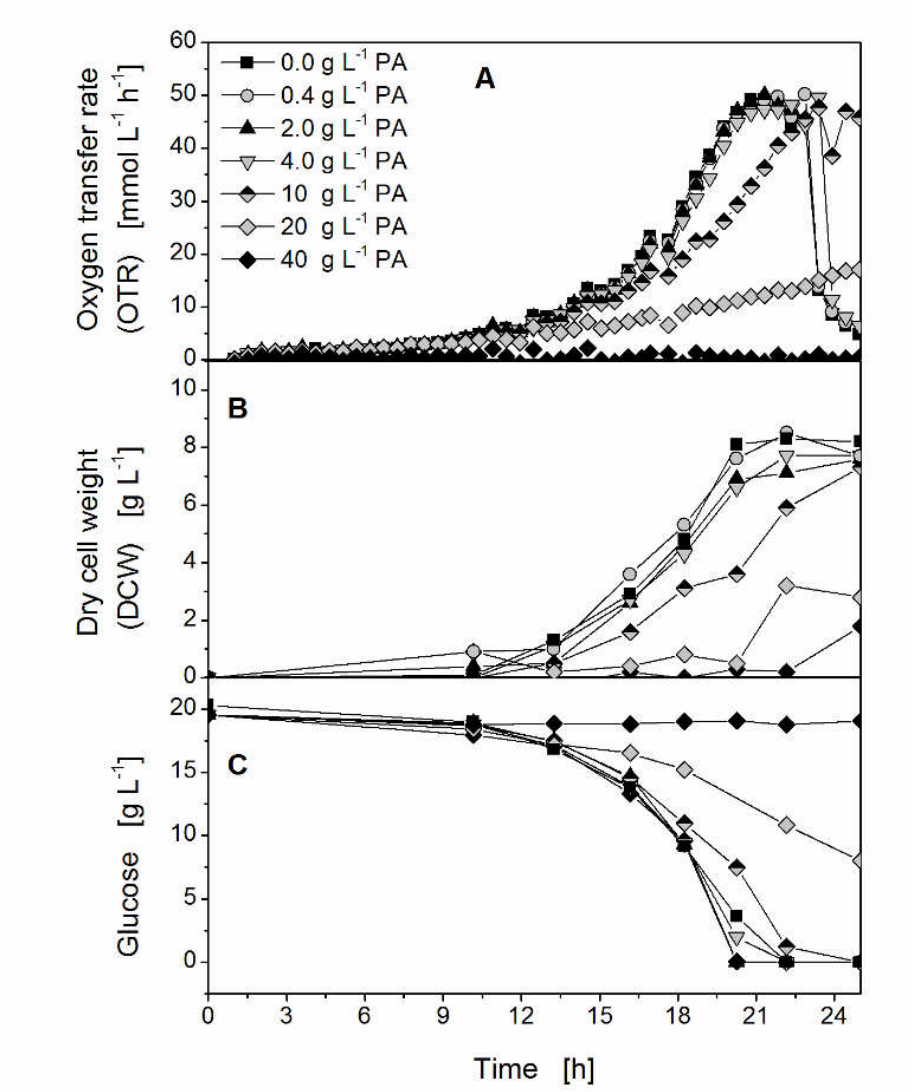

Figure 3-1: Effect of different concentrations of Polyamide 12 (*PA*) tubing (d_i = 4 mm, d_o = 6 mm, black) in the culture medium on the growth behavior and respiration activity of *H. polymorpha* pCoM11sc3625. Culture conditions: Synthetic Syn-6-MES medium, pH value of 6.0, T = 37 °C. The PA in the culture medium was heat sterilized (121 °C, 21 min) and removed before inoculation. The optical density of the culture after inoculation was 0.1. A) Oxygen transfer rate (OTR). B) Dry cell weight (DCW). C) Glucose concentration.

3.1.2 Effect of the Volume of Inoculum

As it was proven before, the volume of inoculum influences the microbial growth behavior (Huber et al., 2010). Therefore, the impact of the volume of inoculum was investigated in a culture medium, which has been heat sterilized together with 20 g L^{-1} PA (Figure 3-2). In contrast to the first experiment, this culture was monitored for 72 h. With media, having an initial optical density of 0.1 after inoculation, a maximal OTR of 22 mmol L^{-1} h^{-1} is reached after 48 h. In comparison to media with an initial optical density of 0.1, those media with higher initial optical densities have shorter culture times and considerably higher OTRs. The medium with an initial optical density of 2.1 reaches a maximal OTR of 40 mmol L^{-1} h^{-1} after 11 h of culture. Another additional peak is visible after the first peak in all cultures. These peaks indicate the consumption of overflow metabolites, formed in the first phase of the culture. This is a typical phenomenon found in *Hansenula polymorpha* cultures (Stöckmann et al., 2003). A similar OTR curve would have been detected in the corresponding culture in Figure 3-, if the culture time would have been longer.

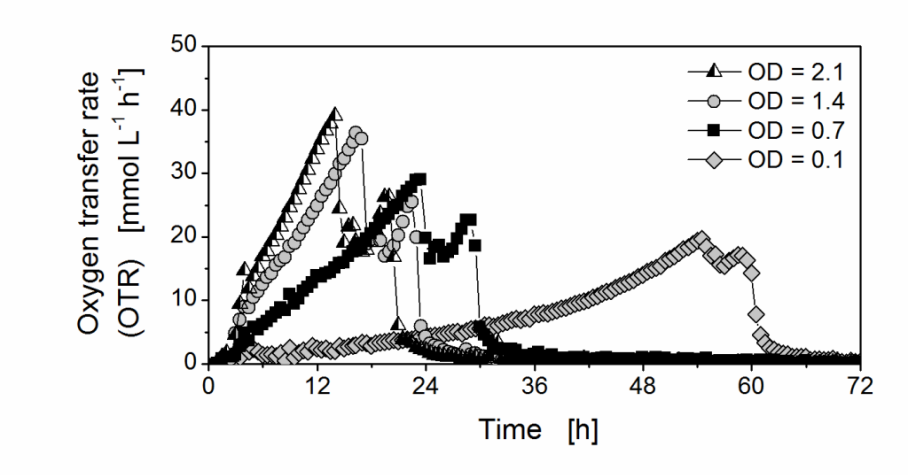

Figure 3-2: Effect of different volumes of inoculum on the respiration activity of *H. polymorpha* pCoM11sc3625 in synthetic Syn-6-MES medium, pH value of 6.0, T = 37 °C and 20 g polyamide per L medium. The Polyamide 12 tubing (d_i = 4 mm, d_o = 6 mm, black) was heat sterilized once in culture medium (121 °C, 21 min) and removed before inoculation.

In this experiment the inhibiting effect of PA could be reduced, even if the PA concentration is far above the threshold. If the volume of inoculum is increased, initial growth rates increases considerably, so the method is less sensitive (Figure 3-2). Consequently, a low initial optical density can result in an inhibition or even termination of metabolic activities, although no influence of polymer additives was observed at higher initial optical densities with offline data.

3.1.3 Effect of Several Heat Sterilization Cycles

To study, whether leaching of polymer additives occurs only during the first heat sterilization cycle, or appears multiple times, 40 g of the same tubing was heat sterilized in 1 L culture medium for one to five cycles at 121 °C for 20 min. For every sterilization cycle, fresh medium was used. Then, respiration activity curves were recorded for each of those culture media as well as for a reference medium without any PA. Figure 3-3 depicts the results. Whereas no respiration activity can be detected for one and two heat sterilization cycles, a slight increase in the oxygen transfer rate was measured for the culture medium with the PA heat sterilized for the 3rd cycle. The respiration activity curves of each subsequent sterilization cycle increasingly resemble the microbial respiration activity of the reference culture. Culture medium with the PA heat sterilized for the 4th and 5th cycle have a maximal OTR of 26 mmol L^{-1} h^{-1} reached after 36 h and 37 mmol L^{-1} h^{-1} reached after 28 h, respectively. In these two OTR curves two further peaks are visible after the first one, indicating the conversion of overflow metabolites.

A GC-MS analysis of the culture media extracted with ethyl acetate revealed the presence of N-Butylbenzenesulfonamide (NBBS) in the sample. NBBS is a widely used plasticizer in polyacetals, polycarbonates, polysulfones, Nylon 11 and Nylon 12 and in flexible tubing (Rider et al., 2012; Skjevrak et al., 2005). NBBS is known to be toxic to human at concentrations above $3.7 \cdot 10^6$ g L^{-1} if inhaled (National Toxicology Program, 2010). It belongs to the group of sulfonamides. Some members of this group serve as antibiotics, based on their nature as competitive inhibitors of the enzyme dihydropteroate synthetase (DHPS), which is active in folic acid synthesis (Fiege et al., 2000). Thus, the observed effect of decreasing inhibition at increasing initial biomass concentration may be explained by a decreasing ratio of NBBS to biomass or rather enzyme concentration (DHPS) (Figure 3-2).

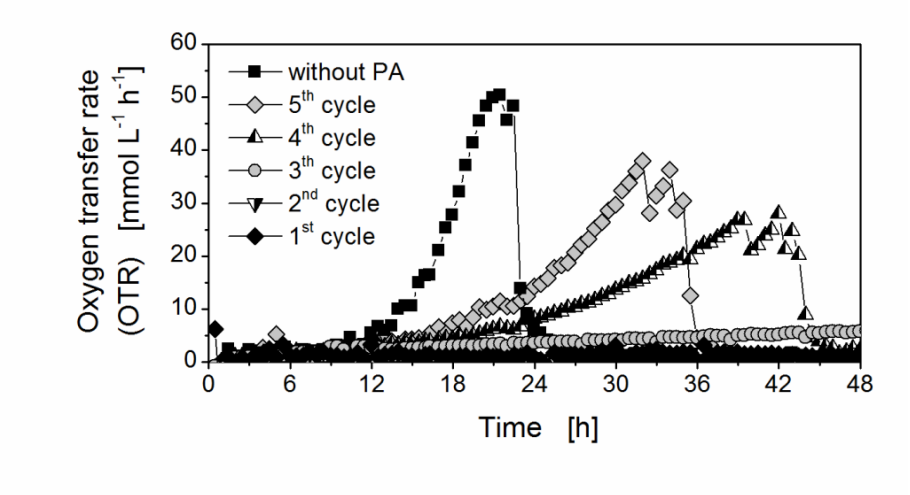

Figure 3-3: Impact of repeated heat sterilization cycles of Polyamide 12 tubing (d_i = 4 mm, d_o = 6 mm, black) in culture medium on the respiration activity of *H. polymorpha* pCoM11sc3625. For multiple numbers of sterilizations, culture medium was refreshed after every sterilization cycle (121 °C, 21 min). Culture conditions: Synthetic Syn-6-MES medium, pH value of 6.0, T = 37 °C and 40 g polyamide per L medium. The optical density after inoculation was 0.1.

The concentrations of NBBS were determined in the culture media after the aforementioned PA sterilization cycles. As shown in Figure 3-4, approx. 0.8 g L^{-1} is present in the medium containing 40 g L^{-1} PA that was heat sterilized for the first cycle. The concentration of NBBS declines in a non–linear fashion to approx. 0.52 g L^{-1} after the 5th sterilization cycle.

To validate the GC-MS data, the determined concentrations of liquid NBBS were added to the culture medium, and, thus, respiration activity curves were measured. Figure 3-5 shows the respiration activity curves corresponding to the 1st, 4th and 5th sterilization cycle with a NBBS concentration of 0.8 g L^{-1}, 0.55 g L^{-1} and 0.52 g L^{-1}, respectively, as well as a reference respiration activity curve for the medium without any additional NBBS. Whereas no respiration activity is detectable in the medium with 0.8 g L^{-1} additional NBBS, those media having 0.52 g L^{-1} and 0.55 g L^{-1} NBBS show a longer lag-phase and a lower respiration

activity. They reach a maximal OTR of 41 mmol L^{-1} h^{-1} after 28 h and 25 mmol L^{-1} h^{-1} after approx. 44 h, respectively.

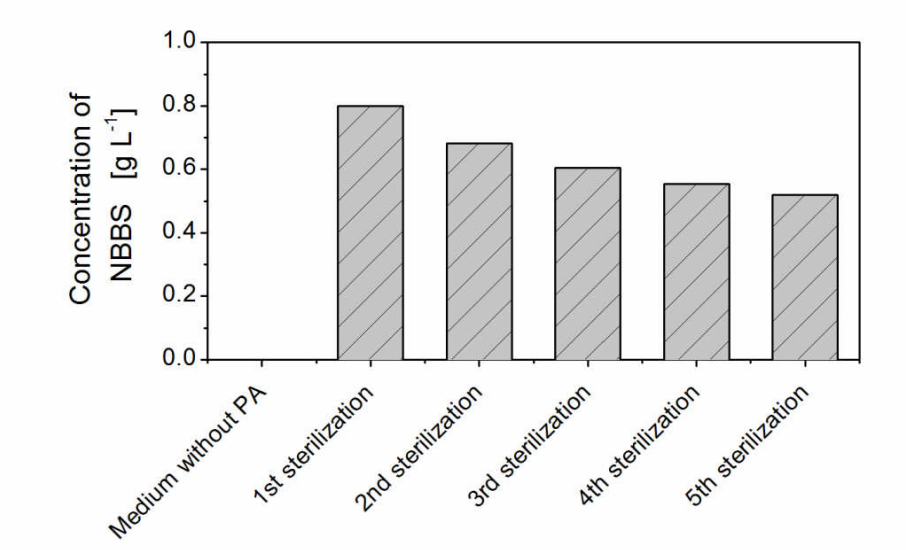

Figure 3-4: Concentrations of N-Butylbenzenesulfonamide (NBBS) determined in the culture medium after repeated cycles of heat sterilization with 40 g per L Polyamide 12 tubing (d_i = 4 mm, d_o = 6 mm, black). New Syn 6 culture medium was used after every sterilization cycle (121 °C, 21 min).

A comparison of Figure 3-3 and Figure 3-5 shows a good agreement of the culture with NBBS added as pure compound and the culture with different PA concentrations. This proofs NBBS to be the direct cause of altered respiration activity of the microbial cultures. It appears to be processed in PA in large amounts, as even five sterilization cycles of PA are not sufficient to lower the leaching concentrations below the threshold (Figure 3-3). NBBS was also found to leach out from PA cooking utensils (Skjevrak et al., 2005). This fact is giving cause for concern, considering the effect of this plasticizer on microbial activity.

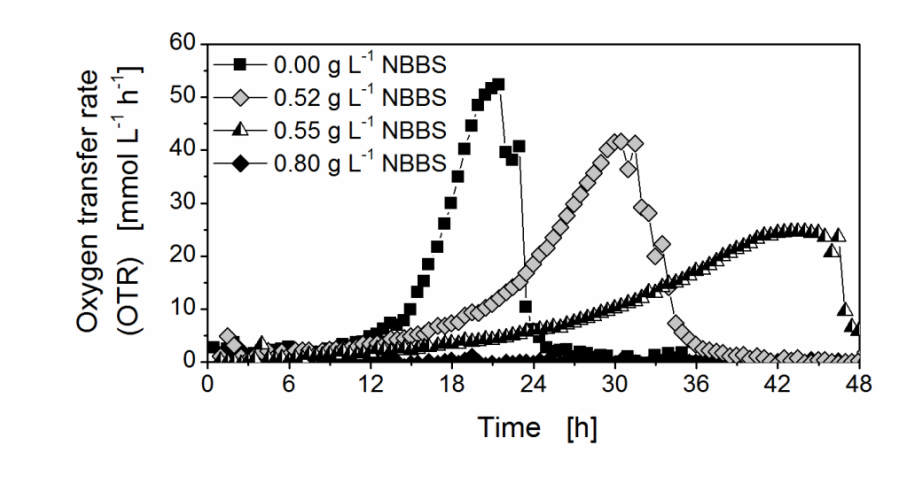

Figure 3-5: Effect of different concentrations of N-Butylbenzenesulfonamide on the respiration activity of *H. polymorpha* pCoM11sc3625. Culture conditions: Synthetic Syn-6-MES medium, buffered at pH value of 6.0, T = 37 °C. The optical density after inoculation was 0.1.

The deviation in Figure 3-3 and Figure 3-5 regarding the maximal OTR value is ± 4 mmol L^{-1} h^{-1}, which is reached after ± 8 h. Hence, within the range of 4 – 20 g L^{-1} PA, changes in the NBBS-concentration can be accurately and reproducibly revealed by using the RAMOS device. In this range even small changes of 0.03 g L^{-1} NBBS have a clear and non-linear impact on the culture (Figure 3-5, 0.52 and 0.55 g L^{-1} NBBS). Consequently, a determination of the concentration of a compound leaching out from a polymer by chemical analysis is insufficient without investigations of its effect on microbial growth and metabolic activity.

3.1.4 Effect of Polyamide 12 Tubing on Bacteria and Fungi

To demonstrate that PA affects microorganisms in general, the same concentrations of PA as in chapter 3.1.1 were studied on the bacterium *E. coli* as well as the fungus *U. maydis*. All respiration activity curves measured via the RAMOS device are illustrated in Figure 3-6. In

both cultures the organisms do not respire when they are subjected to PA in a concentration of 40 g L^{-1} PA. Moreover, PA concentrations of 10 g L^{-1} and 20 g L^{-1} lead to a delayed respiration activity of *E. coli* as well as to a delayed or even terminated respiration activity of *U. maydis*.

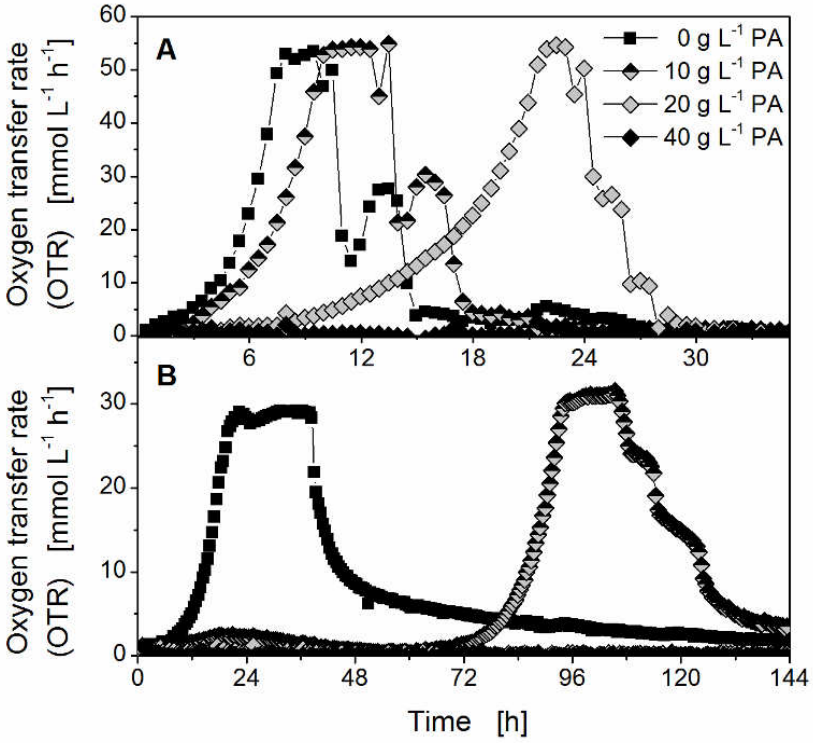

Figure 3-6: Effect of different concentrations of Polyamide 12 tubing (d_i = 4 mm, d_o = 6 mm, black) in the culture medium on the respiration activity of *Escherichia coli* BL21 (DE3) piRhotHi-2-EcFbFP and *Ustilago maydis* MB215. A) *E. coli*. Culture conditions: Synthetic Wilms-Mops medium, 12.5 mL filling volume, pH value of 7.5, T = 37 °C. The optical density after inoculation was 0.1. B) *U. maydis.* Culture conditions: Synthetic Verduyn medium, 20 mL filling volume, pH value of 6.0, T = 30 °C. The optical density after inoculation was 0.1.

Although PA affects *E. coli* and *U. maydis* differently (Figure 3-6), leaching of NBBS clearly influences also those microorganisms. Thus, materials intended for heat sterilized single-use culture systems and other biological applications should be tested for biocompatibility with the respective microorganism. A predication about the effect of polymer additives on microorganism based on the investigation of other microorganism is hardly possible (Cairns, 1986).

3.1.5 Effect of Various Polymers on Yeast

As PA appears to be ill suited for applications in heat sterilized culture vessels, the following polymers were investigated regarding their biocompatibility as well: Polyether ether ketone bloc (PEEK), polytetrafluoroethylene tubing (Teflon), polypropylene pipette tips (PP), Polyurethane tubing (PUR), Polyamide 6.6 cable tie (Nylon) and polyethersulfone membrane (PES). Figure 3-7 illustrates the microbial respiration activity curves with these polymers and PA as well as one reference curve of a culture without a polymer. PUR, PP, Teflon, PEEK and PES do not show an influence on the respiration activity curves, whereas Nylon extends the respiration activity lag-phase as observed for PA, though the effect on the metabolic activity for Nylon is smaller than for PA.

GC-MS measurements of the sample containing Nylon revealed the UV stabilizer and antioxidant 2,6-Di-tert-butylphenol (2,6-DTBP) as well as the monomer 1,8-Diazacyclotetradecane-2,7-dione (*1,8-DACTD-2,7-D*). Whereas 2,6-DTBP has a low toxicity (Fiege et al., 2000), 1,8-DACTD-2,7-D is known to inhibit yeasts (NCI Yeast Anticancer Drug Screen) and thus, may cause the inhibiting effect of Nylon *H. polymorpha*.

This chapter demonstrates the need to test polymers regarding their biocompatibility prior to application in bioreactors. Predication of leaching behavior and its influence on microorganisms is hardly possible. Thus, the here established biocompatibility test is used for all polymers applied in this study.

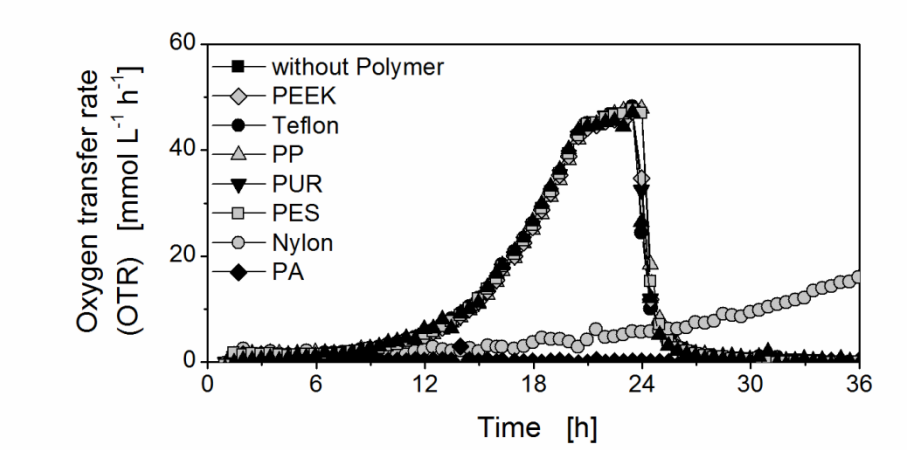

Figure 3-7: Effect of different polymers heat sterilized in the culture medium on the respiration activity of *Hansenula polymorpha* pCoM11sc3625. The polymers were removed after sterilization. The amount of polymer was 0.5 g per flask (40 g L^{-1} culture medium) each. Culture conditions: Synthetic Syn-6-MES medium, buffered at pH value of 6.0, T = 37 °C. The optical density after inoculation was 0.1.

3.2 Establishment of a Protein Quantification Assay

An assay to determine the concentration of the single-chain antibody secreted by *H. polymorpha* was not established before the beginning of this work. Thus, two assays were analyzed regarding their suitability within this chapter: Bicinchoninic Acid (BCA) Protein Assay, a standard method to determine protein concentration and Fast Protein Liquid Chromatography (FPLC), originally a device for purification of proteins.

3.2.1 Bicinchoninic Acid (BCA) Protein Assay

BCA Protein Assay was investigated regarding its ability to determine the single-chain antibody concentration in a sample of supernatant of *H. polymorpha* broth. The calibration with protein standards of BSA reveals good results with a coefficient of determination of 0.976 (Figure 3-8, open diamonds). For validation one sample of *H. polymorpha* was diluted in various ratios and its absorption measured (closed triangles). Concentrations determined by correction of the measured values by the dilution factor (closed circles) should yield the same concentration as the same sample was analyzed. Thus, the closed circles should be on a vertical line, if the BCA Protein Assay is reliable. However, the determined concentrations of the same sample differ widely. The culture medium is composed of EDTA among other. EDTA is known to interfere with the BCA Protein Assay (Lottspeich and Zorbas, 1998) and, thus, may cause this deviation. As a conclusion, the BCA Protein Assay is considered as not suitable for analysis of the samples obtained in this study.

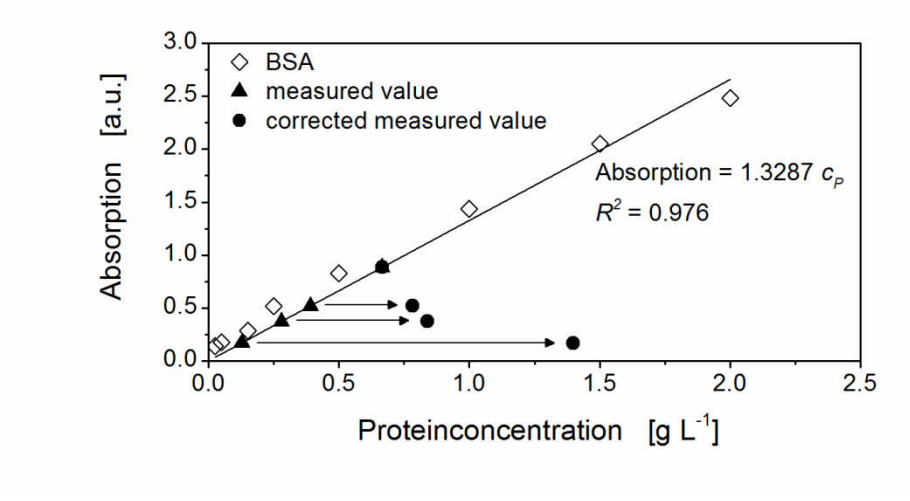

Figure 3-8: Calibration of BCA Protein Assay with BSA standards and sample analysis. Linear trend line is determined by double measurement of BSA standard (open diamonds) with intersection at (0/0). The same sample was measured with different dilutions (closed triangles) and corrected by the dilution factor (closed circles).

3.2.2 Fast Protein Liquid Chromatography (FPLC)

Fast protein liquid chromatography is a size exclusion method known for purification (Jager et al., 2011). Bigger molecules such as proteins result in a UV peak at the beginning of the purification procedure whereas small molecules elute latter. Thus, if the sample contains solely the target protein and smaller molecules such as salts, a distinct peak is visible for the protein. Hence, FPLC may be used to determine the peak area of the target protein, the single-chain antibody.

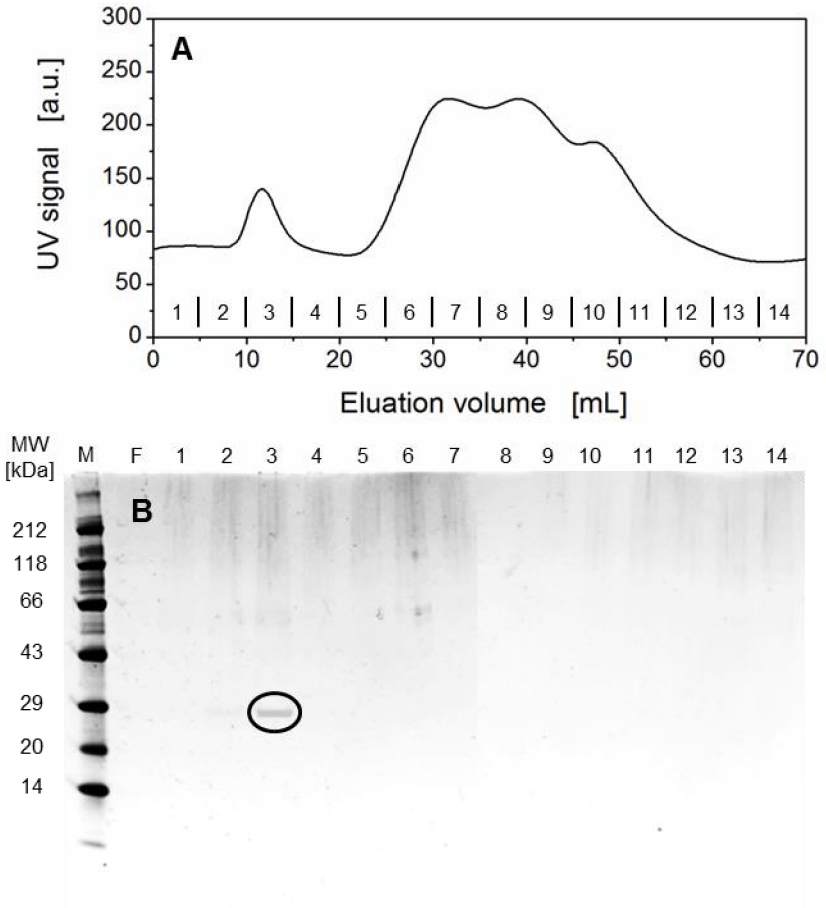

Figure 3-9: Determination of antibody concentration in supernatant of *H. polymorpha* pCoM11sc3625 broth using FPLC. Conditions: Synthetic Syn6 medium, 20 g L^{-1} Glycerol. A) UV signal. B) SDS Page of 15 µL sample volume (fractions obtained by FPLC), 8 µL Marker, M: marker, F: free, 1 – 14: number of fractions.

The UV signal of one exemplary *H. polymorpha* sample measured by FPLC and the obtained fractions are depicted in Figure 3-9 A. The fractions are marked with vertical lines and numbers from 1 – 14. A distinct peak is visible at an eluation volume of approximately 12 mL (mainly fraction 3) and various overlapping peaks are detected in the range from 25 – 60 mL eluation volume (fraction 6 – 12). All fractions obtained by FPLC of the exemplary sample were investigated by a western blot to verify the protein being in fraction 3 and salts causing the peaks at higher eluation volumes. The corresponding western blot of the fractions (Figure 3-9 B) show a clear band in fraction 3 in the expected size range for the single-chain antibody. No bands were visible in other samples. Thus, the first distinct peak in the UV signal can be used for the calculation of the protein concentration.

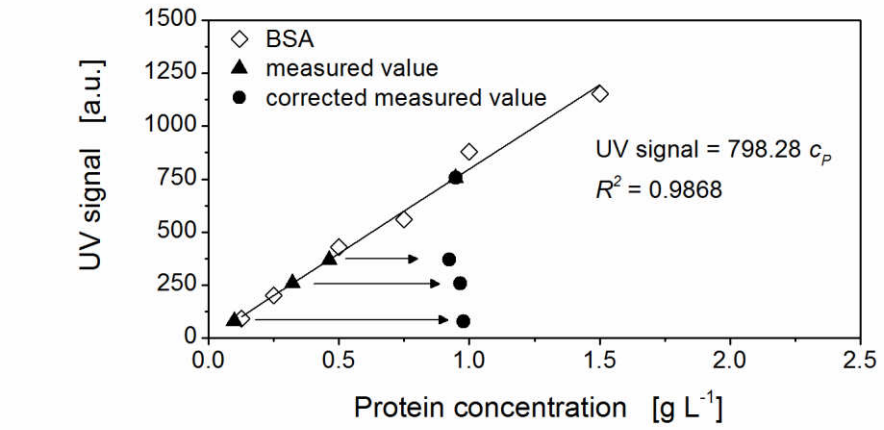

Figure 3-10: Calibration of FPLC Assay with BSA standards and sample analysis. Linear trend line and standard deviation was calculated out of five samples of BSA standard (open diamonds) with intersection at (0/0). The same sample was measured with different dilutions (closed triangles) and corrected by the dilution factor (closed circles).

To verify reproducibility of the FPLC measurement a standard calibration was conducted with five samples each of six concentrations of BSA. For validation the same sample of *H. polymorpha* supernatant was measured diluted in various ratios. The result is depicted in Figure 3-10. The calibration via BSA (Figure 3-10, open diamonds) reveals a linear trend with

a coefficient of determination of 0.9871. The standard deviation of the five BSA samples is less than 5% for all samples. The corrected *H. polymorpha* samples are almost on a vertical line (Figure 3-10, closed circles), indicating that the sample is measured reproducibly independent of the dilution. Hence, the FPLC assay proved to be suitable for determination of the single-chain antibody used in this study and will be applied in this study.

3.3 Determination of Yeast Cell Viability

The viability of cells is of interest in every biotechnological process as in some cases higher product concentrations are yield under stress conditions, whereas other processes demand a high viability of cells. *H. polymorpha* secrets single-chain antibody to a greater extend if the viability of the culture is high. Thus, viability should be investigated for the special conditions of reverse-flow diafiltration in comparison to a conventional continuous culture without cell retention. Therefore, three different viability assays were investigated and compared with regard to their application for *H. polymorpha*.

3.3.1 Hemocytometer

Examination of vivid as well as heat treated *H. polymorpha* cells in a Neubauer improved chamber were conducted with a 40-fold magnification (Figure 3-11). All samples were stained with methylene blue. Cells were hard to detect at this magnification and no significant difference between vivid (Figure 3-11 A) and heat treated (Figure 3-11 B) cells could be determined. A clear image could not be obtained at 100-fold magnification. Thus, the hemocytometer method was considered as not suitable for the determination of viability of *H. polymorpha.*

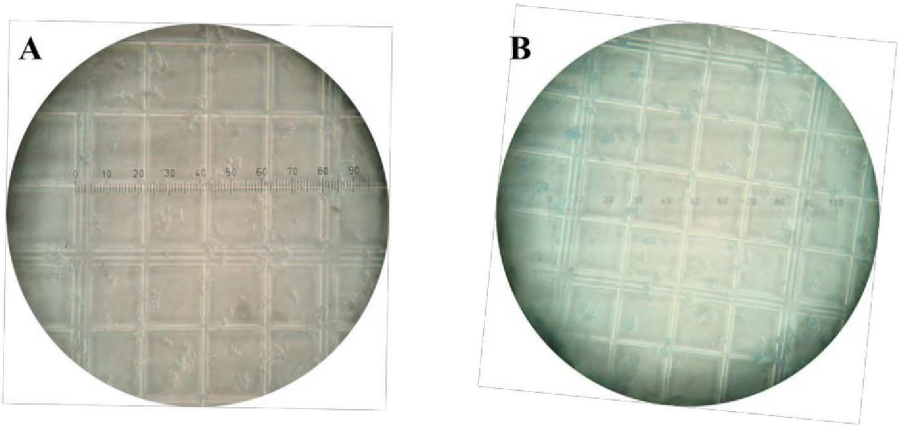

Figure 3-11: Determination of dead cells in a Neubauer improved chamber. Samples of *Hansenula polymorpha* pCoM11sc3625 were stained with methylene blue in a dilution of 1:20 and microscopically analyzed at a 40-fold magnification. A) Vivid cells. B) Heat treated cells (95 °C for 15 min).

3.3.2 Methylene Blue Assay

In the Methylene Blue Assay the concentration of dead cells in a sample was analyzed by measuring indirectly the amount of dye diffused into dead cells. Prior, a correlation of the spectrometric measured OD_{440} and the methylene blue concentration has to be determined. The two values correlate linear with a coefficient of determination of 0.985 as shown in Figure 3-12.

After calibration the specific parameters k and n (Equation 2.2) have to be determined experimentally by measuring the methylene blue concentration for various concentrations of treated *H. polymorpha* cells. Heat treated cells as well as cells treated with isopropanol and starved cells (compare Table 2-2) were examined. Figure 3-13 depicts the measured data for all three treatment methods (dots) as well as the resulting fitted data (continuous line). Depending on the threatening method the resulting values for k and n vary from 0.05 – 0.09 and 0.558 – 1.499, respectively. This range of values leads to a deviations of the dead cell concentration higher than the initial concentration. Thus, the parameters k and n cannot be determined with an accurateness necessary for resilient results with *H. polymorpha*. Thus, the methylene Blue Assay was not used in this study for the determination of the viability of *H. polymorpha*.

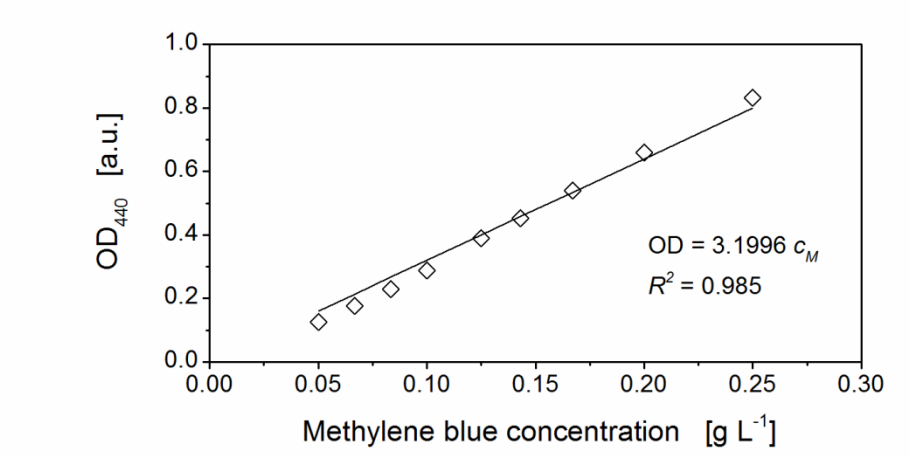

Figure 3-12: Correlation of methylene blue concentration and spectrometric measured OD_{440}. A linear trend line is determined with an intersection at (0/0) and used for further calculations.

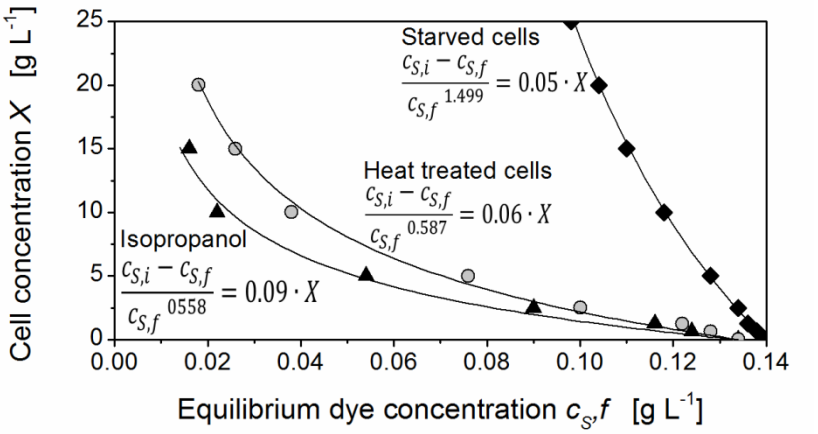

Figure 3-13: Determination of parameters *k* and *n* for different treatment methods of *Hansenula polymorpha* pCoM11sc3625 broth. Treatment with 40% of Isopropanol for 15 min (black triangles), 95 °C applied for 15 min (grey circles) or starved cells (72 h without respiration activity, black diamonds). Data points represent measured values; continuous lines represent the modelled values. Initial dye concentration $c_{S,i} = 0.014$ g L^{-1}.

3.3.3 Flow Cytometry

Determination of dead yeast cell concentrations was conducted with the *LIVE/DEAD*® Funga*Light*™ Yeast Viability Kit applied in a flow cytometer. Every sample is split in two portions; one is stained with SYTO® 9 (green), the other with SYTO® 9 mixed with Propidiumiodid (red). Whereas SYTO® 9 diffuses in all cells, Propidiumiodid only diffuses through ruptured cell membranes causing a shift in the fluorescence spectrum. Thus, an overlay of the obtained dot plots of both portions reveals the percentage of dead cells. Dot plots of vivid and starved cells as well as heat and Isopropanol treated cells are depicted in Figure 3-14. Whereas both portions (green and red) of the vivid cells overlay directly, a shift can be observed for the treated cell samples. Hence, a clear discrimination between dead and vivid cells is possible for a sample of solely dead cells independent of the treatment method. This was also reported in literature before (Attfield et al., 2000; Deere et al., 1998; Garcia et al., 2006; Mernier et al., 2011).

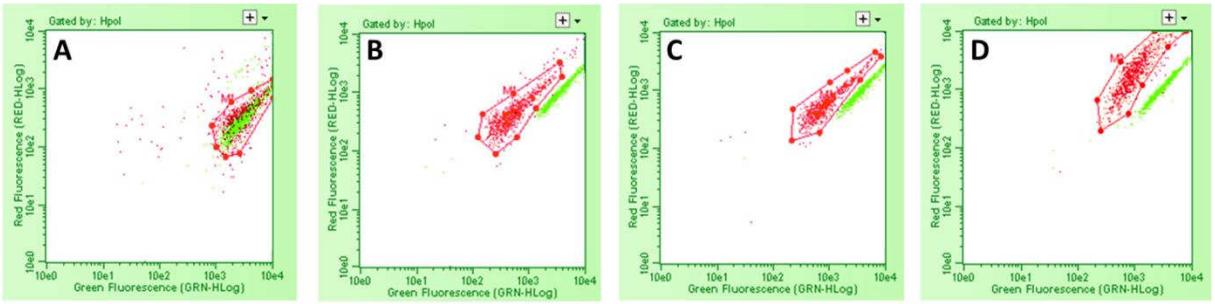

Figure 3-14: Determination of viability of *Hansenula polymorpha* pCoM11sc3625 samples analyzed by flow cytometry. Cells stained with SYTO® 9 (green) are overlaid by cells stained with SYTO® 9 and Propidiumiodid (red). The latter are gated. A) Vivid cells. B) Treatment with 40% of Isopropanol for 15 min. C) Treatment with 95 °C for 15 min. D) Starved cells (72 h without respiration activity).

As fermentation samples are not homogenous dead or vivid, different preset concentrations of dead cell were analyzed. The obtained data is shown in Figure 3-15. Except for 0 and 100% dead cells, the measured value is slightly higher than the preset one. The overestimation of

dead cells could be a result of vivid cells being at the beginning of cell death. Propidiumiodid can diffuse into the ruptured but not yet dead cell causing a shift in the dot plot. The coefficient of determination was calculated as 0.9766. Thus, the *LIVE/DEAD*® Funga*Light*™ Yeast Viability Kit applied in a flow cytometer proved to be accurate enough for this study and is used for viability measurements of *H. polymorpha* in subsequent experiments.

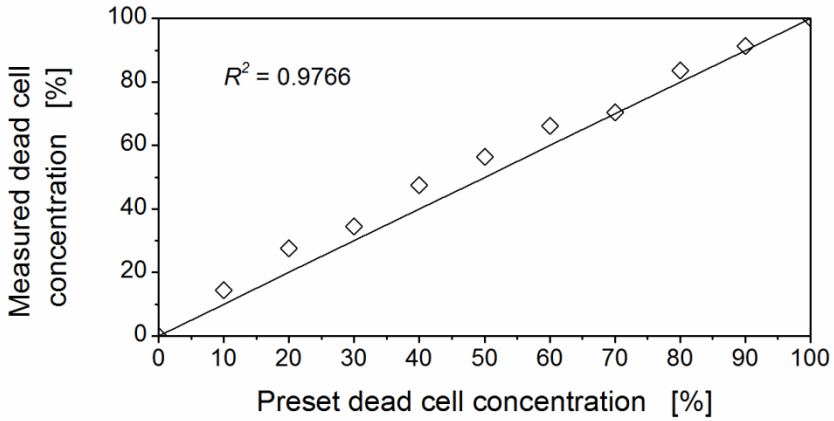

Figure 3-15: Validation of preset dead cell concentrations of *Hansenula polymorpha* pCoM11sc3625 samples analyzed by flow cytometry. Cells were heat treated at 95 °C for 15 min and mixed in set portions with untreated cells. Measured data points (open diamonds) are compared to theoretical values (continuous line).

Chapter 4

Configuration and Evaluation of Process Parameters of Reverse-flow Diafiltration

RFD was designed to achieve maximal space-time-yield, prevent substrate loss and enable stable long-term operation. Both, mathematical calculations and experimental data, as well as process requirements are the design basis for the configuration discussed in this chapter. Whereas the initial configuration was conducted based on data of *Hansenula polymorpha*, data of CHO cultures were used for adjustment if mammalian cell lines are the target cells. An evaluation of the resulting configuration is conducted by comparison of the performance of RFD to conventional membrane-based cell retention systems. This chapter is partly published in Meier et. al (2014) and partly submitted to Biotechnology Progress (Meier et al., June 2014). Experiments regarding transmembrane pressure increase were conducted by Frederike Carstensen (AVT.CVT) and Suzana Djeljadini in the context of her master thesis (2014).

4.1 Permeate Step

During the permeate step (Figure 2-4 A), supernatant is withdrawn from the reactor through a membrane. To determine the maximum flux without formation of an irreversible fouling layer, flux step experiments were performed. Therefore, the irreversible TMP increase was measured for different fluxes (Figure 4-1).

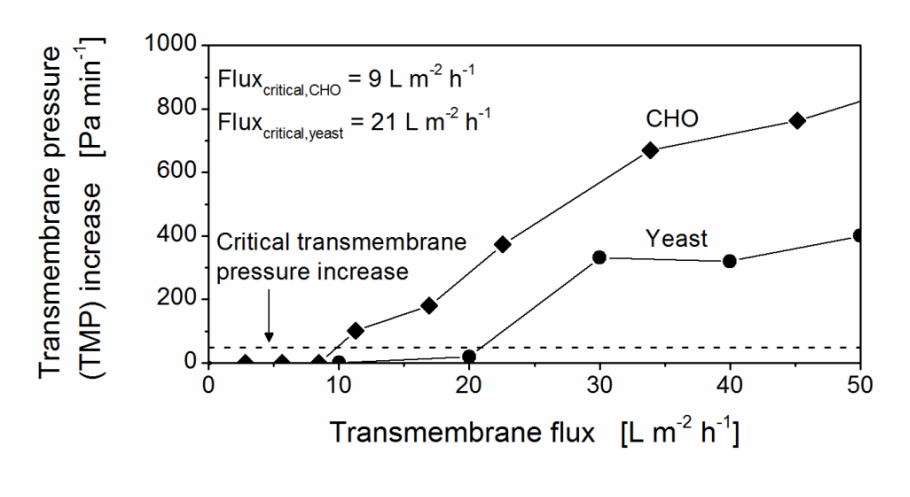

Figure 4-1: Flux step experiments for a microfiltration hollow–fiber membrane with a nominal pore size of 0.2 µm with culture broth of *Hansenula polymorpha* pCoM11sc3625 and CHO DG44. Conditions *H. polymorpha*: Flux time = 300 s, relaxation time = 300 s, no backflushing. Conditions CHO DG44: Flux time = 340 s, relaxation time = 20 s, backflushing time = 120 s.

The critical TMP increase is defined as 45 Pa min^{-1} based on earlier experiments, and should not be exceeded in order to maintain stable conditions. According to Figure 4-1, a transmembrane flux of 21 L m^{-2} h^{-1} was determined to be the maximum flux if yeasts were

examined. The maximum flux is valid under the investigated conditions for this membrane: 300 s filtration without backflushing, 300 s relaxation. The same filtration time of 300 s was set for the permeate step time (t_P) of RFD (see also Table 4-1) to achieve comparable conditions to the flux step experiment. However, in RFD mode, fluxes twice as high as the maximum flux of the flux step experiments led to TMP increases below the critical value (data obtained by Frederike Carstensen, AVT.CVT, RWTH Aachen University). This is due to the worst-case conditions used in the flux step experiments. Therefore, the maximum flux over the membrane for RFD mode is approximately 40 L m^{-2} h^{-1}. Further calculations regarding necessary membrane area were based on the maximum flux of 40 L m^{-2} h^{-1}.

The critical transmembrane flux for CHO cells using the same membrane is 9 L m^{-2} h^{-1} under the following conditions (Figure 4-1): 340 s filtration, 120 s backflushing and 20 s relaxation (Djeljadini, 2014). In contrast to yeast cells, conditions of RFD were applied for the determination of the critical transmembrane flux of CHO cells as RFD settings were know at that time point. Thus, a flux 9 L m^{-2} h^{-1} was expected to be the maximum applicable flux and used for the calculation of the necessary membrane area for the cultivation of CHO cells.

As stated above the permeate step time (t_P) of RFD was set to 300 s to achieve comparable TMP results to the flux step expierment. The setting of the permeate flux was calculated based on the dilution rate (D) and the filtered portion of the reactor outlet (1- NF). It was considered that the filtration time (t_P) is only a part of the cycle time (t_C) and thus, the flux has to be corrected by a time factor $\frac{t_C}{t_P}$. The permeate volume gained during flushing (V_F) (compare also Figure 2-4 B) was also accounted in the calculation of the permeate flux. The resulting formula is given in Table 4-1.

4.2 Flushing Step

During the flushing step (compare also Figure 2-4 B), permeate in the membrane is replace with medium so that only a minimal amount of permeate is pumped into the reactor during the subsequent feed step. However, the medium should not reach the permeate tubing behind the membrane in order to keep the permeate free from medium and to prevent a loss of substrate.

The time necessary for the tip feed flow to arrive at the end of the membrane (Figure 2-4 B) is defined as the flushing time (t_F). It is given by the membrane length (L) and the maximum velocity of the feed flow (v_{max}) during the flushing step. The maximal velocity of a laminar flow in a tube is twice the average velocity ($\bar{v}$) according to the law of Hagen-Poiseuille (Beitz et al., 1994):

$$t_F = \frac{L}{v_{max}} = \frac{L}{2\,\bar{v}} \tag{4.1}$$

The average velocity of fluid during the flushing step is defined as the flow generated by the pumps ($\rightarrow F_{F,F} \cdot A_M = F_{P,F} \cdot A_M$) divided by the cross section area of the membrane (A_Q):

$$\bar{v} = \frac{F_{F,F} \cdot A_M}{A_Q} \tag{4.2}$$

The flushing volume (V_F) is defined as the flushing time (t_F) multiplied by the flow ($F_{F,F} \cdot A_M$):

$$V_F = t_F \cdot F_{F,F} \cdot A_M \tag{4.3}$$

Equations (4.1) and (4.2) into (4.3) results in:

$$V_F = \frac{L \cdot F_{F,F} \cdot A_M}{2\,\bar{v}} = \frac{L \cdot F_{F,F} \cdot A_M \cdot A_Q}{2 F_{F,F} \cdot A_M} = \frac{1}{2} L \cdot A_Q \tag{4.4}$$

The volume of the membrane (V_M) is the the membrane length (L) multiplied by the cross section area of the membrane (A_Q):

$$V_M = L \cdot A_Q \tag{4.5}$$

The ratio (a_F) of the flushing volume (V_F) to the membrane volume (V_M) is therefore:

$$\mathrm{a_F} = \frac{\mathrm{V_F}}{\mathrm{V_M}} = \frac{1}{2}\frac{\mathrm{L \cdot A_Q}}{\mathrm{A_Q \cdot L}} = 0.5 \tag{4.6}$$

Hence, the flushing ratio is independent of membrane length and diameter.

The calculated value of a_F = 0.5 applies to an ideal tube, it has to be validated for membranes, where pores were partially flushed. Experiments with dye were conducted to measure the flushing time needed for the dye to pass the membrane. The experimental value for a_F was determined to be 0.7 as shown in Figure 4-2. This value was chosen for the RFD in subsequent biological experiments.

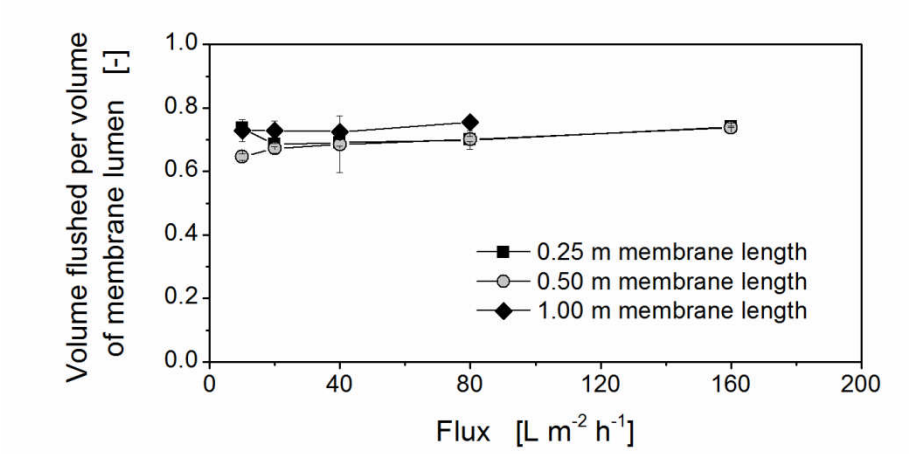

Figure 4-2: Volume flushed per volume of the membrane lumen for different membrane length und fluxes. Methylene blue was flushed at different velocities; the time needed for the first drop of dye to pass the membrane was measured. The volume flushed was calculated based on the flux and the time, the membrane lumen was calculated on the membrane properties: PES hollow fiber membrane with a porosity of 40%, d_i = 1.5 mm, d_o = 2.35 mm.

In the flushing step the tip of the medium flow should just reach the permeate tube. Thus, the permate and feed pump generate a laminar flow, where a_F = 0.7 of the volume of the lumen (V_{Lu}) is flushed (Flushing volume V_F). The flushing time (t_F) was set to 20 s, which was half of the emptying time. The resulting equation to calculate the pump settings for the flushing step is given in Table 4-1.

4.3 Feed Step

The feeding step (Figure 2-4 C) provides the bioreactor with nutrients. Simultaneously, the reverse direction of the feed flux through the membrane relative to the permeate flux removes the reversible cake layer formed during the permeate step. A uniform removal over the whole length of the membrane can be assumed as pressure loss is negligible for the used membrane length. For efficient removal the feed flux should generate a pressure of at least 0.3 bar (Baker, 2004). For the lowest dilution rate this can be achieved with a flux twice as high as the permeate flux. Therefore, the step time for the feed step (t_{Feed}) was set to 150 s, which is half the time of the permeate step (t_P).

The feed flux is calculated based on the dilution rate (D) and the liquid volume (V_L) in the reactor. The flux is corrected by a time factor as the feed is only conducted for 150 s (t_{Feed}) of the whole cycle time (t_C). Furthermore, the permeate volume in the feed tubing due to the emptying (Figure 2-4 D) and flushing step (Figure 2-4 B) was also accounted for ($+V_E - V_F$). The resulting equation for the pump settings in the feed step is given in Table 4-1.

4.4 Emptying Step

During the emptying step (Figure 2-4 D), medium inside the membrane is replaced by permeate to prevent mixing with medium during the subsequent permeate step (Figure 2-4 A). For the emptying step it was assumed that: i) the flow inside the membrane is laminar, ii) the velocity profile ($v(z)$) is linear, and iii) the membrane pores were partially flushed (Bütehorn et al., 2011). Thus, the membrane diameter flushed (d) is larger than the membrane diameter without pores (d_i) and smaller than the membrane diameter with pores (d_o). If the feed ($\rightarrow F_{F,E} \cdot A_M$) and permeate pump ($\rightarrow F_{P,E} \cdot A_M$) are emptying the membrane (Figure 2-4 D), the emptying time (t_E) for a membrane with length (L) and the velocity profile results in:

$$dt_E = v(z) \cdot dz \qquad ,0 < z < L \tag{4.7}$$

$$v(z) = \frac{(F_{F,E} - F_{P,E})A_M}{1/4 \pi d^2 L} z + \frac{F_{P,E} \cdot A_M}{1/4 \pi d^2} \qquad , d_i < d < d_o \tag{4.8}$$

Insertion of equation (4.8) in (4.7) and integration leads to:

$$t_E = \left(log\left(\frac{(F_{F,E}-F_{P,E})A_M}{1/4\pi d^2} + \frac{F_{P,E}\cdot A_M}{1/4\pi d^2}\right) - log\left(\frac{F_{P,E}\cdot A_M}{1/4\pi d^2}\right)\right) \Big/ \left(\frac{(F_{F,E}-F_{P,E})A_M}{1/4\pi d^2}\right), d_i < d < d_o \quad (4.9)$$

The time necessary for the membrane to be completely emptied (t_E) was calculated using equation (4.9) with different ratios of feed flux ($F_{F,E}$) and permeate flux ($F_{P,E}$).

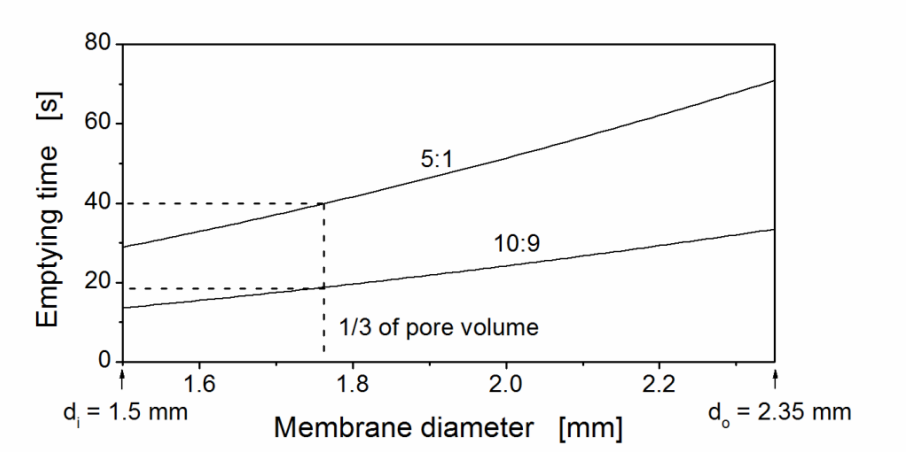

Figure 4-3: Calculation of time needed for membrane emptying step depending on which portion of the membrane pores are flushed. According to Bütehorn et al. (2011), this portion is approximately $\frac{1}{3}$ of all membrane pores. Membrane properties: d_i = 1.5 mm, d_o = 2.35 mm. Flux generated by feed pump = 50 L m^{-2} h^{-1} (reverse direction), flux generated by permeate pump = 10 L m^{-2} h^{-1} (Feed flux / permeate flux ratio of 5:1) or 45 L m^{-2} h^{-1} (Feed flux / permeate flux ratio of 10:9), respectively.

For example, the emptying time (t_E) for a feed flux (F_F) to permeate flux (F_P) ratio of 5:1 and 10:9 as a function of the diameter flushed is shown in Figure 4-3. The feed flux during emptying is fixed at 50 L m^{-2} h^{-1}, which is higher than the critical flux but leads to an emptying time as short as possible. As this flux is applied only for a short period the impact on the membrane is negligible. According to Bütehorn et al. (2011), approxitmatly $\frac{1}{3}$ of all

membrane pores are flushed. Thus, 40 s or 19 s are necessary to empty the membrane if a feed flux to permeate flux ratio of 5:1 or 10:9, respectively, is applied. As only $\frac{1}{3}$ of membrane pores are flushed, the remaining $\frac{2}{3}$ of pores have to be filled with permeate recovered from the fermenter. Hence, a driving force in the form of a pressure difference over the membrane is needed. If the feed and permeate fluxes are almost equal, hardly no driving force over the membrane exists. Smaller ratios result in greater pressure differences, but also in longer emptying times and a worse overall process performance. Therefore, a ratio of 5:1 and thereby an emptying time of 40 s was determined to be a good compromise between short emptying time and high driving force (Table 4-1).

The overall emptying volume (V_E) can be calculated with the chosen emptying time (t_E = 40 s) and the feed and permeate pump flow. The ratio between the emptying volume (V_E) and the membrane volume (V_M) is defined as a_E. For the selected feed flux to permeate flux ratio of 5:1, a_E equals 1.69. The resulting equation for the settings of the feed and permeate pump in the emptying step is given in Table 4-1.

4.5 Step Times and Fluxes for Overall Processes

RFD was configured in this chapter with focus on the maximum flux over the membrane and avoidance of a mixture of permeate and fresh medium. Furthermore, every dilution rate can be applied exactly, as time factors and the small volumes of the emptying and flushing step were considers for the feed and permeate step. The relevant equations to apply RFD are summarized in Table 4-1 and presented in the most general mode. Thus, membrane area (A_M), dilution rate (D) and retention rate ($1\text{-}NF$) as well as step times can be chosen freely. However, steps times as given in the table are recommended for microbial cultures. Table 4-1 is the basis for all RFD experiments conducted in this thesis.

Table 4-1: Calculation of fluxes and applied step times for all four steps of RFD.

Step	Time [s]	Flux [L m^{-2} h^{-1}]
Permeate 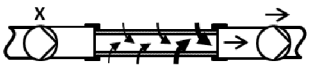	$t_P = 300$	$F_{P,P} = \frac{D\,V_L(1-NF)\,t_C - V_F}{A_M t_P}$
Flushing 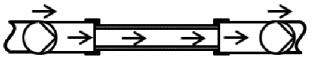	$t_F = 20$	$F_{P,F} = F_{F,F} = \frac{a_F V_{Lu}}{A_M t_F} = \frac{V_F}{A_M t_F}$
Feed 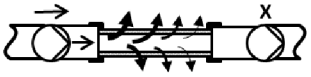	$t_{Feed} = 150$	$F_{F,Feed} = \frac{D\,V_L\,t_C - V_F + V_E}{A_M t_{Feed}}$
Emptying 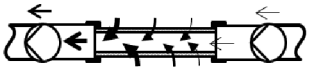	$t_E = 40$	$F_{F,E} = \frac{a_E V_M}{A_M t_E} = \frac{V_E}{A_M t_E}$ $F_{P,E} = \frac{a_E V_M}{5A_M t_E} = \frac{V_E}{5A_M t_E}$

4.6 Benchmark of Reverse-flow Diafiltration

In RFD small amounts of permate are pumped backed into the reactor during the feeding step as there is a mixture of permate and feed in the feed tubing caused by the emptying step (Figure 2-4 D). The amount of pemerate pumped back should be small as the permate contains high value products. To evaluate this aspect, RFD is compared to conventional backflushing membrane bioreactors, where permeate is used to reduce the fouling layer

The permeate volume pumped back into the bioreactor in RFD equals the volume pumped during the emptying step (V_E) minus the volume of the membrane (V_M), which was filled with medium before. This volume subtracted from the total permeate withdrawn over the

membrane ($F_P \cdot A_M \cdot t_P$) is defined as gained permeate ($V_{P,g}$). The amount of gained permeate per total permeate was plotted over the dilution rate in Figure 4-4 for one and three membranes applied. The selected feed flux to permeate flux ratio was set to 5:1 as discussed in chapter 4.4.

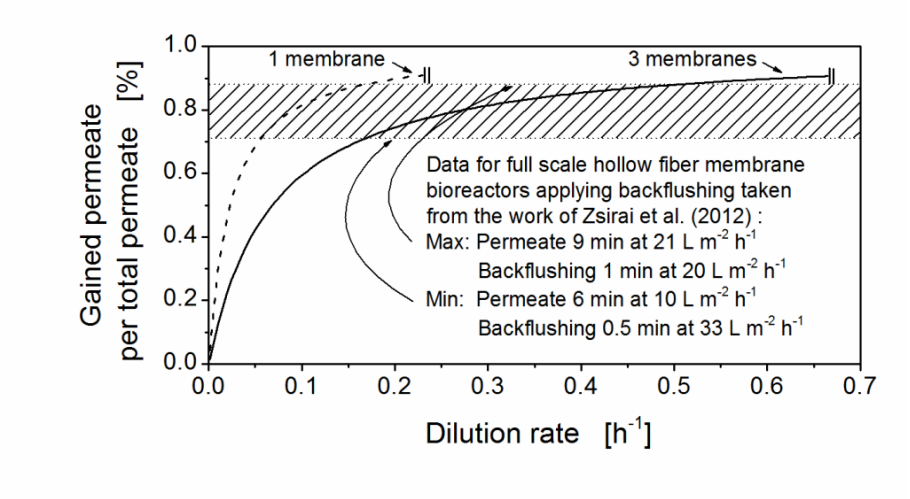

Figure 4-4: Gained permeate per total gained permeate for different dilution rates in comparison to conventional backflushing. Permeate is pumped back into the fermenter due to emptying and flushing steps or backflushing. RFD conditions: 1 or 3 microfiltration membranes with 1 m length each and a nominal pore size of 0.2 µm, NF = 0.5, a_E = 1.69, a_F = 0.7, t_C = 510 s, feed flux / permeate flux of 5 : 1.

The maximum specific flow rate over the membrane, determined in chapter 4.1, limits the applied dilution rate if the membrane area is fixed. This is indicated in Figure 4-4 by two vertical lines. One membrane applied allows dilution rates up to D = 0.22 h^{-1}, three membranes applied triple the maximum dilution rate to D = 0.66 h^{-1}. Furthermore, Figure 4-4 contains a striped area depicting how much permeate is lost due to backflushing in full scale hollow fiber membrane bioreactors for waste water treatment. Data for minimum and maximum value is taken from Zsirai et al. (2012). The values of RFD at the maximum dilution rates are above the striped area. Hence, if the selected membrane area is as small as

possible, RFD recovers more permeate than full scale hollow fiber membrane bioreactors that apply backflushing.

Evaluation of membrane-based bioreactors is often conducted based on the membrane area. The critical transmembrane flux determined in chapter 4.1 defines the required membrane area of RFD. The critical flux specifies the maximum volume [L] that can be filtered by the membrane area [m^{-2}] per time [h^{-1}]. Thus, if the factor time is provided in terms of the perfusion rate [d^{-1}], the specific filtration area [m^{-1}] indicating the membrane area [m^2] per filtered volume [L] can be calculated based on the critical flux. The result of this calculation for CHO cells with a critical flux of 9 L m^{-2} h^{-1} (Figure 4-1) is given in Figure 4-5 as a continuous line for RFD. Furthermore, Figure 4-5 depicts data for other commonly used perfusion systems applying membrane based cell retention systems taken from reviews by Voisard et al. (2003) and Su et al. (2010). Here, data points represent applied specific filtration areas in single studies; a linear fit of the data is shown as dashed-dotted or dashed line for the rotating filter and cross-flow membranes, respectively. Recently, the commercially available ATF system (Alternating Tangential Flow, Refine Technology, New Jersey, USA) is widely applied in industry. As data in literature hardly exist, theoretical data (Su, 2010) was used for the correlation of the specific filtration area and the perfusion rate (dotted line). Although the data points scatter as different media and filtration settings were used, the necessary filtration area for cross-flow membranes and the ATF system is larger than the calculated values for RFD. In contrast, rotating filters were applied with less membrane area. However, it was reported that fouling is a major issue (Su, 2010; Voisard et al., 2003) for commonly available rotating filters. Rotating filter screens are made of stainless steel with pore sizes larger than the average cell size. As stainless steel is highly positively charged, cell debris and proteins are likely to stick to the steel enhancing membrane fouling and reducing antibody transmission through the filter (Su, 2010; Voisard et al., 2003). Thus, the required membrane area, based on the critical flux of 9 L m^{-2} h^{-1} for CHO cells for the chosen membrane-medium combination, is competitive with commercially available membrane-based cell retention systems.

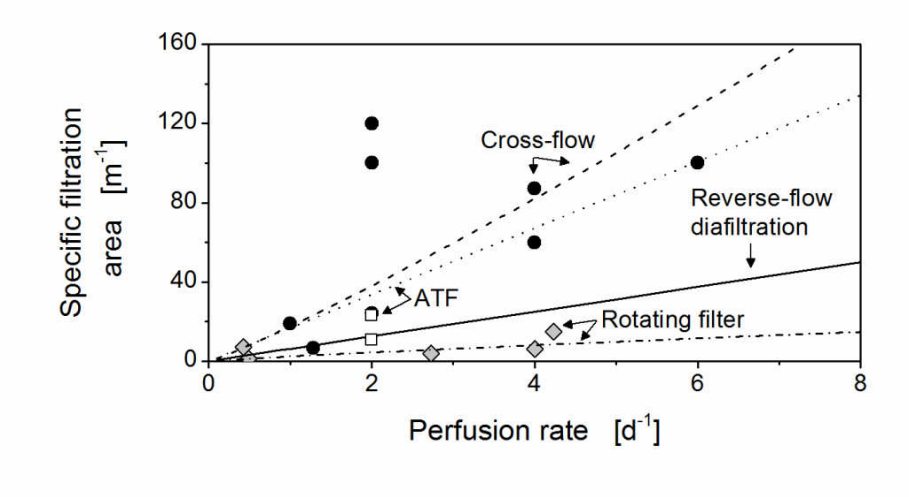

Figure 4-5: Specific filtration areas of membranes in perfusion cultures applying different cell retention systems. The continuous line (reverse-flow diafiltration) was calculated based on the critical flow rate. Data points for the ATF system (white squares) and the theoretical data for the calculation of the dotted line (ATF) were taken from the review paper of Su et al. (2010). Data points for cross-flow (black circles) were taken from the review paper Voisard et al. (2003) and fitted linear (dashed line). Rotating filter data (grey diamonds) was also taken from Voisard et al. (2003) and fitted linear (dashed-dotted line). The media used for in data from the review papers were from all kinds: Dulbecco's modified Eagle's medium with 5 – 10% fetal calf serum, alone or mixed with Ham's nutrient mixture F-12. One study used Grace's powdered medium, one study Roswell Park Memorial Institute basal medium.

Chapter 5

Production of (Single-chain) Antibodies in a Reverse-flow Diafiltration Membrane Bioreactor

This chapter focuses on the application of RFD in a membrane bioreactor cultivating the yeast *H. polymorpha* as well as the mammalian cell line CHO DG44. Therefore, the influence of RFD on yeast cell viability was examined in the first part. Furthermore, the production of single-chain antibodies secreted by *H. polymorpha* is investigated in a continuous culture using RFD. In the second part applicability of RFD with CHO cells is examined by a biocompatibility test of the used polymer materials. Also a perfusion culture using RFD for the production of human full length antibodies secreted by CHO is conducted. Key aspects for the evaluation of RFD with yeast and mammalian cells are product yield, viability of cells as well as long term stability indicated by the filtration performance. Experiments discussed in this chapter were performed by Christoph Scheeren (2012), Anne Worsch (2013) und Suzana Djeljadini (2014). A part of this chapter was published in Meier et al. (2014), another part is submitted to Biotechnology Progress (June 2014).

5.1 Production of Single-chain Antibodies Secreted by Yeasts

5.1.1 Influence of Reverse-flow Diafiltration on Yeast Cell Viability

A continuous fermentation without cell retention was performed in acceleration-stat mode (Paalme et al., 1995) as a reference for the RFD process. Results are illustrated in Figure 5-1. With 20 g L^{-1} glycerol as a carbon source, a constant dry cell weight between 10 and 13 g L^{-1} was observed and, therefore, a yield of approximately 0.55 could be achieved. The washout point was around 0.32 h^{-1}, but slightly delayed due to acceleration-stat operating mode. The antibody concentration was consistently in the range of 0.12–0.15 g L^{-1}. Until the washout point, the glycerol concentration was close to zero as anticipated for a continuous fermentation limited by the carbon source (Figure 5-1 A). As expected, the oxygen transfer rate increased linearly with the dilution rate (Figure 5-1 B). The vivid cell concentration was 86% for a dilution rate of 0.08 h^{-1} and increased to 100% for dilution rates of 0.26 h^{-1} or higher, where the exchange of cells in the reactor is faster. The dead cell concentration was in agreement with the vivid cell concentration (Figure 5-1 C).

To investigate the influence of pulsed feeding and the membrane on cell viability, RFD was applied, but the gained permeate was directed back into the fermenter, creating a shortcut (Figure 2-6, dashed line). Consequently, removal of fluid from the fermenter system was only conducted through the non-filtered product stream. Thus, feed streams and non-filtered product streams in this particular experiment equal a continuous fermentation without cell retention, however, were pumped in a pulsed mode. The viabilities of cells with pulsed feeding and without cell retention did not differ significantly from the reference (Figure 5-1 C). Dry cell weight, antibody concentration, glycerol concentration, as well as the oxygen transfer rate, were also very similar to Figure 5-1 A & B and, thus, not shown for clarity reasons.

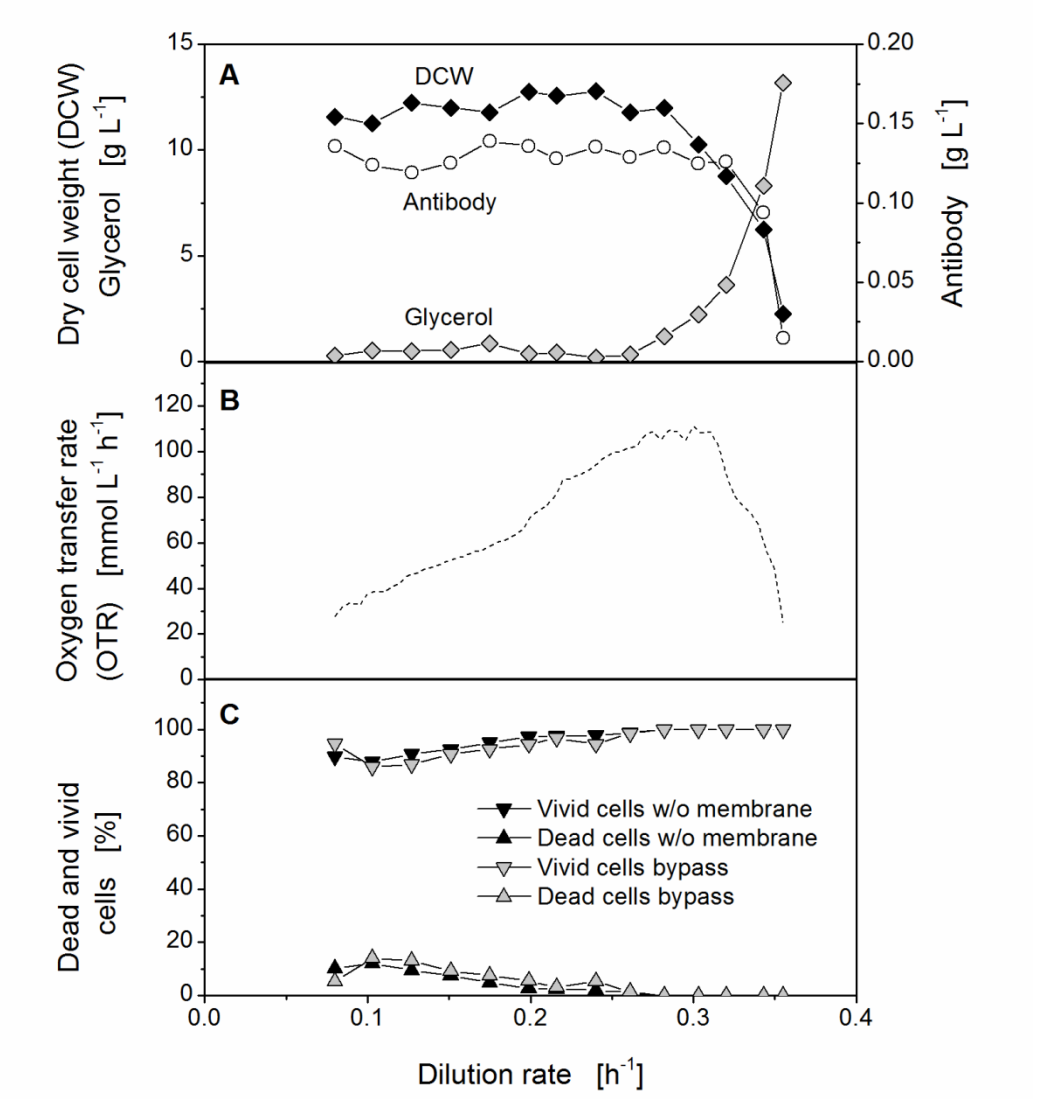

Figure 5-1: Continuous acceleration-stat fermentation of *Hansenula polymorpha* pCoM11sc3625 with (A, B, C) and without (C) reverse-flow diafiltration. Culture conditions: synthetic medium Syn-6, 20 g L^{-1} glycerol, V_L = 1.5 L, pO_2 > 30%, n = 500 – 1800 rpm, q = 1 vvm, pH value of 5.5, T = 37 °C, acceleration rate a = 0.001 h^{-2} for D = 0.08 – 0.34 h^{-1}. A) Dry cell weight (DCW) and antibody concentration. B) Oxygen transfer rate (OTR). C) Viability of cells measured by flow cytometry.

5.1.2 Production of Single-chain Antibodies in a Reverse-flow Diafiltration Membrane Bioreactor

Continuous fermentations with 50% cell retention were performed in RFD mode. Results are summarized in Figure 5-2. The dry cell weight consistently ranged between 20 – 22 g L^{-1}, which was nearly twice as high as without cell retention (Figure 5- A and Figure 5-2 A). Also, the washout point approximately doubled as a dilution rate of 0.65 h^{-1} was achieved (Figure 5-2 A). Doubling of these values is expected for 50% cell retention. Glycerol was not detectable, neither in the broth nor in the permeate (Figure 5-2 A). Since the presence of glycerol in the permeate would be an indication of mixing of the permeate and medium, the absence of glycerol demonstrates successful emptying and flushing.

The average antibody concentration in broth and permeate was approximately 0.2 g L^{-1} (Figure 5-2 A). This is unexpectedly high as a constant product concentration over a range of dilution rates as measured in Figure 5-1 A implies growth associate product formation. The growth rate of the biomass does not change if cell retention is applied. Thus, cells have the same growth rate for the same dilution rate in fermentation with and without cell retention. Hence, the product concentration should be similar in both experiments. The difference between the antibody concentration in the reference fermentation (Figure 5-1 A) and the fermentation with cell retention could be explained by a higher number of dead cells in the experiment with cell retention. For a dilution rate of 0.1 h^{-1}, nearly 30% of cells died if retained (Figure 5-2 C). This value was nearly constant until the washout point. The percentages of vivid and dead cells are coherent. Cell disruption experiments demonstrated that a fraction of antibodies remain in and attached to the cells. Therefore, a higher concentration of dead cells implies greater release of antibodies into the supernatant.

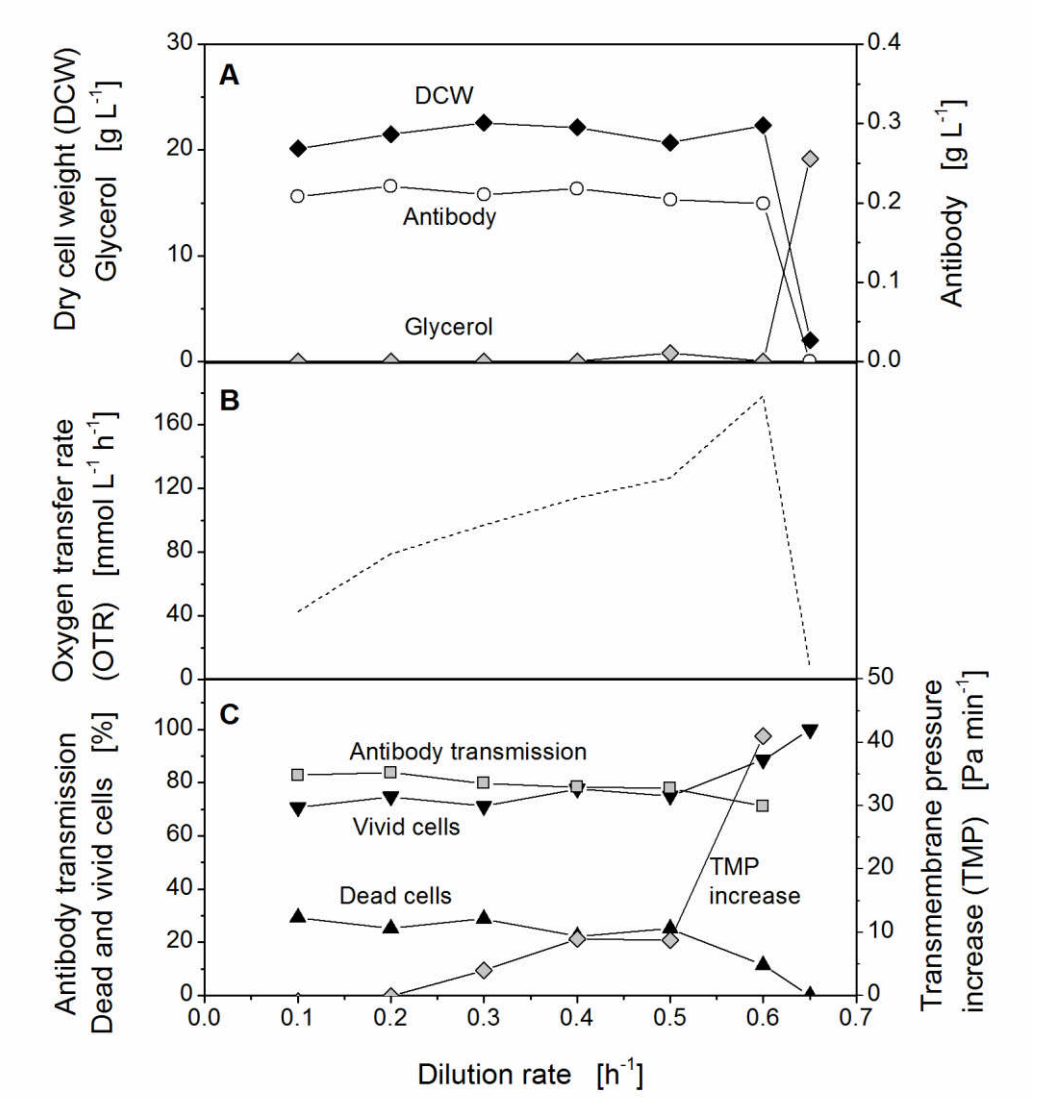

Figure 5-2: Continuous fermentation of *Hansenula polymorpha* pCoM11sc3625 with reverse-flow diafiltration. Culture conditions: synthetic medium Syn-6, 20 g L^{-1} glycerol, V_L = 1.5 L, pO_2 > 30%, n = 500 – 1800 rpm, q = 1 - 3 vvm, pH value of 5.5, T = 37 °C, 3 parallel microfiltration membranes with 1 m length each and a nominal pore size of 0.2µm, a_E = 1.69, a_F = 0.7, NF = 0.5, t_C = 510s. A) Dry cell weight (DCW), glycerol concentration and antibody concentration (average of permeate and broth). B) Oxygen transfer rate (OTR). C) Antibody transmission, dead and vivid cells and transmembrane pressure (TMP) increase.

As expected, the oxygen transfer rate increased linearly with dilution rate (Figure 5-2 B). OTR values with or without cell retention were comparable at the same dilution rate (Figure 5-1 B and Figure 5-2 B). Antibody transmission was constantly high, ranging from 70 – 80% (Figure 5-2 C). However, antibody transmission decreased slightly with higher dilution rates due to a slightly larger fouling layer. The increase in TMP also became greater with higher dilution rates, but remained below the critical TMP increase of 45 Pa min^{-1} over the whole range of dilution rates. Therefore, a stable filtration process could be maintained for all applied dilution rates. Hence, it can be suggested that long-term application of RFD would show constant performance for high dilution rates. Direct comparison of productivity, cell viability or filtration stability from the current study to literature values cannot be done since only mammalian cultures for antibody production have been investigated so far.

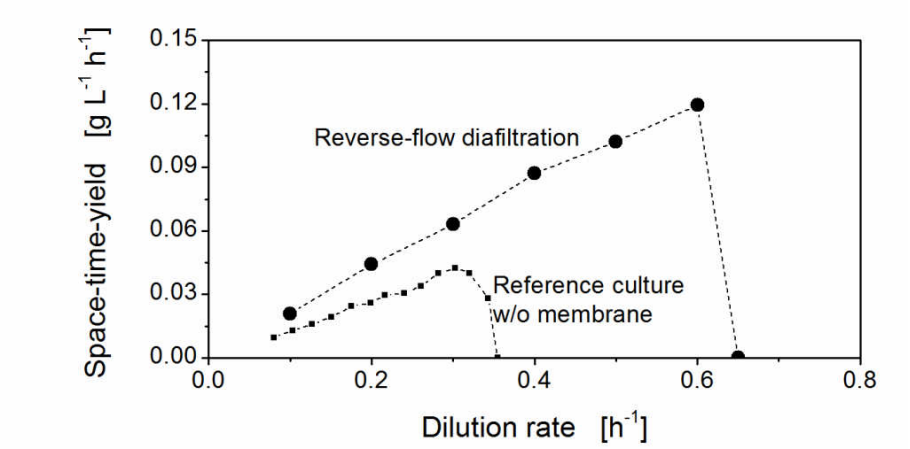

Figure 5-3: Comparison of space-time-yields of a continuous acceleration-stat fermentation and a continuous fermentation with reverse-flow diafiltration of *Hansenula polymorpha* pCoM11sc3625. Culture conditions: synthetic medium Syn-6, 20 g L^{-1} glycerol, V_L = 1.5 L, pO_2 > 30%, n = 500 – 1800 rpm, q = 1 - 3 vvm, pH value of 5.5, T = 37 °C, 1 to 3 parallel microfiltration membranes with 1 m length each and a nominal pore size of 0.2 µm, acceleration rate $a = 0.001$ h^{-1} for $D = 0.08 - 0.34$ h^{-1}, a_E = 1.69, a_F = 0.7, NF = 0.5, t_C = 510s.

Evaluation of RFD from an economic standpoint was done by examining the space-time-yield of antibodies gained with or without cell retention (Figure 5-3). The space-time-yield from the reference fermentation without cell retention increased linearly from approximately 0.01 g L^{-1} h^{-1} at a dilution rate of 0.08 h^{-1} to 0.04 g L^{-1} h^{-1} at a dilution rate of 0.32 h^{-1}. Fermentation with RFD mode led to a space-time-yield of 0.02 g L^{-1} h^{-1} at a dilution rate of 0.1 h^{-1} and 0.12 g L^{-1} h^{-1} at a dilution rate of 0.6 h^{-1}. Consequently, a stable filtration process could be achieved for high dilution rates, leading to a triplication of the space-time-yield.

5.2 Production of Antibodies Secreted by Mammalian Cells

5.2.1 Biocompatibility of Reverse-flow Diafiltration Materials

Plastic materials can leach out chemical compounds which may be toxic above a certain concentration for microbial and cell cultures. As it is not possible to predict the toxicity of the leached compounds for individual cultures, a biocompatibility test should be conducted prior to each new combination of culture and plastic material. Comparison of growth behaviors of culture in the presence and absence of plastic materials is a common biocompatibility test setup (Meier et al., 2013). The used plastic materials in this study namely the polyethersulfone membrane, heat shrink tubing and silicon tubing were added separately to a culture of CHO DG44 cells in T75 flasks. Viable cell densities of these cultures were compared to the viable cell density of a culture without additional plastic material. Figure 5-4 depicts the result. After 4 days of culture the viable cell density of all cultures approximately quadrupled. No significant difference could be noticed between the cultures in presence or absence of the examined plastic materials.

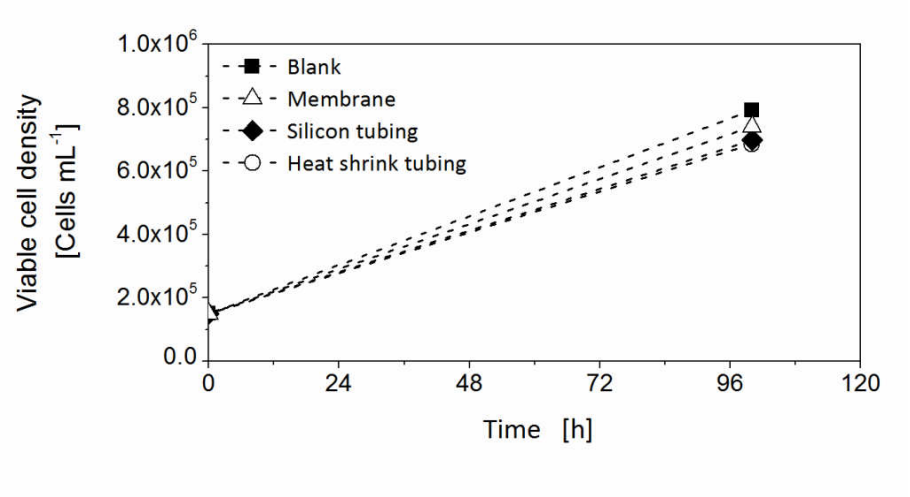

Figure 5-4: Investigation of biocompatibility of applied materials in the perfusion culture setup applying reverse-flow diafiltration and CHO DG44 cells. Culture conditions: PowerCHO 2 medium with 4 mM L-glutamine, T75 flask, T = 37 °C, 5% CO_2, V_L = 20 mL.

5.2.2 Production of Antibodies in a Batch Culture

A batch culture of CHO DG44 cells without a membrane module was conducted as a reference for the subsequent perfusion culture applying RFD. The obtained data is depicted in Figure 5-5. The viable cell concentration increases from $0.1 \cdot 10^6$ cells mL^{-1} to a maximum of $3.5 \cdot 10^6$ cells mL^{-1} after 286 h (Figure 5-5 A). After a stagnation phase lasting until 387 h the viable cell concentration starts to decrease. The capacity signal is a mixed signal of viable biomass and metabolic activities. It has a similar progress as the viable cell concentration in the conducted batch experiment (Figure 5-5 A). It increases simultaneously with the viable cell concentration until 288 h and decreases afterwards with a small peak at 378 h. The peak could indicate a change of the metabolic activity as apoptosis of the cell line starts approximately at that time point. This can also be noticed in the viability of the cell culture dropping below 80% (Figure 5-5 B).

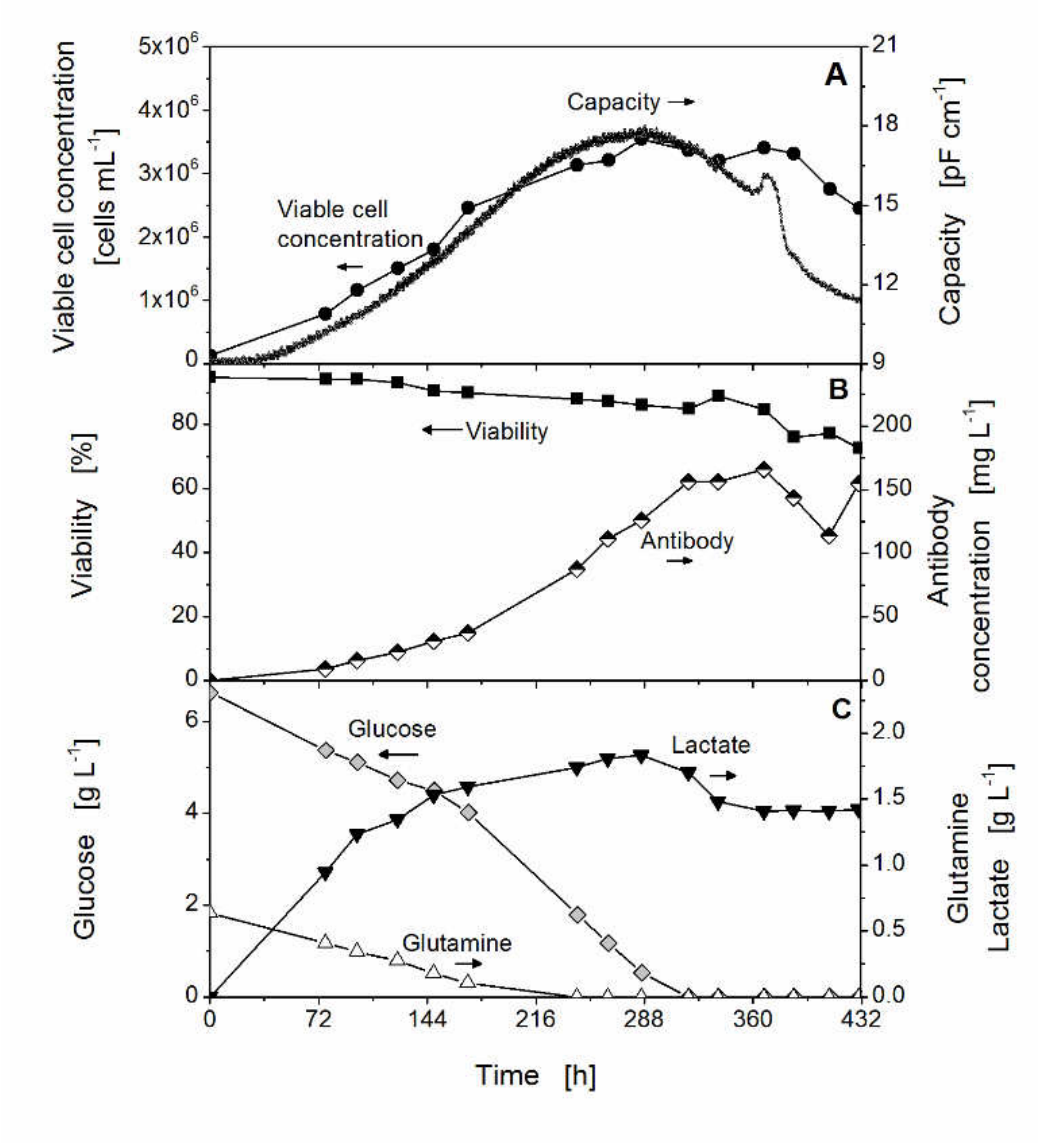

Figure 5-5: Batch culture of CHO DG44 cells expressing a H10 antibody. Culture conditions: PowerCHO 2 medium with 4 mM L-glutamine, T = 37 °C, V_L = 1 L, n = 120 rpm, $pO_2 > 40\%$, pH of value = 6.8. A) Viable cell concentration and capacity. B) Viability C) Glucose, glutamine and lactate concentration.

The H10 antibody was efficiently produced and accumulated up to 156 mg L^{-1} after 317 h and remained constant until 368 h (Figure 5-5 B). Following, a steep drop in H10 concentration to 114 mg L^{-1} that occurred at 411 h, the antibody concentration finally increased again and reached 155 mg L^{-1} at the end of the cultivation (430 h). The concentration drop could have been caused by degradation. The subsequent increase may result from rupturing cells due to

apotosis releasing antibodies. The sharp decrease of product formation followed by an increase was observed during several cultivations of this specific CHO DG44 cell line according to Tanja Holland (Fraunhofer IME). The glucose concentration steadily decreases from its initial value of 6.6 g L^{-1} and was fully depleted after 317 h (Figure 5-5 C). The glutamine concentration decreased from initially 0.64 g L^{-1} and was no longer detectable in the medium after 244 h (Figure 5-5 C). The maximum concentration of the byproduct lactate was 1.8 g L^{-1}, which was reached after 244 h and remained constant (Figure 5-5 C).

The integrity of the H10 antibody chains was verified by a reduced western blot that is shown in Figure 5-6. Protein bands of heavy and light chain at 50 and 25 kDa, respectively indicate the correct protein sizes displayed in Figure 5-5 B. More degradation products became visible in samples corresponding to later time points of the cultivation, most likely because of the higher antibody concentration applied.

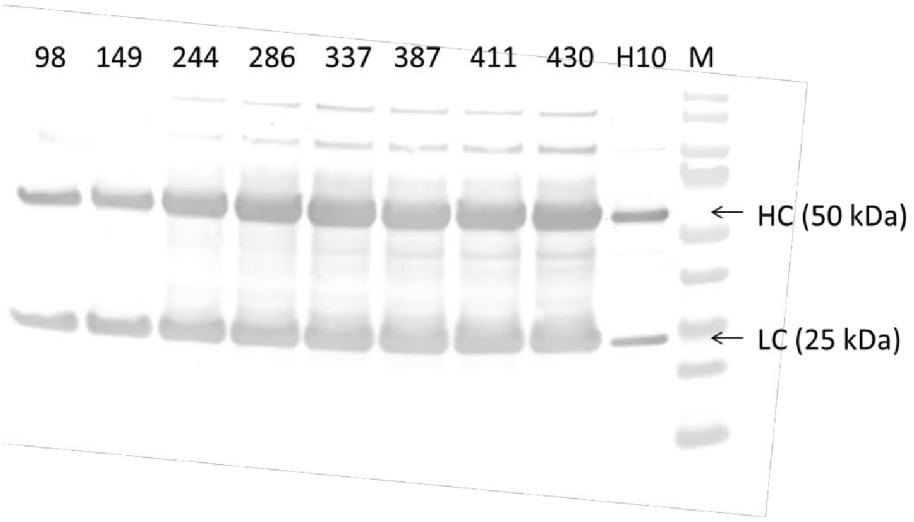

Figure 5-6: Reduced western blot of batch samples. 20 µL sample volume (supernatant), 4 µL standard (50 µg mL^{-1} H10), 8 µL pre-stained marker (Fermentas), HC: heavy chain, LC: light chain.

5.2.3 Production of Antibodies in a Reverse-Flow Diafiltration Membrane Bioreactor

Until now, RFD has only been described for microbial culture processes (Carstensen et al., 2013; Carstensen et al., 2012b; Meier et al., 2014; Meier et al., May 2014). However, recombinant protein production in mammalian cell lines could also be efficiently carried out using RFD. In mammalian cell terminology continuous cultures applying cell retention are called perfusion cultures. Perfusion cultures are not C-source limited as continuous cultures for microbial processes and therefore, perfusion cultures do not reach steady state. Thus, results of perfusion cultures are plotted over time in contrast to microbial continuous cultures, which are plotted time independent over the dilution rate.

A perfusion culture of CHO DG44 cells applying RFD with a retention rate of 90% ($NF = 0.1$) is shown in Figure 5-7. The first days of the perfusion culture were conducted in batch mode until a viable cell concentration of $1.8 \cdot 10^6$ cells mL^{-1} was achieved (Figure 5-7 A) after 114 h. The increase of the viable cell concentration of the perfusion culture until 114 h was comparable with the data that was obtained for the batch culture of CHO DG44 cells without a membrane module (Figure 5-5 A and Figure 5-7 A), confirming the results of the biocompatibility test (Figure 5-4). At 114 h, the perfusion mode was started with a dilution rate of D = 0.5 d^{-1}. The viable cell density increased to $4.5 \cdot 10^6$ cells mL^{-1} at 146 h and remained rather constant at 3.9 – $4.5 \cdot 10^6$ cells mL^{-1} until 216 h. When the dilution rate was set to D = 1 d^{-1} at 216 h the viable cell concentration remained high at 4.2 – $4.6 \cdot 10^6$ cells mL^{-1} until 340 h. The temporary drop of the viable cell concentration was caused by two short operation failures of Labview cause a failure of both pumps between 170 h and 242 h which led to a dilution of the culture. A further increase of the dilution rate to D = 2 d^{-1} at 383 h cause a decrease of viable cell density of finally $1.5 \cdot 10^6$ cells mL^{-1} at 428 h indicating a dilution of the culture. The maximum growth rate (μ_{max}) of this CHO DG44 cell line is 0.672 d^{-1}, thus, dilution rates (D_{max}) up to 6 .72 d^{-1} ($D_{max} = \frac{\mu_{max}}{NF}$) should be possible.

The dilution rate of D = 0.5 d^{-1}, 1 d^{-1} and 2 d^{-1} correspond to permeate flow rates of 4.2 L m^{-2} h^{-1}, 8.6 L m^{-2} h^{-1} and 18.2 L m^{-2} h^{-1}, respectively (Table 2-6). Whereas the flow rates for D = 0.5 d^{-1} and 1 d^{-1} are below the critical flow rate of 9 L m^{-2} h^{-1} (Figure 4-1), the flow rate for D = 2 d^{-1} is above the critical value. Thus, membrane fouling was expected to occur. Concurrent membrane blocking causes a decrease of the amount of permeate gained over the

membrane. Data obtained by the permeate balance (data not shown) confirm an increasing deviation of the set permeate and the gained permeate. As a result, the volume of the non-filtered product stream increased because the corresponding pump was controlled by the balance weighing the bioreactor. Hence, the retention rate decreased and, thus, a lower cell density was obtained.

For every dilution rate a distinct transmembrane pressure plateau could be measured (Figure 5-7 A). The plateaus were at 0.13 bar, 0.28 bar and 0.34 bar for the dilution rates of $D = 0.5\ d^{-1}$, $1\ d^{-1}$ and $2\ d^{-1}$, respectively. The transmembrane pressure nearly doubled when the dilution rate was doubled for the first time, but the increase in the transmembrane pressure was only 20% at the second increase of the dilution rate. This indicates membrane blocking at $D = 2\ d^{-1}$ as the pressure required to generate the flux could not be adjusted accurately.

The viability of the cell population remained constant above 90% during the entire culture time of 432 h indicating that optimal growth conditions were sustained (Figure 5-7 B). The antibody concentrations in the reactor and in the harvest were quantified by a Resonance Surface Plasmon Measurement (Figure 5-7 B). During dilution rates of $D = 0.5\ d^{-1}$ and $1\ d^{-1}$ the antibody concentration increased in both fractions, but the antibody concentration in the harvest was always proportionally lower. The antibody transmission ranged between 40 and 60%. Clincke et al. (Clincke et al., 2013b) reported that commercially available membrane-based cell retention systems show antibody transmission of 10% to 60% after a comparable perfusion time of 18 days. In this perfusion experiment maximum antibody concentrations of 189 mg L^{-1} and 122 mg L^{-1} were determined in the reactor and in the harvest, respectively. These values are comparable to those quantified of the batch culture. A sharp decrease in the antibody concentration accompanies the increase of the dilution rate to $D = 2\ d^{-1}$ according to the trend of the viable cell density.

Glucose and glutamine concentrations decreased during the batch phase to values of 4.6 g L^{-1} and 0.2 g L^{-1}, respectively (Figure 5-7 C). After switching to the perfusion culture glucose and glutamine concentrations shortly increased. Then, the glucose concentration steadily decreased to a value of to 2.6 g L^{-1} at 240 h and thereafter remained constant until 340 h, whereas the glutamine concentration alternates around 0.2 g L^{-1} until 340 h. The fluctuations of metabolites can be caused by the pulsed feeding mode of RFD. The subsequent increase of the dilution rate to $D = 2\ d^{-1}$ caused an increase of the glutamine and glucose concentrations

corresponding to the decrease of the viable cell concentration. The lactate concentration increases during the batch phase to a value of 1.4 g L^{-1} and remains constant until the dilution rate was set to $D = 2\ d^{-1}$ when it decreased.

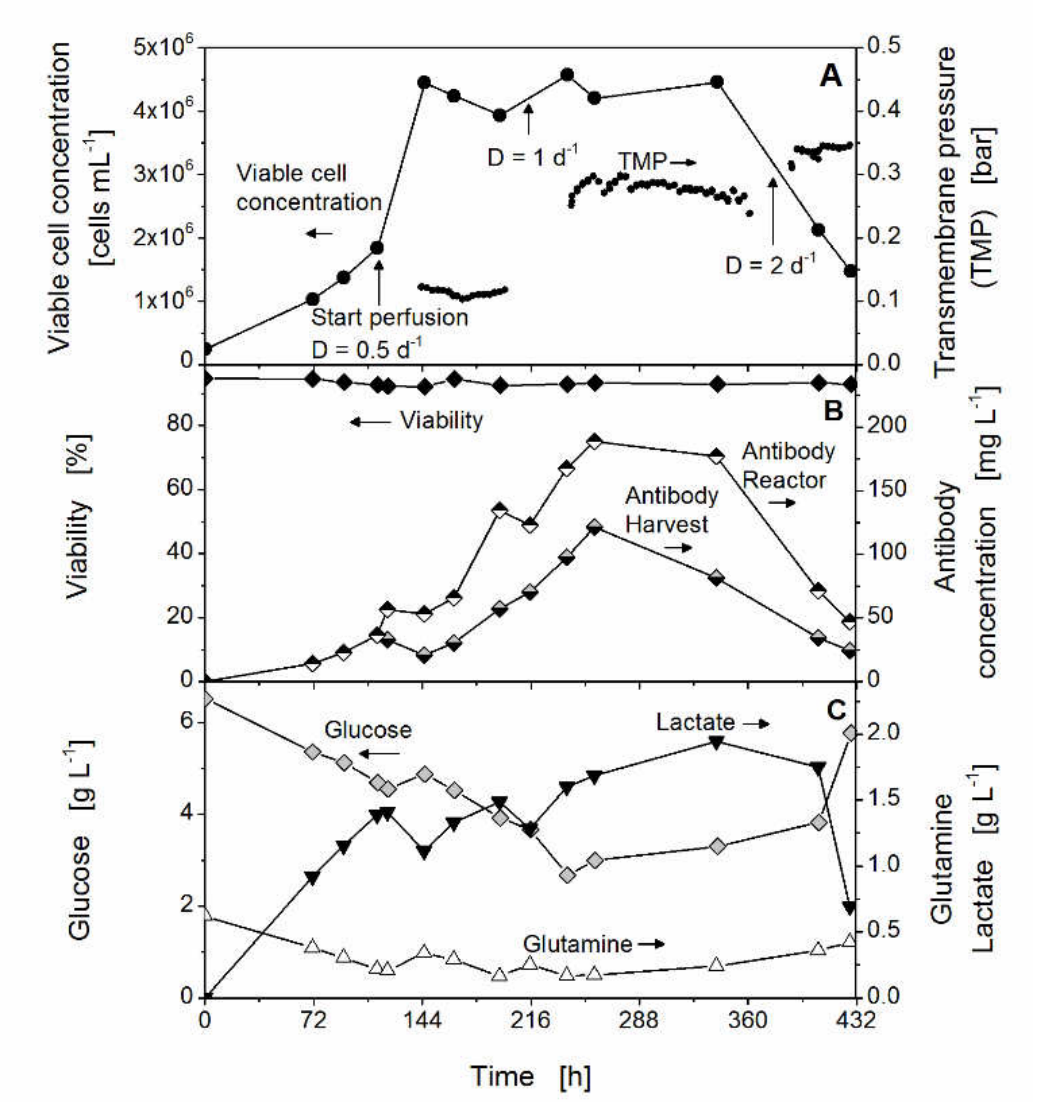

Figure 5-7: Perfusion culture of CHO DG44 cells expressing a H10 antibody applying reverse-flow diafiltration. Culture conditions: PowerCHO 2 medium with 4 mM L-glutamine, $T = 37$ °C, $V_L = 1$ L, $n = 120$ rpm, $pO_2 > 40\%$, pH value of 6.8, $t_C = 510$ s, $a_E = 1.89$, $a_F = 0.7$, $NF = 0.1$. A) Viable cell concentration and transmembrane pressure (data for transition zones not monitored). B) Viability and antibody concentrations C) Glucose, glutamine and lactate.

A reducing western blot was conducted for one sample from each dilution rate to verify integrity of the antibody (Figure 5-8). Bands of heavy and light chain could be detected for all samples at the expected sizes of 50 and 25 kDa, respectively.

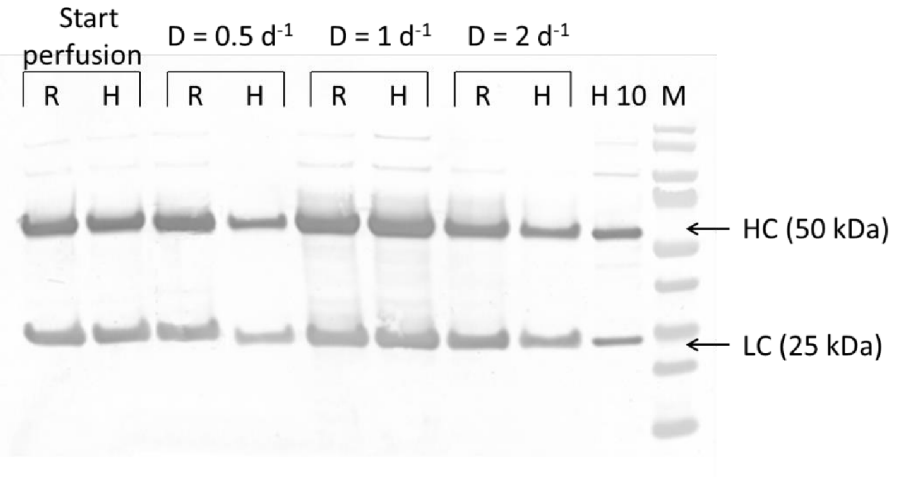

Figure 5-8: Reduced western blot of samples from the perfusion culture. 20 µL sample volume (supernatant), 4 µL standard (50 µg mL^{-1} H10), 8 µL pre-stained Marker (Fermentas), HC: heavy chain, LC: light chain, R: samples reactor, H: samples harvest.

Long-term stability and high space-time yield was proven for RFD culturing yeast or CHO cells. Stable conditions in terms of concentrations and filtration performance were achieved as long as the critical flow rate was not exceeded. Antibody transmission was comparable to published data (Clincke et al., 2013b) for commercially available membrane based cell retention systems. In case higher dilution rates as applied here or larger fermenter volumes are required, a bigger membrane area would have to be applied.

An industrial application would require a scale up from the investigated 3 L reactor to 100 – 1000 L reactors with dilution rates of 1 reactor volume per day. The maximum flux in this study is 21 L m^{-2} h^{-1} or 9 L m^{-2} h^{-1} for *H. polymorpha* or CHO cells, respectively. Hence, the necessary filtration area has to be six-fold to 180-fold higher for a reactor with 100 L or 1000 L filling volume, respectively. Using hollow fiber bundles can solve this issue. In

membrane bundles a uniform driving force in every membrane has to be provided in order to guarantee an effective flushing and emptying. Several bundles spread over the reactor volume will lead to a good distribution of medium avoiding areas with high concentration.

As the application of single-use bioreactors is an emerging trend especially in industry, an integration of submerged membranes in single-use bags and disposable cylindrical vessels was considered. Attachment of membranes in single-use bags was already successfully investigated in the diploma thesis of Lukas Beckmann (Beckmann, 2013). RFD is an easy applicable process with low investment cost. Only the membranes, two ports and a disposable bracket at the bottom of the culture vessel are required modifications. Hence, an integration of RFD in single-use bioreactors is feasible in economic and technical terms.

Chapter 6

Modelling and Simulation of Reverse-flow Diafiltration

Models and simulations are supportive tools for process optimization. The experimental effort can be reduced drastically if establish models predict the progress and the outcome of potential experiments. Especially experiments with mammalian cell cultures are time consuming, cost-intensive and accident sensitive and, thus, particularly appropriate for the application of simulation tools. In this chapter a model for the batch cultivation and reverse-flow diafiltration of mammalian cells conducted in this thesis is developed. The calculation of constants and the estimation of parameters using a Monte Carlo simulation are based on batch data. The developed model is used to determine an optimized perfusion strategy to increase the accumulated product concentration. The main results discussed in this chapter are acquired in the master thesis of Suzana Djeljadini (Djeljadini, 2014).

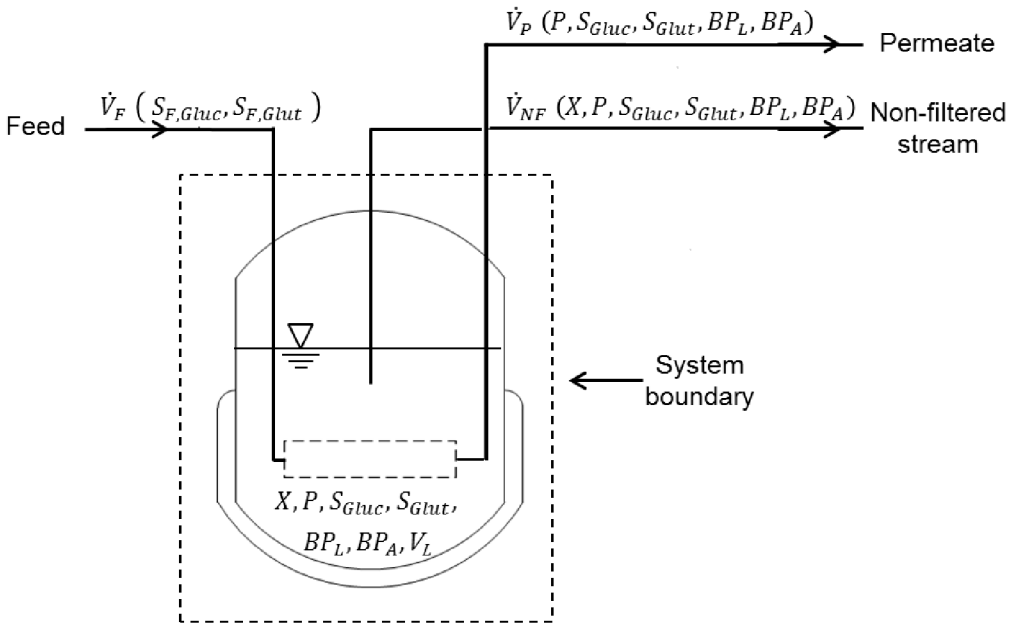

Figure 6-1: System boundaries and relevant variables of RFD. Feed flow ($\dot{V}_F$), permeate flow ($\dot{V}_P$) and non-filtered product stream flow ($\dot{V}_{NF}$), filling volume (V_L) concentration of biomass (X), product (P), substrates glucose (S_{Gluc}) and glutamine (S_{Glut}), byproducts lactate (BP_L) and ammonium (BP_A) as well as concentrations in the feed glucose ($S_{F,Gluc}$) and glutamine ($S_{F,Glut}$).

6.1 Model development of a reverse-flow diafiltration

The developed model focuses on the biological part of the RFD process. Therefore, the system boundary was chosen around the bioreactor as shown in Figure 6-1. The variables of the model describe concentrations and, thus, are determined by mass balances. In general, balances for an extensive property such as mass (Ψ) consist of a conversion term ($\sum_\Psi$) and the flow of the extensive property in ($+\dot{\Psi}_{in}$) and out ($-\dot{\Psi}_{out}$) of the system:

$$\frac{d(\Psi)}{dt} = \sum_\Psi + \dot{\Psi}_{in} - \dot{\Psi}_{out} \tag{6.1}$$

Substitution of mass by concentrations multiplied by the volume of the system ($\Psi = c_\Psi \cdot V_L$) and adaption of equation 6.1 to the flows of bioreactor system shown in Figure 6-1 ($\dot{V}_F$, $\dot{V}_P$ and $\dot{V}_{NF}$) results in:

$$\frac{d(c_\Psi \cdot V_L)}{dt} = \sum_\Psi + \boldsymbol{\dot{V}_F \cdot c_{\Psi,F} - \dot{V}_P \cdot c_{\Psi,P} - \dot{V}_{NF} \cdot c_{\Psi,NF}} \quad (6.2)$$

$$\frac{dc_\Psi}{dt} \cdot V_L + \frac{dV_L}{dt} \cdot c_\Psi = \sum_\Psi + \boldsymbol{\dot{V}_F \cdot c_{\Psi,F} - \dot{V}_P \cdot c_{\Psi,P} - \dot{V}_{NF} \cdot c_{\Psi,NF}} \quad (6.3)$$

The filling volume of the bioreactor is assumed to be constant $\left(\frac{dV_L}{dt} = 0\right)$:

$$\frac{d\boldsymbol{c_\Psi}}{dt} = \sum_\Psi + \frac{\dot{V}_F}{V_L} \cdot \boldsymbol{c_{\Psi,F}} - \frac{\dot{V}_P}{V_L} \cdot \boldsymbol{c_{\Psi,P}} - \frac{\dot{V}_{NF}}{V_L} \cdot \boldsymbol{c_{\Psi,NF}} \quad (6.4)$$

The flow into the bioreactor ($\dot{V}_F$) and the flow out of the bioreactor (Permeate $\dot{V}_P$ and non-filtered $\dot{V}_{NF}$) is set equal, which is a condition for continuous cultures. The ratio between the permeate flow ($\dot{V}_P$) and the non-filtered flow ($\dot{V}_{NF}$) is defined as non-filtered ratio (*NF*):

$$\dot{V}_F = \dot{V}_{NF} + \dot{V}_P = \dot{V} \cdot NF + \dot{V} \cdot (1 - NF) = \dot{V} \quad (6.5)$$

In chemical engineering the residence time (τ) is used to describe the average time a particle remains in a system. In biotechnology the common parameter describing this value is the reciprocal of the residence time, the dilution rate (*D*). It is defined as the flow ($\dot{V}$) through the bioreactor divided by the filling volume (V_L):

$$D = \frac{\dot{V}}{V_L} \quad (6.6)$$

Inserting equations 6.5 and 6.6 in equation 6.4 leads to:

$$\frac{d\Psi}{dt} = \sum_\Psi + \boldsymbol{D \cdot \Psi_F - D \cdot (1 - NF) \cdot \Psi_P - D \cdot NF \cdot \Psi_{NF}} \quad (6.7)$$

This general expression of equation 6.7 is specified for the RFD relevant variables, namely the biomass (*X*), the two substrates glucose (S_{Gluc}) and glutamine (S_{Glut}) as well as the product (*P*) and the two byproducts ammonium (BP_A), produced during glutamine conversion, and lactate (BP_L), produced during glucose conversion, in equations 6.8 – 6.13.

For the conversion term of the different variables the following variables, constants and parameters are taken into account: the growth and death rate (μ) and (μ_d), the yields (Y), the maintenance coefficients (m), the degradation rate of glutamine into ammonium (d_{Glut}) and the removal rate of ammonium due to gas sparging of ammonia (r_A). The product formation is calculated according to the very general approach of Luedeking-Piret (Luedeking and Piret, 1959) with the a growth associated constant (α) and a non-growth associated constant (β) for product formation as well as the monod constants for glucose and glutamine (k_M).

The flow terms into the bioreactor of equation 6.7 are calculated with the medium supplies (S_f). To calculate the flow terms out of the bioreactor a homogenous mixture is assumed. Thus, concentrations in the permeate and the non-filtered product stream are equal ($\Psi_P = \Psi_{NF}$) except for the biomass, which is retained in the bioreactor and only removed through the non-filtered product stream ($X_P = 0$).

$$\frac{dX}{dt} = (\mu - \mu_d) \cdot X - \boldsymbol{D \cdot X \cdot NF} \tag{6.8}$$

$$\frac{dS_{Gluc}}{dt} = -\left(\frac{\mu - \mu_d}{Y_{XS_{Gluc}}} + m_{Gluc}\right) \cdot X + \boldsymbol{D \cdot \left(S_{F,Gluc} - S_{Gluc}\right)} \tag{6.9}$$

$$\frac{dS_{Glut}}{dt} = -\left(\frac{\mu - \mu_d}{Y_{XS_{Glut}}} + m_{Glut}\right) \cdot X - d_{Glut} \cdot S_{Glut} + \boldsymbol{D \cdot \left(S_{F,Glut} - S_{Glut}\right)} \tag{6.10}$$

$$\frac{dBP_L}{dt} = \left(\frac{\mu - \mu_d}{Y_{XS_{Gluc}}} + m_{Gluc}\right) \cdot Y_{BP_L S_{Gluc}} \cdot X - \boldsymbol{D \cdot BP_L} \tag{6.11}$$

$$\frac{dBP_A}{dt} = \left(\frac{\mu - \mu_d}{Y_{XS_{Glut}}} + m_{Glut}\right) \cdot Y_{BP_A S_{Glut}} \cdot X + d_{Glut} \cdot S_{Glut} + r_A \cdot X - \boldsymbol{D \cdot BP_A} \tag{6.12}$$

$$\frac{dP}{dt} = \left(\alpha \cdot \frac{dX}{dt} + \beta \cdot X\right) \cdot \frac{S_{Gluc}}{S_{Gluc} + k_{M,Gluc}} \cdot \frac{S_{Glut}}{S_{Glut} + k_{M,Glut}} - \boldsymbol{D \cdot P} \tag{6.13}$$

The non-bolt parts of the mass balances (Equation 6.8 – 6.13) represent the conversion term and, thus, are valid for batch cultures and RFD. The bolt parts of the equations describe the flow in and out of the bioreactor and, therefore, are only used in the RFD model.

Furthermore, constitutive equations for the growth and death rate of biomass as well as the maintenance of glutamine are implemented in the model based on the model of Xing et al.

(2010). Cell death is accelerated at increased lactate or ammonium concentrations. Thus, terms for the two byproducts are used for calculating the death rate. Also, the maximum growth rate (μ_{max}), the death constant (k_d) and two constant (α_1) and (α_2) are considered:

$$\mu = \mu_{max} \cdot \frac{S_{Gluc}}{S_{Gluc}+k_{M,Gluc}} \cdot \frac{S_{Glut}}{S_{Glut}+k_{M,Glut}} \cdot \frac{k_{M,L}}{BP_L+k_{M,L}} \cdot \frac{k_{M,A}}{BP_A+k_{M,A}} \quad (6.14)$$

$$\mu_d = k_d \cdot \frac{BP_L}{BP_L+k_{d,L}} \cdot \frac{BP_A}{BP_A+k_{d,A}} \quad (6.15)$$

$$m_{Glut} = \frac{\alpha_1 \cdot S_{Glut}}{\alpha_2+S_{Glut}} \quad (6.16)$$

Constants are determined from batch data obtained in chapter 5.2.2 and listed in Table 6-1, parameters are estimated as shown in chapter 6.2. To simulate the lag phase of the culture μ_{max} was substituted by $\mu_{max,S}$ for the first 36 h.

Table 6-1: CHO specific constants obtained from a batch culture.

Constant	**Value**	**Unit**	**Note**
$\mu_{max,s}$	0.0029	h^{-1}	0 – 36 hours to simulate lag phase[a]
μ_{max}	0.028	h^{-1}	36 – 96 hours for exponential phase[a]
k_d	0.0070	h^{-1}	387 – 430 hours for death phase[b]
$Y_{XS_{Gluc}}$	1.23	10^6 cells mL^{-1} mg^{-1}	36 – 172 hours[b]
$Y_{XS_{Glut}}$	5.55	10^6 cells mL^{-1} mg^{-1}	36 – 172 hours[b]
$Y_{BP_LS_{Gluc}}$	0.47	g g^{-1}	36 – 172 hours
$Y_{BP_AS_{Glut}}$	0.095	g g^{-1}	36 – 172 hours

[a]Biomass data obtain from capacity signal [b]Biomass data obtain by CASY measurement

6.2 Parameter estimation for CHO DG44 cells

In contrast to the CHO specific constants (Table 6-1), parameters cannot directly be determined from batch data. Therefore, a parameter estimation using a Monte Carlo simulation (Metropolis and Ulam, 1949) was conducted. In general, a Monte Carlo simulation is a stochastically method to obtain numerical results by repeated random simulations. In this study, repeated simulations were conducted with one million parameter sets, consisting of eleven parameters. Each parameter set was randomly generated to achieve a statistically distribution of possible values for the unknown parameter sets.

Randomly chosen parameters (θ) of the parameter set were generated independently within a given reasonable physical space (p_{min} and p_{max} given in Table 6-2) and a random number (r) between 0 and 1. Within this study, the following algorithm was used:

$$\theta = p_{min} + (p_{max} - p_{min}) \cdot r \tag{6.17}$$

A simulation based on the model developed in chapter 6.1 was conducted with each of the one million generated parameter sets. The simulation was performed in Matlab with "ODE45" as solver for differential equations. The parameter set ($\theta_{i,sim}$) with the best fitting to the batch data ($\theta_{i,exp}$) was determined by the smallest sum square error (*min SSE*):

$$minSSE = \sum_{i=1}^{n} \left(\theta_{i,exp} - \theta_{i,sim}\right)^2 \tag{6.18}$$

The best parameter set was further adapted to the batch data with the Matlab optimizer function "fminsearch". This function examines the neighborhood of each parameter with the aim to minimize the sum square error. The result of the parameter estimation is displayed in Table 6-3.

.

Table 6-2: CHO specific parameter space for parameter estimation.

Constant	**Unit**	$\mathbf{p_{min}}$	$\mathbf{p_{max}}$
$\boldsymbol{m_{Gluc}}$	10^{-12} mg L cells^{-1} h^{-1}	0.09	54
$\boldsymbol{k_{M,Gluc}}$	g L^{-1}	$1.8 \cdot 10^{-5}$	0.18
$\boldsymbol{k_{M,Glut}}$	g L^{-1}	$1.5 \cdot 10^{-5}$	0.15
$\boldsymbol{k_{M,L}}$	g L^{-1}	0.09	9
$\boldsymbol{k_{M,A}}$	g L^{-1}	0.009	0.36
$\boldsymbol{k_{d,L}}$	g L^{-1}	0.09	9
$\boldsymbol{k_{d,A}}$	g L^{-1}	0.009	0.36
$\boldsymbol{\alpha}$	10^{-12} L cells^{-1} h^{-1}	0.001	5
$\boldsymbol{\beta}$	10^{-12} L cells^{-1} h^{-2}	0.001	5
$\boldsymbol{\alpha_1}$	10^{-12} mg L cells^{-1} h^{-1}	0.073	43.8
$\boldsymbol{\alpha_2}$	g L^{-1}	0.073	2.92
$\mathbf{r_A}$	10^{-12} mg L cells^{-1} h^{-1}	0.55	1000
$\mathbf{d_{Glut}}$	h^{-1}	0.001	0.01

Table 6-3: CHO specific estimated parameter using the Monte Carlo method with a parameter set of one million.

Constant	**Unit**	**Value**	**Literature (Xing et a 2010)**
m_{Gluc}	10^{-12} mg L cells^{-1} h^{-1}	7.74	0 – 36000
$k_{M,Gluc}$	g L^{-1}	0.15	0.027 – 0.18
$k_{M,Glut}$	g L^{-1}	0.073	0.0088 – 0.12
$k_{M,L}$	g L^{-1}	0.47	0.72 –12.60
$k_{M,A}$	g L^{-1}	0.31	0.018 – 0.36
$k_{d,L}$	g L^{-1}	2.16	1.35 – 27.99
$k_{d,A}$	g L^{-1}	0.046	0.026 – 0.081
α	10^{-12} L cells^{-1} h^{-1}	2.07	n.a.
β	10^{-12} L cells^{-1} h^{-2}	0.49	n.a.
α_1	10^{-12} mg L cells^{-1} h^{-1}	2.336	0 – 49640
α_2	g L^{-1}	2.628	0.029 – 0.58
r_A	10^{-12} mg L cells^{-1} h^{-1}	350	n.a.
d_{Glut}	h^{-1}	0.0072	n.a.

6.3 Simulation of experimental data

A simulation of the batch model of chapter 6.1 with the constants determined in the same chapter and the parameters estimated in chapter 6.2 is shown in Figure 6-2 as black line. Blue dots in Figure 6-2 display the batch data the simulation is based on. The viable cell density as well as the glucose and product concentrations are fitted accurately with a coefficient of determination $R^2 > 0.9$. As these values are measured with three different analytical assays with respective analytical errors the reliability of model fit can be regarded as very high. The progress of glutamine, lactate and ammonium is represented adequately with the model. However, during the whole cultivation time glutamine and lactate are over- and underestimated, respectively. For ammonium it should be noted that the first measured data points are underestimated as the analytical device is not sensitive enough.

Simulation of the perfusion conducted in chapter 5.2.3 is shown in Figure 6-3. Events were implemented in the Matlab code as they occurred: A switch from batch phase to perfusion at $D = 0.5$ d^{-1} at $t = 114$ h, drop out of pumps at $t = 170$ h for 3 h, switch of perfusion rate to $D = 1$ d^{-1} at 216 h, another drop out of pumps at $t = 242$ h for 8 h and finally, switch of perfusion rate to $D = 2$ d^{-1} at $t = 360$ h. As membrane fouling occurred at the highest dilution rate, the non-filtered ratio (*NF*) decreased. This decrease of *NF* was also considered in the model.

The progress of the simulated data and the measured data are in good accordance. The viable cell density, the concentration of product as well as of the two substrates glucose and glutamine can be simulated sufficiently. The concentration of lactate is underestimated as it was in the batch. Again the concentration of ammonium was not detected sufficiently in the perfusion culture. Hence, a statement about the accuracy of the fit of ammonium is not possible at this time.

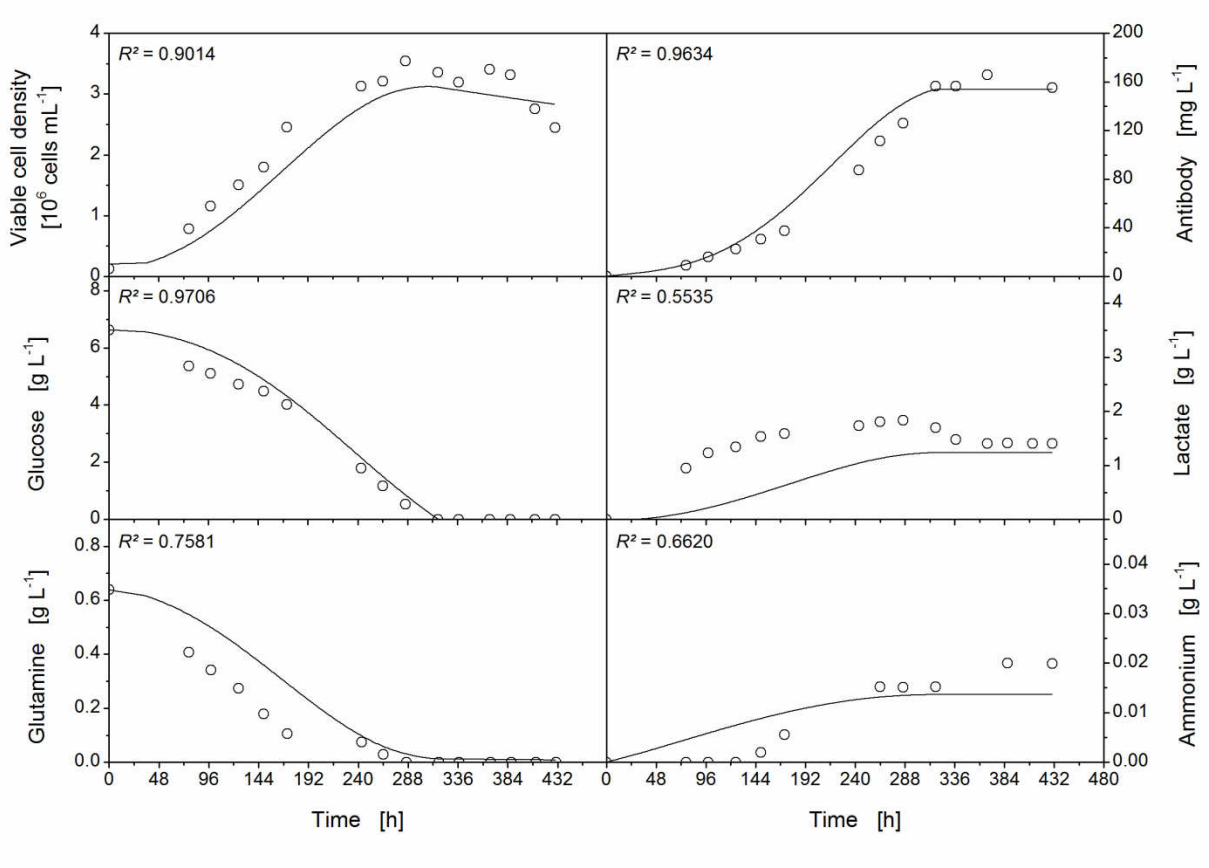

Figure 6-2: Simulation (black line) of a batch fermentation of CHO DG44 cells. Simulation was conducted with Matlab, differential equations were solved with the solver ODE45, and constants were taken from the batch data. Parameters were estimated using the Monte Carlo method based on one million randomly generated parameter sets consisting of eleven parameters. Batch data (open circles) was taken from experiments described in chapter 5.2.2.

It is remarkable that the simulation is based on constants and parameters fitted to solely one batch experiment. The accuracy of the simulation can be improved if the values of the parameters and constants would be an average of more batch experiments. Furthermore, within the perfusion experiment two drop out of the pumps occurred, which also influences the result. Hence, a sound perfusion experiment should be conducted to evaluate the real potential of the simulation. Despite the two mentioned drawbacks, the simulation of the

perfusion is satisfactory. Thus, the simulation was used to predict the optimal dilution rate in terms of productivity.

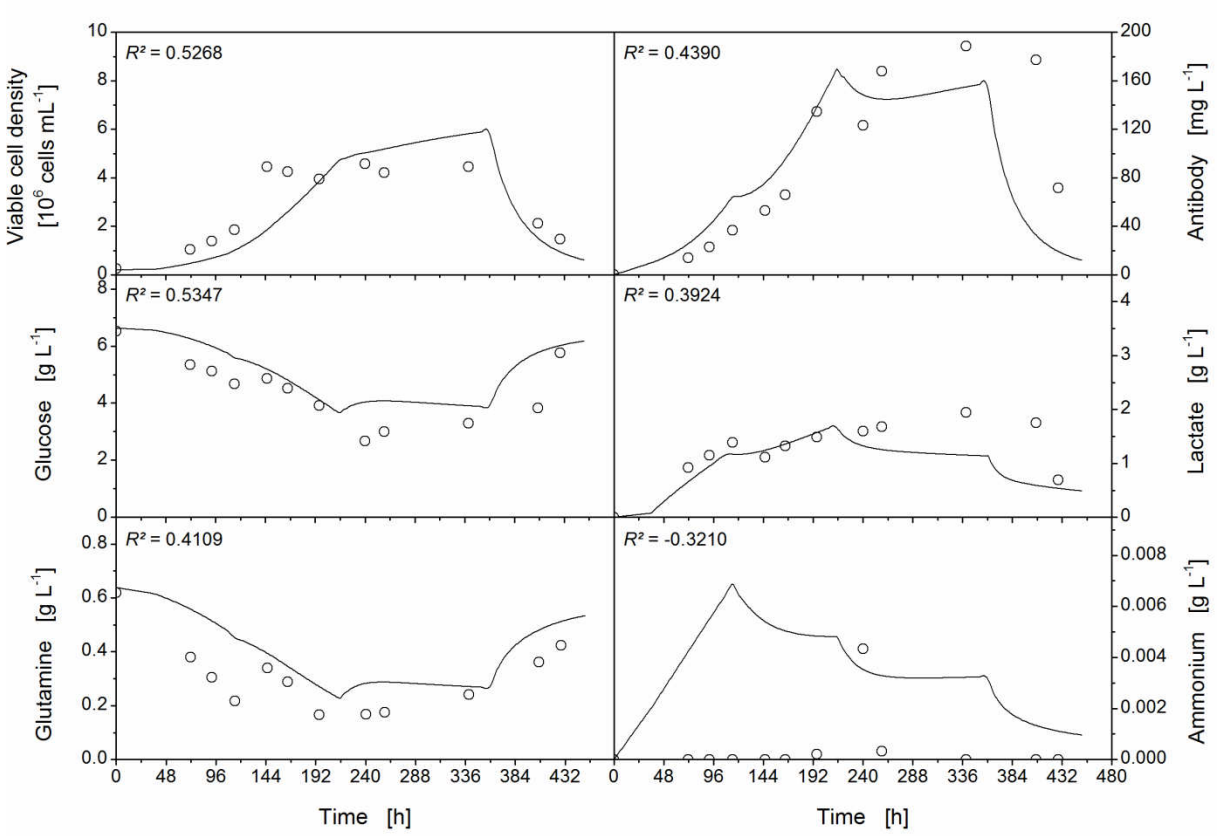

Figure 6-3: Simulation (black line) of the perfusion of CHO DG44 cells applying RFD (open circles) conducted in chapter 5.2.3. Simulation was conducted with matlab, differential equations were solved with the solver ODE45, and constants were taken from the batch data. Parameters were estimated using the Monte Carlo method based on one million randomly generated parameter sets consisting of eleven parameters and fitted to batch data. Batch and perfusion data were taken from chapter 5.2.2 and 5.2.3, respectively.

6.4 Optimized operation conditions for CHO DG 44

In chapters 4 and 5 RFD was optimized regarding the experimental set-up, biocompatibility, long-term stability, minimal membrane area and maximum product recovery. Hence, an optimization of process parameters to improve the productivity of the mammalian cell culture is the next optimization step.

Experiments with CHO cells conducted in chapter 5.2 were used as proof of concept to demonstrate the compatibility of RFD with CHO cells. Three distinct dilution rates of $D = 0.5\ d^{-1}$, $1\ d^{-1}$ and $2\ d^{-1}$ as well as a non-filtered ratio of $NF = 0.1$ were applied based on the critical flux and data provided by Tanja Holland (Fraunhofer IME, Aachen, Germany). An experimental optimization of these parameters was not conducted as this would have been costly in terms of time and money. In contrast, optimized parameters by means of the model developed in chapter 6.1 can be received fast and favorable.

The accumulated product concentration for the experiment conducted in chapter 5.2.3 with and without disturbances is depicted in Figure 6-4. Furthermore, a simulation of a perfusion culture applying RFD is conducted, where the perfusion rate is increased by $D = 0.5\ d^{-1}$ every time a glucose concentration of $4\ g\ L^{-1}$ is reached. Thus, a nearly constant cell concentration is achieved without depletion of the C-source. This strategy is called cell specific perfusion rate (CSPR) and often used for perfusion cultures (Clincke et al., 2013a; Dowd et al., 2003; Ozturk, 1996). CSPR could not be followed in the perfusion experiment of chapter 5.2.3 as glucose could not be detected online. The accumulated product concentration of a RFD simulation following the CSPR perfusion strategy is also shown in Figure 6-4.

According to the simulation results of Figure 6-4 the accumulated product concentration for the perfusion experiment conducted in chapter 5.2.3 would have been approximately three times as high if no disturbances would have occurred. A further increase from 4095 mg L^{-1} accumulated product in the non-filtered stream to 4894 mg L^{-1} can be achieved if the fermentation strategy is adapted to CSPR.

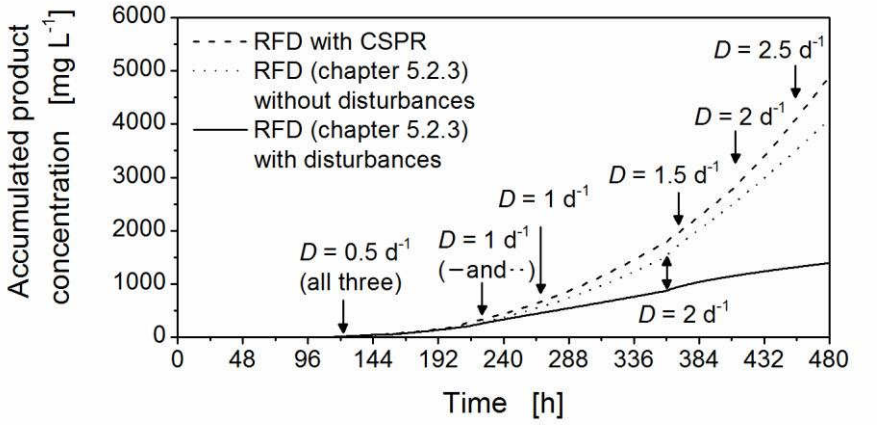

Figure 6-4: Accumulated product concentration for perfusion cultures of CHO DG44 cells applying RFD. *D* was varied according to the perfusion experiment in chapter 5.2.3 or according to the strategy of CSPR. One perfusion culture was simulated with the disturbances which occurred in the respective experiment. Simulation was conducted with Matlab, differential equations were solved with the solver ODE45, and constants were taken from the batch data (chapter 5.2.2.). Parameters were estimated using the Monte Carlo method based on a parameter set of one million randomly generated parameters and fitted to batch data.

The developed model and the parameter estimation conducted in this chapter enable the prediction of perfusion experiments. Optimized setting of non-filtered ratio and dilution rates for higher accumulated product concentration can be chosen based on the predication saving experimental time and costs. However, the experimental proof of the simulation results was not conducted yet. Furthermore, the optimization was conducted exemplarily for one perfusion strategy. Thus, the optimization potential of the model is not tapped. Other optimization strategies with e.g. varying non-filtered ratios during one perfusion experiment can be conducted to enhance the accumulated product concentration further. In addition, the simulation can be used to forecast the impact of disturbances during a perfusion experiment or to improve the feed composition.

Chapter 7

Quasi-continuous Operation of a Reverse-flow Diafiltration Membrane Bioreactor

In this chapter, the improvement of conventional RFD by realizing a quasi-continuous RFD is shown. In conventional RFD the feeding is pulsed, which can cause short-term oxygen limitations and the formation of overflowmetabolites. By sequential operation of three membranes in quasi-continuous RFD feed pulses are avoided. Thus, constant concentration profiles are achieved in the bioreactor. In the first part of this chapter, the pulsed feeding of conventional RFD and its impact on the yeast *H. polymorpha* is investigated. In particular, fermentation conditions which result in repeated short-term oxygen limitations due to pulsed feeding were examined and compared to oxygen unlimited conditions. In the second part, a process scheme for sequential operation of three membranes is introduced. Finally, the sequential operation is experimentally investigated for several dilution and stirring rates.

7.1 Conventional Operation of a Reverse-flow Diafiltration at Two Distinct Dilution Rates

Reverse-flow diafiltration alternates harvesting and feeding over the same membrane, resulting in a continuous C-source limited culture with a pulsed feeding mode. RFD was applied at $D = 0.1\ h^{-1}$ and $D = 0.2\ h^{-1}$ to examine the impact of RFD or rather pulsed feeding on the oxygen supply. As the working volume of the bioreactor was 1.5 L, a homogenous distribution of substrate concentrations such as oxygen or glucose was expected. Hence, the obtained values are representative for the entire bioreactor volume. Figure 7-1 depicts the dissolved oxygen tension (DOT) and the applied stirring rate for the two examined dilution rates. Pulsed feeding of glucose causes an oscillation of the DOT signal as the consumption of glucose and dissolved oxygen is coupled to each other. Whereas the DOT signal oscillates between 25 and 31% and, therewith, has an amplitude of approximately 3% for a dilution rate of $D = 0.1\ h^{-1}$, the oscillation amplitude increases to 30% at a dilution rate of $D = 0.2\ h^{-1}$. In the transition of the dilution rates an excessive amount of glucose reduces the oscillation and the stirring rate is raised until the culture is glucose limited and oscillation of the DOT signal starts again. The average DOT signal for both dilution rates is approximately 30%, which corresponds to the DOT set point of 30% maintained by the stirring rate. However, the minimal DOT signal for the dilution rate of $0.2\ h^{-1}$ is below 10%, which may trigger suboptimal oxygen supply. Whereas a higher DOT set point or a manual adjustment of the stirring rate can both solve this problem for $D = 0.2\ h^{-1}$, the effort to guarantee a sufficient oxygen supply increases with increasing dilution rates as the oscillation amplitude increases as well.

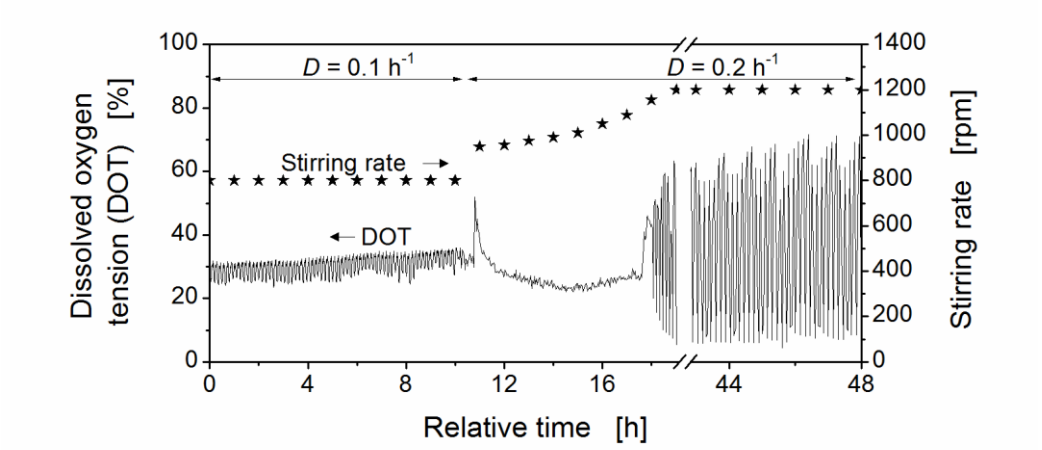

Figure 7-1: Dissolved oxygen tension and stirring rate of a continuous fermentation of *Hansenula polymorpha* pCoM11sc3625 with reverse-flow diafiltration at two dilution rates; all three membranes are operated in parallel. DOT set-point of 30% was maintained by adjusting the stirring rate. Culture conditions: synthetic medium Syn-6, 20 g L^{-1} glucose, V_L = 1.5 L, q = 1 vvm, pH value of 5.5, T = 37 °C, 3 MF02 membranes with a length of 1 m each, a_E = 1.8, a_F = 0.7, NF = 0.5.

7.2 Short Term Oxygen Limitation by Pulsed Feeding

As shown in chapter 7.1, pulsed feeding causes an oscillation of the DOT signal. The higher the dilution rate and, therewith, the amount of glucose fed, the higher the consumption of dissolved oxygen. As a consequence, the oscillation of the DOT signal increases as well. The options to elevate the minimal DOT signal such as increasing stirring rate or aeration rate are limited. Therefore, short-term oxygen limitations cannot be avoided at high dilution rates under feasible fermentation conditions. Thus, the impact of short-term oxygen limitation due to pulsed feeding is examined at a dilution rate of 0.2 h^{-1} using RFD.

Oxygen unlimited fermentation conditions and short-term oxygen limited fermentation conditions caused by a reduction of the stirring rate from 1200 rpm to 1100 rpm are compared in Figure 7-2. The oscillation amplitude of the DOT signal is approximately 30% under oxygen unlimited fermentation conditions at a stirring rate of 1200 rpm or 25% under short-term oxygen limited fermentation conditions at a stirring rate of 1100 rpm, respectively (Figure 7-2 A). The oxygen transfer rate (OTR) signal oscillates with the same frequency as the DOT signal with an amplitude of 30 mmol L^{-1} h^{-1} under oxygen unlimited fermentation conditions or 20 mmol L^{-1} h^{-1} under short-term oxygen limited fermentation conditions, respectively (Figure 7-2 B). The respiratory quotient (RQ) is approximately 1.0 under oxygen unlimited fermentation conditions indicating oxidative growth on glucose. Under short-term oxygen limited fermentation conditions the RQ reaches values of around 1.5 implying the formation of overflow metabolites.

The formation of overflow metabolites is also evident by HPLC measurements (Figure 7-2 C). Ethanol could not be detected under oxygen unlimited fermentation conditions, whereas under short-term oxygen limited fermentation conditions its concentration increases to 1.6 g L^{-1}. Furthermore, short-term oxygen limited fermentation conditions lead to a decrease of 25% of the secreted protein concentration, a single-chain antibody. The concentration of the antibody was approximately 0.2 g L^{-1} under oxygen unlimited and 0.15 g L^{-1} under oxygen short-term limited conditions. It is known that the biomass yield decrease under oxygen limiting fermentation conditions (Enfors et al., 2001). However, the dry cell weight is not notably affected by the examined short-term oxygen limitation and remains at approximately 19 g L^{-1} for both conditions. The concentration of glucose remains undetectable for both settings.

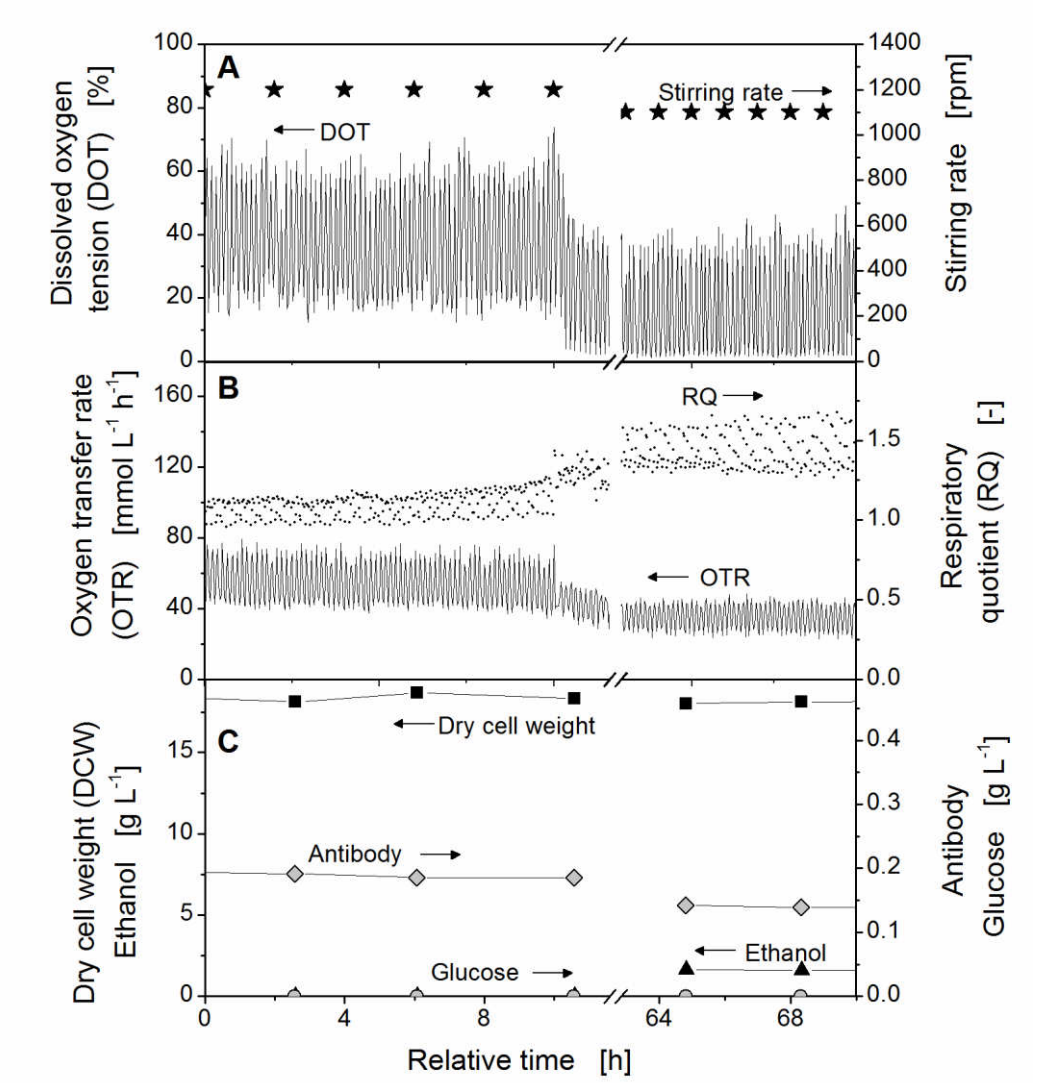

Figure 7-2: Continuous fermentation of *Hansenula polymorpha* pCoM11sc3625 with reverse-flow diafiltration at oxygen unlimited and short-term limited conditions caused by different stirring rates; all three membranes are operated in parallel. Stirring rate was adjusted manually; DOT set-point was not maintained. Culture conditions: synthetic medium Syn-6, 20 g L^{-1} glucose, V_L = 1.5 L, q = 1 vvm, pH value of 5.5, T = 37 °C, 3 MF02 membranes with 1 m length each, a_E = 1.8, a_F = 0.7, NF = 0.5, D = 0.2 h^{-1} A) Dissolved oxygen tension (DOT) and stirring rate. B) Oxygen transfer rate (OTR) as well as respiratory quotient (RQ). C) Dry cell weight (DCW), antibody, ethanol and glucose concentration.

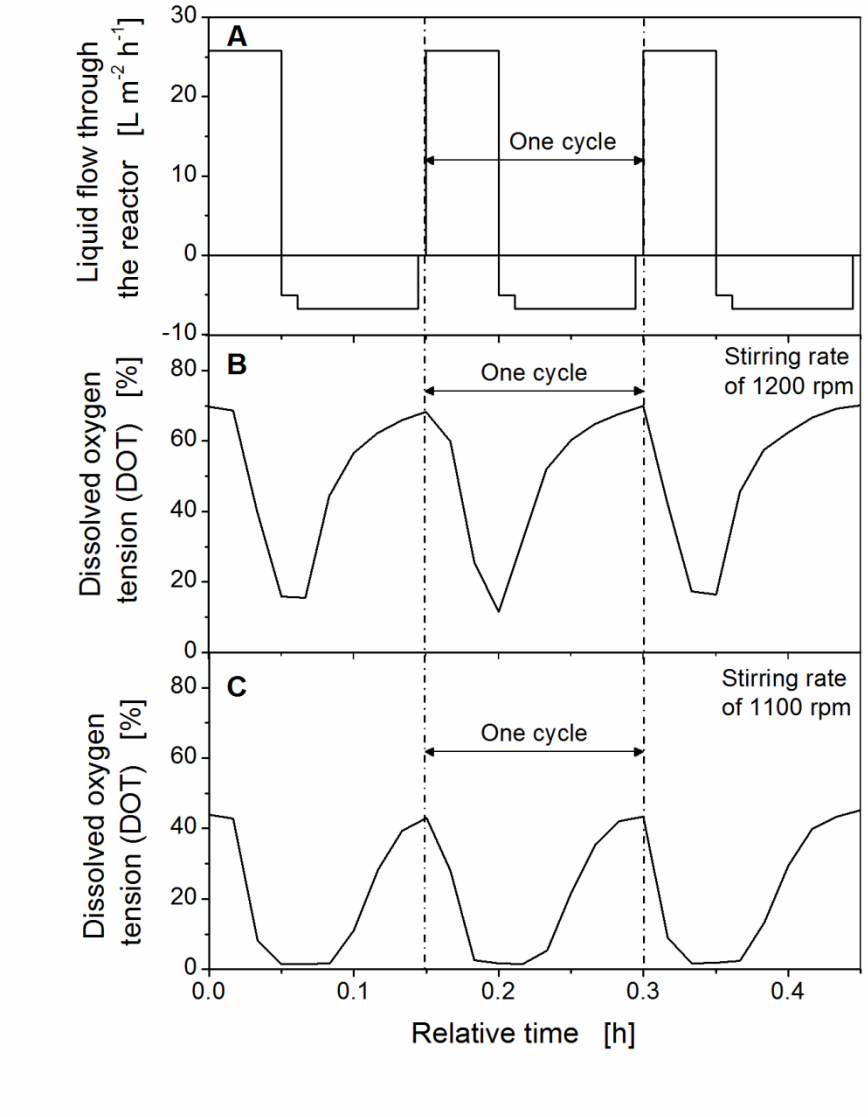

Figure 7-3: True to scale time dependent liquid flow of reverse-flow diafiltration and the resulting dissolved oxygen tension at different stirring rates for a continuous fermentation of *Hansenula polymorpha* pCoM11sc3625 at a dilution rate of D = 0.2 h^{-1}; all three membranes are operated in parallel. Culture conditions: synthetic medium Syn-6, 20 g L^{-1} glucose, V_L = 1.5 L, q = 1 vvm, pH value of 5.5, T = 37 °C, 3 MF02 Membranes a 1 m a_E = 1.8, a_F = 0.7, NF = 0.5. A) True to scale time dependent liquid flow B) Dissolved oxygen tension (DOT), not oxygen limited C) Dissolved oxygen tension (DOT), oxygen limited.

A magnification of the DOT signal under oxygen unlimited and short-term oxygen limited fermentation conditions is compared in Figure 7-3 for the reverse-flow diafiltration mode using all three membranes in parallel. The examined time span is plotted relative to each other to synchronize the reverse-flow diafiltration sequences in all diagrams of Figure 7-3. The step sequence starts with feeding into the membrane bioreactor. Simultaneously, a sharp decrease of the DOT signal can be noticed as long as feeding is proceeded. The DOT signal remains at the lower level for a few seconds before it rises to the higher level until feeding starts again. Whereas under oxygen unlimited fermentation conditions at a stirring rate of 1100 rpm the DOT signal reaches a minimum of approximately 10% for a few seconds (Figure 7-3 B), the DOT signal remains close to zero for a short period of time indicating the oxygen limitation (Figure 7-3 C). The simultaneous behavior of the DOT signal of both fermentation conditions in correlation with the flow generated by the RF in Figure 7-3 proofs that the pulsed feeding is the main reason for the oscillating DOT signal.

Beside the pulsed feeding, the other three steps of RFD (flushing, emptying and permeate) or the feeding through the membrane could contribute to the oscillating DOT signal as these properties are unique in RFD and not applied in conventional continuous cultures. To verify that pulsed feeding is the main cause of the oscillating DOT signal, an experiment with pulsed feeding was performed in the bioreactor without membranes (see also Figure 2-6, set up with dashed-dotted line and dotted line). To achieve comparable fermentation conditions, the feeding frequency and duration was adjusted according to the RFD experiments. Thus, 180 s of feeding alternated with 360 s of feeding stop (compare also Table 2-4). All other fermentation parameters were kept as in the previous experiment including the setting of the stirring rate of 1200 rpm and 1100 rpm (compare Figure 7-2).

Figure 7-4 depicts the obtained data. The DOT signal oscillates between 10 and 70% or 0 and 50% under oxygen unlimited fermentation conditions or short-term oxygen limited fermentation conditions, respectively (Figure 7-4 A). In this experiment, the oscillation of the DOT signal is more uniform than in the experiment with RFD (compare Figure 7-2 A and Figure 7-4 A). This may be caused by the medium provided through the membrane. In the membrane concentration gradients may occur due to RFD mode in contrast to pulsed feeding via a feed inlet. However, the frequency and the average DOT signals in both experiments are comparable. Also, data from the exhaust gas analysis – OTR and RQ – are similar regarding

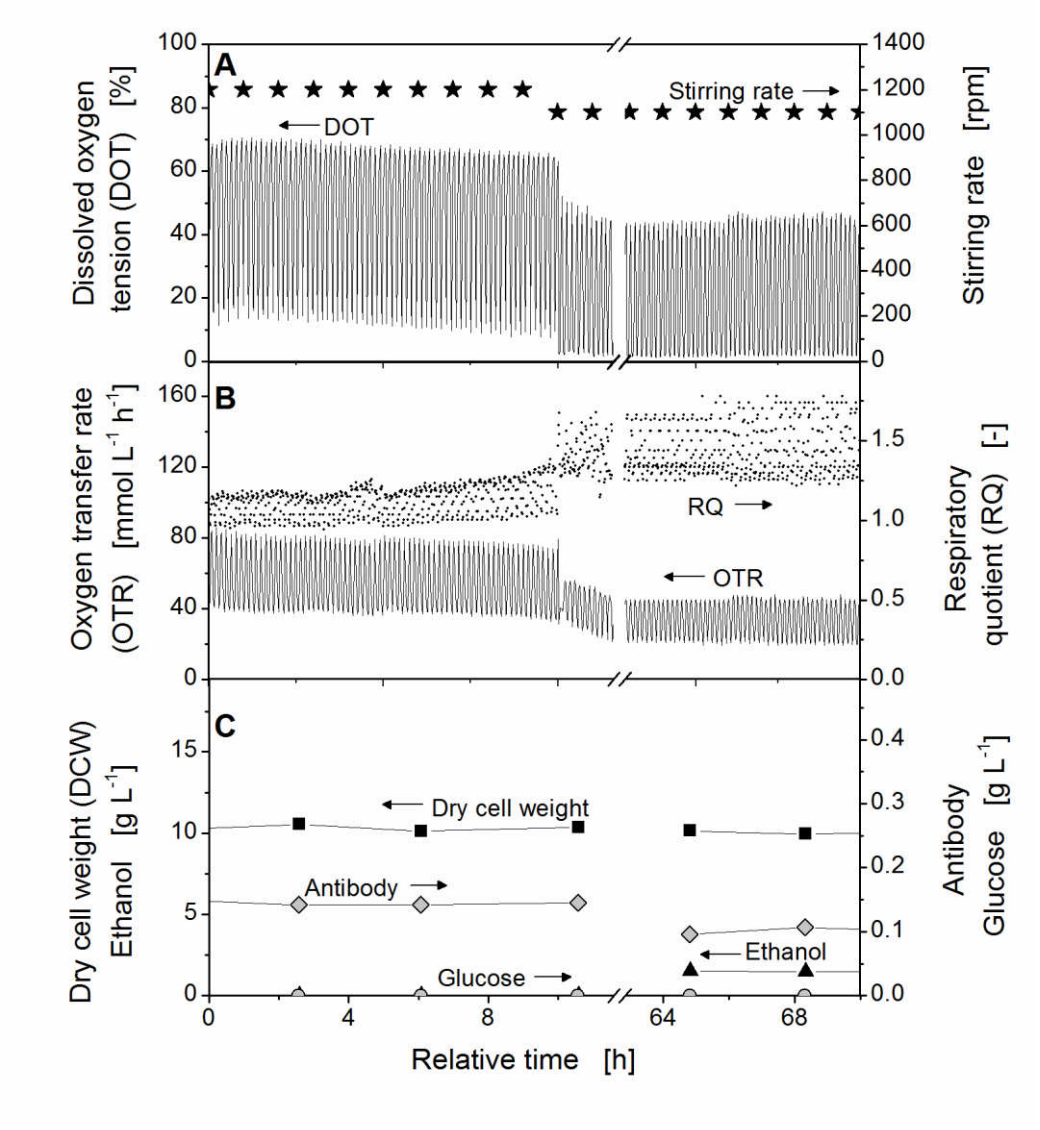

Figure 7-4: Continuous fermentation of *Hansenula polymorpha* pCoM11sc3625 without membranes applying pulsed feeding at different stirring rates: 180 s of feeding alternates with 360 s of feeding stop. Stirring rate was adjusted manually; DOT set-point was not maintained. Culture conditions: synthetic medium Syn-6, 20 g L^{-1} glucose, V_L = 1.5 L, q = 1 vvm, pH value of 5.5, T = 37 °C, D = 0.2 h^{-1}. A) Dissolved oxygen tension (DOT) and stirring rate. B) Oxygen transfer rate (OTR) as well as respiratory quotient (RQ). C) Dry cell weight (DCW), antibody, ethanol and glucose concentration.

the measured values as well as glucose and ethanol concentrations. The amount of dry cell weight is 10 g L^{-1}, which is half of the concentrations detected in the experiment with RFD. As cell retention in RFD was set to 50% this value was expected for an experiment without membranes. Furthermore, the absolute level of antibody concentration is decreased in the experiment without membrane (Figure 7-4) in comparison to the experiment with RFD (Figure 7-2). This can also be explained by the absence of cell retention (Meier et al., 2014). However, deviations regarding DOT, OTR, RQ, glucose and ethanol concentrations in Figure 7-2 and 6-4 could not be noticed. Hence, the pulsed feeding of glucose can be regarded as the main reason for an oscillating DOT signal during RFD operation.

A decrease of the product concentration has to be prevented as antibodies are high-value products. Thus, pulsed feeding in RFD has to be avoided.

7.3 Sequential Operation of Membranes in Reverse-flow Diafiltration

RFD alternates harvest and feeding causing an oscillation of DOT signal. A more uniform feeding by reducing the step times of the non-feeding steps – permeate, emptying and flushing – cannot be conducted without a loss of efficiency. Therefore, three membranes arranged in parallel operating sequentially were used to provide a uniform feed supply into the membrane bioreactor.

A true to scale representation of the time dependent flows in and out of the bioreactor for the sequential operation mode is shown in Figure 7-5. At the left hand side the liquid flows for the single membranes (① - ③) are depicted, operated at their particular time sequences. Each sequence is time-shifted by 180 s as this is the feed step time. Summing up the flows of the three membranes results in an overall flow illustrated at the top right hand side. The flow into

the bioreactor is continuous as the three membranes seamlessly alternate in their feeding action. Also the non-filtered product stream is purged continuously as the pump control is too

slow to respond to the small volume changes due to RFD mode. Only the flushing, emptying and permeate step affect the overall permeate output resulting in a step pattern. Hence, the fermenter volume merely varies slightly, which is often observed in cell retention systems (Clincke et al., 2013a; Tang et al., 2007). The average permeate output is depicted as a dotted line in the true to scale representation of the overall flows in Figure 7-5. A permeate output slightly below the average indicates that one membrane is operated in the permeate step and one membrane is conducting the emptying step (compare start of the cycle in Figure 7-5: membranes no. 2 and 3 at left hand side as well as overall permeate output at right hand side). Followed by this step combination, two membranes are operated in the permeate step resulting in a permeate output above the average. Afterwards one of the membranes is flushed causing the lowest permeate output. After all four steps were conducted by every membrane, one cycle is completed. The step sequence and the step times for a cycle of three membranes operated sequentially are shown in a tabular form in Figure 7-5.

Settings of the feed and the permeate pumps for the four steps of RFD are given in Table 2-5 depending on the dilution rate. For instance, at the beginning of a cycle membrane 1 is operated in the feed step, membrane 2 in the permeate step and membrane 3 in the emptying step (compare Figure 7-5). If a dilution rate of 0.1 h^{-1} should be applied, the feed pump of membrane 1 generates a flow rate of 29.3 L m^{-2} h^{-1} whereas the permeate pump of membrane 1 stops (feed step). Simultaneously, the feed pump of membrane 2 stops while the permeate pump generates a flow rate of 6.0 L m^{-2} h^{-1} (permeate step). At the same time the feed and the permeate pump of membrane 3 operates with a flow rate of 50 L m^{-2} h^{-1} and 10 L m^{-2} h^{-1} into the direction of the feed tank, respectively (emptying step).

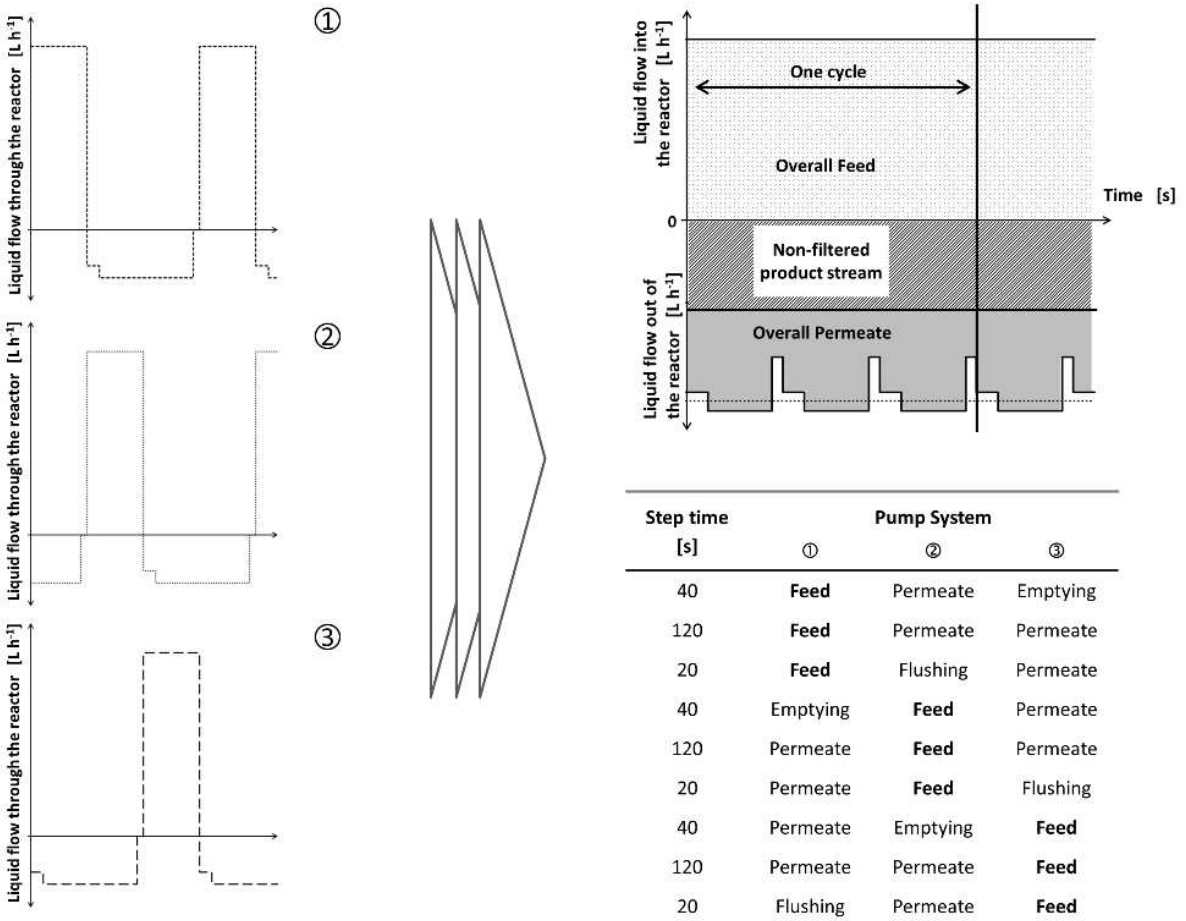

Step time [s]	Pump System ①	②	③
40	**Feed**	Permeate	Emptying
120	**Feed**	Permeate	Permeate
20	**Feed**	Flushing	Permeate
40	Emptying	**Feed**	Permeate
120	Permeate	**Feed**	Permeate
20	Permeate	**Feed**	Flushing
40	Permeate	Emptying	**Feed**
120	Permeate	Permeate	**Feed**
20	Flushing	Permeate	**Feed**

Figure 7-5: True to scale representation of time dependent flow into and out of the reactor of three membranes operated sequentially in the reverse-flow diafiltration mode (① - ③ left hand side) and the resulting overall feed, permeate and non-filtered product stream flow (right hand side) for a cell retention of 50%. The average permeate output is represented by a dotted line. It should be noted that the integral of the flows pumped in and out of the bioreactor equals zero in every cycle. The non-filtered product stream is 50% of the overall feed, equal to Figure 2-5. Relative heights of feed and non-filtered product stream differ in comparison to Figure 2-5 as the overall feed is split into three membranes operated sequentially. Furthermore, steps and step times for the sequential operation of all three membranes are stated in the Table.

7.4 Preventing Oxygen Limitation by Sequential Operation

The implementation of sequential operation for a dilution rate of 0.2 h^{-1} is illustrated in Figure 7-6. For better comparison, the same fermentation conditions as in Figure 7-2 were applied, except for the sequential feeding. The DOT signal oscillates around 45 – 55% and 35 - 45% for a stirring rate of 1200 rpm and 1100 rpm, respectively (Figure 7-6 A). Although the oscillation of the DOT signal cannot be completely prevented as in common continuous fermentations, a significant reduction of the amplitude of the oscillation could be observed. The small oscillation could be caused by the mixture of feed and permeate present in the feed tubing at the beginning of the feed step. Thus, a lower glucose concentration is pumped into the bioreactor for a short period of time, every time the membrane feeding operation is sequentially changed. Another explanation for the small oscillation of the DOT signal could be differences in the feed flow of the three manually calibrated feed pumps. However, sequential feeding strongly reduces the oscillation. Thus, fermentation conditions are more constant and oxygen limitation could be completely avoided.

The OTR and RQ signals are slightly oscillating for both stirrer settings (Figure 7-6 B), though the RQ remains around 1.0 indicating oxidative growth on glucose. This observation is verified by the measurement of metabolites (Figure 7-6 C). Neither glucose nor ethanol could be detected for the chosen stirrer settings. The concentration of antibodies and the dry cell weight remain constant for both settings. Thus, the oxygen supply at a stirring rate of 1100 rpm is not sufficient for membranes operated in parallel to avoid short-term oxygen limitations (Figure 7-2), but completely sufficient for membranes operated sequentially.

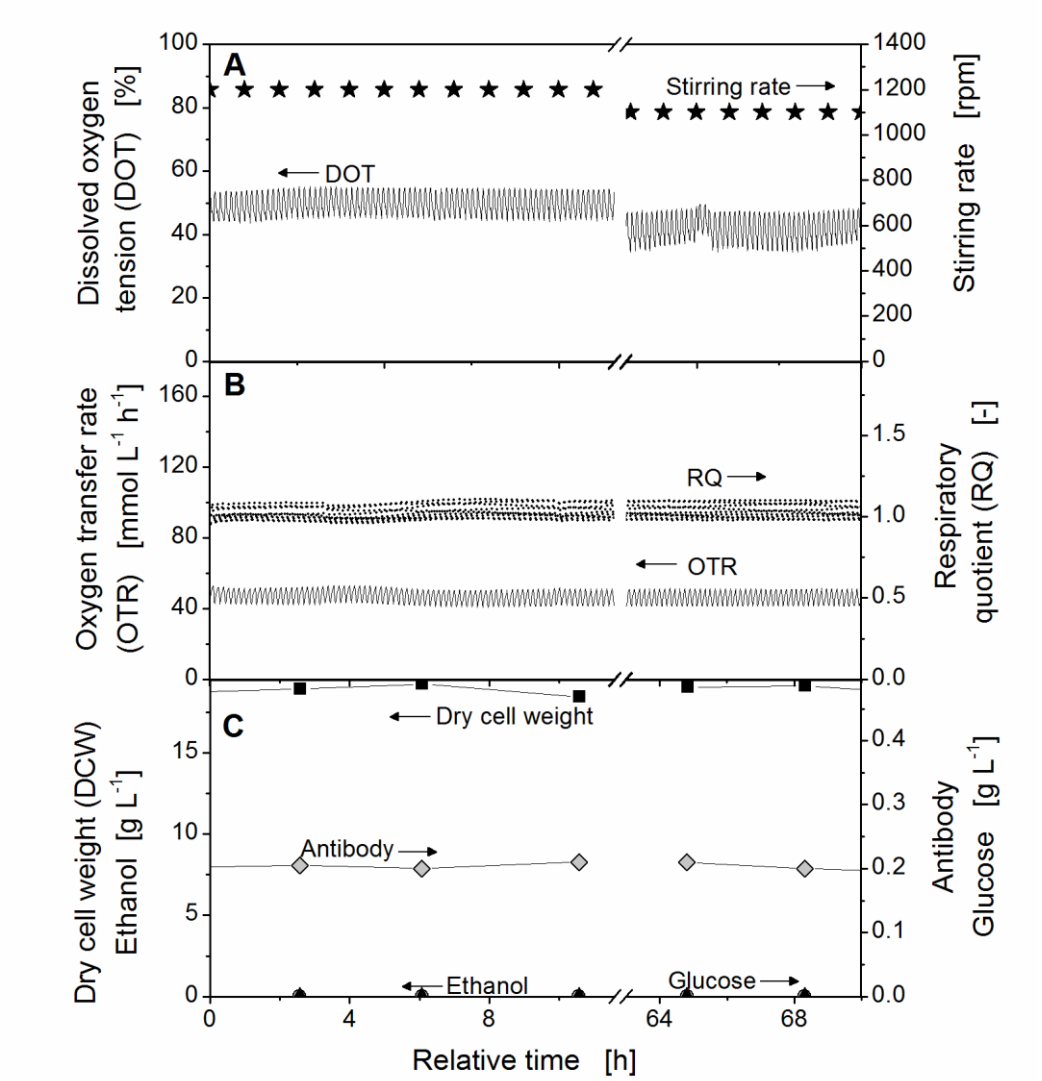

Figure 7-6: Continuous fermentation of *Hansenula polymorpha* pCoM11sc3625 with reverse-flow diafiltration at different stirring rates; three membranes are operated sequentially. Culture conditions: synthetic medium Syn-6, 20 g L^{-1} glucose, V_L = 1.5 L, q = 1 vvm, pH value of 5.5, T = 37 °C, 3 MF02 Membranes a 1 m, a_E = 1.8, a_F = 0.7, NF = 0.5, t_C = 510s, D = 0.2 h^{-1} A) Dissolved oxygen tension (DOT) and stirring rate. B) Oxygen transfer rate (OTR) as well as respiratory quotient (RQ). C) Dry cell weight (DCW), antibody, ethanol and glucose concentration.

7.5 Sequential Operation at Several Distinct Dilution Rates

The effect of an oscillating DOT signal due to pulsed feeding by membranes operated in parallel increases with increasing dilution rates. Hence, the sequential feeding was examined for dilution rates in the range of 0.1 h^{-1} to 0.5 h^{-1}. The results are depicted in Figure 7-7. As already observed in the last chapter for a dilution rate of 0.2 h^{-1}, small oscillations of the DOT signal occur with sequential operation of the membranes for the applied dilution rates (Figure 7-7 A). Sequential feeding at a dilution rate of 0.5 h^{-1} causes the biggest oscillations in the range of 20 to 60%. Nevertheless, the oscillations for this dilution rate are smaller than the oscillations of membranes operated in parallel at a dilution rate of 0.2 h^{-1} (Figure 7-2 A). Whereas a stirring rate of 1200 rpm was necessary to provide a sufficient oxygen supply for membranes operated in parallel (Figure 7-2 A), this rate could be reduced to 900 rpm if membranes are operated sequentially saving energy and reducing cell damage. Sufficient oxygen supply for all dilution rates is also indicated by the OTR and RQ (Figure 7-7 B). The RQ for all applied dilution rates is around 1.0 implying oxidative growth on glucose. This conclusion is confirmed by measurement of metabolites as neither ethanol nor glucose could be detected (Figure 7-7 C). The dry cell weight remains constant for all applied dilution rates. The concentration of antibodies decreases at higher dilution rates. This effect is caused by the formation of a minimal fouling layer and was observed before in chapter 5.1.2. Sequential feeding proves to minimize oscillations of the DOT signal. Thus, higher dilution rates can be applied at lower stirring or aeration rates to supply sufficient oxygen saving energy and reducing cell damage.

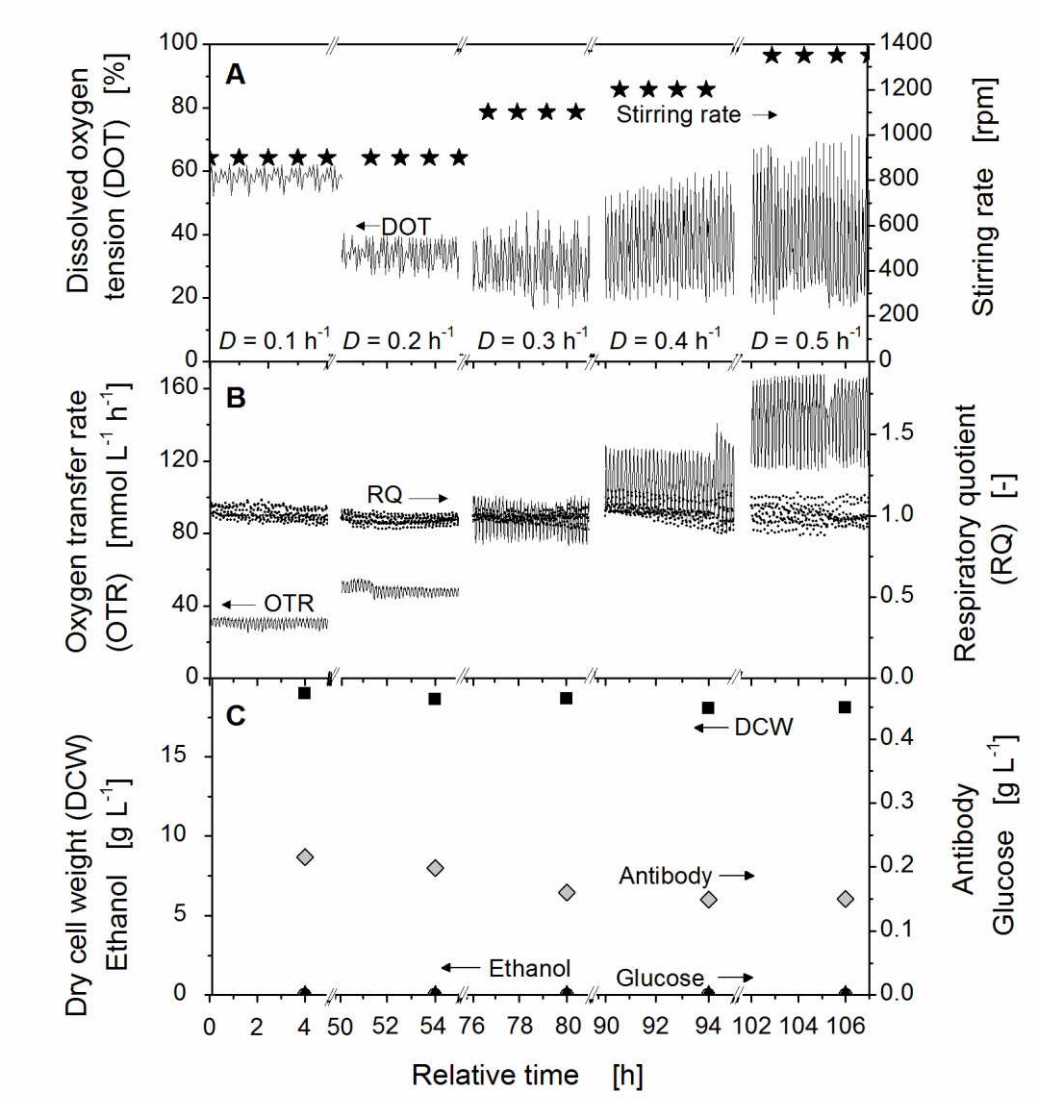

Figure 7-7: Continuous fermentation of *Hansenula polymorpha* pCoM11sc3625 with reverse-flow diafiltration at different dilution rates; three membranes are operated sequentially. Culture conditions: synthetic medium Syn-6, 20 g L^{-1} glucose, V_L = 1.5 L, q = 1 vvm, pH value of 5.5, T = 37 °C, 3 MF02 Membranes a 1 m, a_E = 1.8, a_F = 0.7, NF = 0.5, t_C = 510s, D = 0.2 h^{-1} A) Dissolved oxygen tension (DOT) and stirring rate. B) Oxygen transfer rate *(OTR*) as well as respiratory quotient (RQ). C) Dry cell weight (DCW), antibody, ethanol and glucose concentration.

Chapter 8

Conclusion and Outlook

The aim of this thesis was the enhancement and establishment of Reverse-flow diafiltration (RFD), an *in situ* product recovery process. In RFD medium supply alternates with product recovery over the same submerged hollow fiber membrane. Thus, cells are retained gently while simultaneously a potential fouling layer is minimized. The requirements for this process were expressed in the project MoBiDiK "Modulare Bioproduktion – Disposable und Kontinuierlich":

- Biocompatible
- Sterile
- Robust
- Long-term stable
- Continuous high cell retention
- High antibody transmission
- Producible as single-use system

Non-biocompatible additives from polymer materials may leach out in the culture medium especially during heat sterilization or in presence of solvents and inhibit metabolic activity. Thus, it is crucial to precisely understand this leaching behavior. This thesis has shown the Respiration Activity MOnitoring System (RAMOS) to be an easy to apply and very sensitive device to qualify materials before their application in culture systems. Being fast, reliable and cost-effective, the RAMOS device can prevent the use of detrimental polymers, whose

plasticizers might leach out and retard the growth of microorganism. This online technique ultimately precludes the need for multiple sampling and may be used to determine a metabolic activity inhibition threshold of leaching from polymer materials.

Heat sterilization accelerates leaching of polymer additives. Since biotechnical processes may require heat sterilization, it is relevant to include this kind of pretreatment for the evaluation of leaching. Otherwise, if e.g. gamma-sterilization is applied (with no need for heat-sterilization), the polymer material under investigation could be placed in the culture medium for a time span corresponding to an average culture time at culture temperature. Thus, application conditions are mimicked with this test. A culture with this medium could afterwards be monitored by RAMOS to identify the influence of compounds which have potentially leached out of the polymer.

This work and other investigations in literature prove that plasticizers leach out from polymer materials. Some plasticizers are toxic to human, animals, mammalian cells and, as shown here, to microorganisms. Therefore, the processing as well as the amount of these kinds of plasticizers and other harmful additives should be considered and tested by the producers as well as the manufactures of polymer materials. In this thesis a biocompatibility test was conducted for all applied polymers with the respective organism prior application.

RFD consists of four subsequent steps: feed, emptying, permeate and flushing. The optimal emptying and flushing steps prevented mixing of permeate with medium and increase the permeate output. Based on calculations of fluid flows the four steps were configured with respect to pump settings and step times. The flow of the feed and permeate steps as well as the number of applied membranes are calculated as a function of the applied dilution rate. The results of the configuration are formulas to calculate the pump settings for the single steps and the resulting step times, which are summarized in Table 4-1. This table was the basis for all settings applied in biological experiments within this thesis.

A critical transmembrane pressure increase of 45 Pa min^{-1} should not be exceeded by the chosen membrane-medium-culture system to maintain stable filtration properties. The critical specific flow rate over the membrane for yeast and CHO cultures applying RFD were

determined as 21 L m^{-2} h^{-1} and 9 L m^{-2} h^{-1}, resulting in a maximum applicable dilution rate of approximately D = 0.7 h^{-1} and D = 1 d^{-1} for stable long-term applications, respectively. The resulting necessary filtration area for RFD is smaller than most conventional available retention systems. Systems with less filtration area were reported to tend to irreversible fouling.

Alternating substrate and product streams results in a feed pulse instead of a continuous feeding, causing oscillations of the dissolved oxygen tension. The amplitude of the oscillation increases with increasing dilution rate. Hence, also the effort to guarantee a sufficient oxygen supply increases e.g. increasing the stirring and / or aeration rate. Short-term oxygen limitations cause the formation of overflow metabolites like ethanol as it was shown in this study for *H. polymorpha*. Furthermore, the product concentration decreases during short-term oxygen limitation.

In this thesis, a quasi-continuous feeding was achieved by sequential operation of three membranes. The membranes were operated according to the step sequence of reverse-flow diafiltration, but time-shifted by 180 s to generate a continuous flow into the membrane bioreactor. Thus, oscillation of the dissolved oxygen tension signal can be minimized. The oscillation amplitude, which occurs at a dilution rate of 0.5 h^{-1} for sequential operation, is smaller than the amplitude corresponding to a dilution rate of 0.2 h^{-1} for membranes operated parallel. Thus, sequential operation results in more constant fermentation conditions than parallel operation. This is particularly relevant for microorganisms with a fast aerobic metabolism to reduce the effort for a sufficient oxygen supply and avoid a decrease of product concentration.

Oscillations could not be completely prevented due to a mixture of feed and permeate liquid pumped into the bioreactor at the beginning of the feed step. A higher flow rate at the beginning of the feed step could lead to a constant total amount of glucose pumped into the bioreactor and, thus, a steady dissolved oxygen tension.

A continuous fermentation of *H. polymorpha* with 50% cell retention could be conducted with dilution rates ranging from 0.1 h^{-1} to 0.65 h^{-1}. Dry cell weight concentration and the washout point could be doubled. Antibody transmission was constantly between 70 – 80%, which is a high value in comparison with data presented in literature. The TMP increase became greater with higher dilution rates, but did not exceed the critical value of 45 Pa min^{-1}, indicating that a stable long-term filtration process was achieved. Space-time-yields were three-times that of a continuous fermentation without cell retention due to the higher applicable dilution rates.

A CHO perfusion culture applying RFD yields high viabilities of over 90% for the whole culture time. The antibody transmission was between 40 and 60%, which is a common value for filtration of proteins in literature. Presumably, the utilization of membranes which do not tend to form a polar layer can enhance this value. The filtration performance of RFD was predictable and stable for dilution rates up to D = 1 d^{-1}. Thus, RFD proved to be also an *in situ* cell retention device appropriate for cultivation of CHO cells.

Simulations are powerful tools to predict experiments while saving time and costs. Within this work, a model for batch and RFD cultivations of CHO DG44 cells was developed. Based on the batch data constants and parameters of the cell line were calculated and estimated in Matlab, respectively. The batch culture could be simulated with a high accuracy; the perfusion culture was simulated satisfying taking into account that solely one batch experiment was the basis for the parameter estimation and the calculation of the constants. The simulation of RFD was used to optimize the fermentation strategy. The accumulated product concentration of the experiment conducted was 1390 mg L^{-1}. The same perfusion experiment without disturbances would achieve 4095 mg L^{-1} according to the simulation. The perfusion strategy of CSPR achieves an accumulated product concentration of 4894 mg L^{-1}.

Simulations with varying dilution rates or non-filtered ratios during one perfusion experiment can be conducted to enhance the space-time-yield further. In addition, the simulation can forecast the impact of disturbances during a perfusion experiment or used to improve the feed composition. Thus, the developed model is an efficient tool for investigations of cultivation systems and should be to support experiments.

Reverse-flow diafiltration proved to fulfil the requirements stated in MoBiDiK: RFD is a fail-safe and easy applicable *in situ* product recovery process with low investment costs and minimal equipment requirements. Long-term stable filtration performance and a sufficient antibody transmission as well as the possibility to integrate it in single-use bags characterize RFD as a convenient process for MoBiDiK especially suitable for shear sensitive cells or organism prone to oxygen limitation.

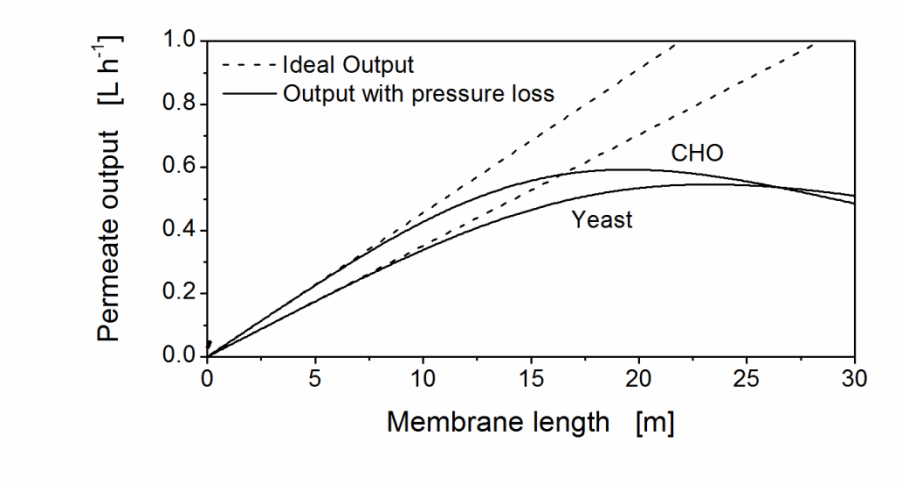

Figure 8-1: Ideal and reduced permeate output due to pressure loss for yeast and CHO cells. Permeate output was calculated based on the critical transmembrane flux of 21 L m^{-2} h^{-1} or 9 L m^{-2} h^{-1} for *H. polymorpha* or CHO cells, respectively. Settings of RFD: a_E = 1.69, a_F = 0.7, t_C = 510s and *NF* = 0.5 or 0.9 for *H. polymorpha* or CHO cells, respectively.

To realize an industrial application of RFD for CHO cells, an up scaling to a fermenter volume of 10 L should be conducted. In comparison to the experiments conducted in 1 L scale in this thesis, a 10-fold membrane area should be applied. Thus, applying the same membrane, a total membrane length of 10 m has to be integrated into the bioreactor. Three membranes with 3.3 m length each are recommended to minimize spatial heterogeneities as shown in chapter 7. A noticeable pressure loss accompanied with decreased filtration performance is not expectable for a 3.3 m membrane length as shown in Figure 8-1. Reduced permeate output due to pressure loss is calculated for various membrane lengths and the

settings of RFD based on the principal of pipe flow. Furthermore, for an industrial application, sterile single-use bags with integrated membrane modules have to be commercially produced. The integration of membranes has to be conducted by the bag producer as he guarantees for sterility.

Application of RFD for filamentous organisms or organisms, which tend to grow on superficies, would be challenging as membrane blocking is more likely to occur. However, based on filtration experiments to determine the transmembrane pressure increase, the required membrane area to achieve long-term stability can be calculated and, thus, application of RFD should be possible.

Bibliography

Anderlei T, Büchs J. 2001. Device for sterile online measurement of the oxygen transfer rate in shaking flasks. Biochemical Engineering Journal 7:157-162.

Anderlei T, Zang W, Papaspyrou M, Büchs J. 2004. Online respiration activity measurement (OTR, CTR, RQ) in shake flasks. Biochemical Engineering Journal 17:187-194.

Attfield PV, Kletsas S, Veal DA, van Rooijen R, Bell PJL. 2000. Use of flow cytometry to monitor cell damage and predict fermentation activity of dried yeasts. Journal of Applied Microbiology 89:207-214.

Avgerinos GC, Drapeau D, Socolow JS, Mao J, Hsiao K, Broeze RJ. 1990. Spin filter perfusion system for high-density cell culture - production of recombinant urinary tpye plasminogen-activator in CHO cells. Nature Biotechnology 8:54-58.

Badrilla Ltd. 2014. Antibodies. http://badrilla.com/antibodies.html (accessed 10.07.2014).

Baker RW. 2004. Membrane technology and applications West Sussex, England: John Wiley & Sons, Ltd.

Banik GG, Heath CA. 1995. Partial and total cell retention in a filteration-based homogeneous perfusion reactor. Biotechnology Progress 11:584-588.

Baptista RP, Fluri DA, Zandstra PW. 2013. High density continuous production of murine pluripotent cells in an acoustic perfused bioreactor at different oxygen concentrations. Biotechnology and Bioengineering 110:648-655.

Bastidas O. 2013. Cell counting with neubauer chamber basic hemocytometer usage http://www.celeromics.com/en/resources/docs/Articles/Cell-counting-Neubauer-chamber.pdf (accessed 18.10.2013).

Beckmann L. 2013. A Novel Disposable ISPR Membrane Bioreactor: Conceptual Design, Development and Performance Testing [Diploma thesis]. Aachen: RWTH Aachen.

Beitz W, Küttner K-H, Davies BJ, editors. 1994. Dubbel - Handbook of mechanical engineering. Berlin: Springer.

Bleckwenn NA, Golding H, Bentley WE, Shiloach J. 2005. Production of recombinant proteins by vaccinia virus in a microcarrier based mammalian cell perfusion bioreactor. Biotechnology and Bioengineering 90:663-674.

Borzani W, Vairo MLR. 1958. Quantitative adsorption of methylene blue by dead yeast cells. Journal of Bacteriology 76:251-255.

Brooks JD, Meers JL. 1973. Effect of discontinuous methanol addition on growth of a carbon-limited culture of *Pseudomonas*. Journal of General Microbiology 77:513-519.

Brunner D, Frank J, Appl H, Schoffl H, Pfaller W, Gstraunthaler G. 2010. Serum-free cell culture: The serum-free media interactive online database. Altex-Alternatives to Animal Experimentation 27:53-62.

Büntemeyer H, Bödeker BG, Lehmann J. 1987. Membranes-stirrer-reactor for bubble free aeration and perfusion. Modern approaches to animal cell technology: European Society for Animal Cell Technology, the 8. Meeting. London: Butterworth. p 411–419.

Bütehorn S, Utiu L, Kuppers M, Blumich B, Wintgens T, Wessling M, Melin T. 2011. NMR imaging of local cumulative permeate flux and local cake growth in submerged microfiltration processes. Journal of Membrane Science 371:52-64.

Cacciatore JJ, Chasin LA, Leonard EF. 2010. Gene amplification and vector engineering to achieve rapid and high-level therapeutic protein production using the Dhfr-based CHO cell selection system. Biotechnology Advances 28:673-681.

Cairns J. 1986. The myth of the most sensitive species. Bioscience 36:670-672.

Caron AW, Tom RL, Kamen AA, Massie B. 1994. Baculovirus expression system scaleup by perfsuion of high density SF-9 cell cultures. Biotechnology and Bioengineering 43:881-891.

Carstensen F. 2013. *In situ* product recovery from fermentation processes using reverse-flow diafiltration [Dissertation]. Aachen, Germany: RWTH Aachen.

Carstensen F, Apel A, Wessling M. 2012a. *In situ* product recovery: Submerged membranes vs. external loop membranes. Journal of Membrane Science 394:1-36.

Carstensen F, Klement T, Büchs J, Melin T, Wessling M. 2013. Continuous production and recovery of itaconic acid in a membrane bioreactor. Bioresource Technology 137:179-187.

Carstensen F, Marx C, André J, Wessling M. 2012b. Reverse-flow diafiltration for continuous *in situ* product recovery. Journal of Membrane Science 421:39-50.

Castilho L, Medronho R. 2002. Cell retention devices for suspended-cell perfusion cultures. In: Schügerl K, Zeng AP, Aunins JG, Bader A, Bell W, Biebl H, Biselli M, Carrondo MJT, Castilho LR, Chang HN and others, editors. Tools and Applications of Biochemical Engineering Science: Springer Berlin Heidelberg. p 129-169.

Choo CY, Tian Y, Kim WS, Blatter E, Conary J, Brady CP. 2007. High-level production of a monoclonal antibody in murine myeloma cells by perfusion culture using a gravity settler. Biotechnology Progress 23:225-231.

Clincke M-F, Mölleryd C, Zhang Y, Lindskog E, Walsh K, Chotteau V. 2013a. Very high density of CHO cells in perfusion by ATF or TFF in WAVE bioreactor™. Part I. Effect of the cell density on the process. Biotechnology Progress 29:754-767.

Clincke MF, Molleryd C, Samani PK, Lindskog E, Faldt E, Walsh K, Chotteau V. 2013b. Very high density of chinese hamster ovary cells in perfusion by alternating tangential flow or tangential flow filtration in WAVE bioreactorpart II: Applications for antibody production and cryopreservation. Biotechnology Progress 29:768-777.

Coelho S. 2012. Implementation and optimization of the reverse-flow diafiltration for *in situ* product recovery [Master thesis]. Aachen: RWTH Aachen University.

da Silva TL, Reis A, Roseiro JC, Hewitt CJ. 2008. Physiological effects of the addition of n-dodecane as an oxygen vector during steady-state *Bacillus licheniformis* thermophillic fermentations perturbed by a starvation period or a glucose pulse. Biochemical Engineering Journal 42:208-216.

Dalm MCF, Jansen M, Keijzer TMP, van Grunsven WMJ, Oudshoorn A, Tramper J, Martens DE. 2005. Stable hybridoma cultivation in a pilot-scale acoustic perfusion system: Long-term process performance and effect of recirculation rate. Biotechnology and Bioengineering 91:894-900.

Deere D, Shen J, Vesey G, Bell P, Bissinger P, Veal D. 1998. Flow cytometry and cell sorting for yeast viability assessment and cell selection. Yeast 14:147-160.

Delabroise D, Noiseux M, Lemieux R, Massie B. 1991. Long-term perfusion culture of hybridoma - a grow or die cell-cycle system. Biotechnology and Bioengineering 38:781-787.

Delafosse A, Delvigne F, Collignon ML, Crine M, Thonart P, Toye D. 2010. Development of a compartment model based on CFD simulations for description of mixing in bioreactors. Biotechnologie Agronomie Societe Et Environnement 14:517-522.

Delvigne F, Boxus M, Ingels S, Thonart P. 2009. Bioreactor mixing efficiency modulates the activity of a prpoS::GFP reporter gene in *E. coli*. Microbial Cell Factories 8:15.

Delvigne F, Lejeune A, Destain J, Thonart P. 2006. Stochastic models to study the impact of mixing on a fed-batch culture of *Saccharomyces cerevisiae*. Biotechnology Progress 22:259-269.

Deo YM, Mahadevan MD, Fuchs R. 1996. Practical considerations in operation and scale-up of spin-filter based bioreactors for monoclonal antibody production. Biotechnology Progress 12:57-64.

Djeljadini S. 2014. Model-based and experimental analysis of mammalian cell cultivation in a continuous membrane bioreactor [Master thesis]. Aachen: RWTH Aachen University.

Dowd J, Jubb A, Kwok K, Piret J. 2003. Optimization and control of perfusion cultures using a viable cell probe and cell specific perfusion rates. Cytotechnology 42:35-45.

Duffield P, Bourne D, Tan K, Garruto RM, Duncan MW. 1994. Analysis of the neurotoxic plasticizer n-butylbenzenesulfonamide by gas chromatography combined with accurate mass selected ion monitoring. Journal of Analytical Toxicology 18:361-368.

Eibl R, Löffelholz C, Eibl D, editors. 2011. Single-Use bioreactors - An overview. Hoboken: John Wiley & Sons, Inc. 34 - 51 p.

Elsayed EA, Medronho RA, Wagner R, Deckwer WD. 2006. Use of hydrocyclones for mammalian cell retention: Separation efficiency and cell viability (Part 1). Engineering in Life Sciences 6:347-354.

Endo H, Hayashi T, Nakayama J, Mukada Y, Watanabe E. 1998. Rapid determination of the number of viable yeast cells during fermentation by flow cytometry. Journal of the Tokyo University of Fisheries 85:65-72.

Enfors SO, Jahic M, Rozkov A, Xu B, Hecker M, Jurgen B, Kruger E, Schweder T, Hamer G, O'Beirne D and others. 2001. Physiological responses to mixing in large scale bioreactors. Journal of Biotechnology 85:175-185.

Fiege H, Voges H-W, Hamamoto T, Umemura S, Iwata T, Miki H, Fujita Y, Buysch H-J, Garbe D, Paulus W. 2000. Phenol Derivatives. Ullmann's Encyclopedia of Industrial Chemistry: Wiley-VCH Verlag GmbH & Co. KGaA.

Furey J. 2000. Continuous cell culture using the ATF system - A new way to grow suspension- or anchorage-dependent cells. Genetic Engineering News 20:52-52.

Garcia MT, Sanz R, Galceran MT, Puignou L. 2006. Use of fluorescent probes for determination of yeast cell viability by gravitational field-flow fractionation. Biotechnology Progress 22:847-852.

George S, Larsson G, Enfors SO. 1993. A scale-down 2-compartment reactor with controlled substrate oscillations - matabolic response of saccaromyces-cerevisiae. Bioprocess Engineering 9:249-257.

Ghaderi D, Zhang M, Hurtado-Ziola N, Varki A. 2012. Production platforms for biotherapeutic glycoproteins. Occurrence, impact, and challenges of non-human sialylation. In: Harding SE, Adams GG, editors. Biotechnology and Genetic Engineering Reviews Vol 28, Issue 1. p 147-175.

Haxthausen N. 2012. Flex-facilities management biopharmaceuticals on demand. Bioprocess International 10:46-48.

Herweg E. 2012. Untersuchungen zur Biokompatibilität von Feststoffen am Beispiel von Polyamid 12 mittels RAMOS [Research internship]. Aachen: RWTH Aachen University.

Hewitt CJ, Nienow AW. 2007. The scale-up of microbial batch and fed-batch fermentation processes. In: Laskin AI, Sariaslani S, Gadd GM, editors. Advances in Applied Microbiology, Vol 62. San Diego: Elsevier Academic Press Inc. p 105-135.

Hewitt CJ, Onyeaka H, Lewis G, Taylor IW, Nienow AW. 2007. A comparison of high cell density fed-batch fermentations involving both induced and non-induced recombinant *Escherichia coli* under well-mixed small-scale and simulated poorly mixed large-scale conditions. Biotechnology and Bioengineering 96:495-505.

Holland T, Sack M, Rademacher T, Schmale K, Altmann F, Stadlmann J, Fischer R, Hellwig S. 2010. Optimal nitrogen supply as a key to increased and sustained production of a monoclonal full-size antibody in BY-2 suspension culture. Biotechnology and Bioengineering 107:278-289.

Huber R, Palmen T, Ryk N, Hillmer A-K, Luft K, Kensy F, Büchs J. 2010. Replication methods and tools in high-throughput cultivation processes - recognizing potential variations of growth and product formation by on-line monitoring. BMC Biotechnology 10:22.

Hülscher M, Scheibler U, Onken U. 1992. Selective recycle of viable animal-cells by coupling of airlift reactor and cell settler. Biotechnology and Bioengineering 39:442-446.

Ihssen J, Kowarik M, Dilettoso S, Tanner C, Wacker M, Thony-Meyer L. 2010. Production of glycoprotein vaccines in *Escherichia coli*. Microbial Cell Factories 9:61.

International Conference on Harmonization. 2000. Good manufacturing practice guide for active pharmaceutical ingedients. Geneva, Switzerland. .

International Organization for Standardization. 2009. Biological evaluation of medical devices - Part 5: Tests for in vitro cytotoxicity. ISO 10993-5.

Jager G, Girfoglio M, Dollo F, Rinaldi R, Bongard H, Commandeur U, Fischer R, Spiess AC, Buchs J. 2011. How recombinant swollenin from Kluyveromyces lactis affects cellulosic substrates and accelerates their hydrolysis. Biotechnology for Biofuels 4.

Jain E, Kumar A. 2008. Upstream processes in antibody production: Evaluation of critical parameters. Biotechnology Advances 26:46-72.

Jenke D. 2007a. Evaluation of the chemical compatibility of plastic contact materials and pharmaceutical products; safety considerations related to extractables and leachables. Journal of Pharmaceutical Sciences 96:2566-2581.

Jenke D. 2007b. An extractables/leachables strategy facilitated by collaboration between drug product vendors and plastic material/system suppliers. PDA journal of pharmaceutical science and technology / PDA 61:17 - 23.

Jenke DR, Story J, Lalani R. 2006. Extractables/leachables from plastic tubing used in product manufacturing. International Journal of Pharmaceutics 315:75-92.

Jockwer A, Medronho RA, Wagner R, Anspach FB, Deckwer WD. 2001. The use of hydrocyclones for mammalian cell retention in perfusion bioreactors. In: LindnerOlsson E, Chatzissavidou N, Lullau E, editors. Animal Cell Technology: From Target to Market. Dordrecht: Springer. p 301-306.

Johnson M, Lanthier S, Massie B, Lefebvre G, Kamen AA. 1996. Use of the Centritech lab centrifuge for perfusion culture of hybridoma cells in protein-free medium. Biotechnology Progress 12:855-864.

Jostock T. 2011. Expression of Antibody in Mammalian Cells. In: Al-Rubeai M, editor. Cell Engineering, Vol 7: Antibody Expression and Production. Dordrecht: Springer. p 1-24.

Junne S, Klingner A, Kabisch J, Schweder T, Neubauer P. 2011. A two-compartment bioreactor system made of commercial parts for bioprocess scale-down studies: Impact of oscillations on *Bacillus subtilis* fed-batch cultivations. Biotechnology Journal 6:1009-1017.

Kawahara H, Mitsuda S, Kumazawa E, Takeshita Y. 1994. High-density culture of FM-3A cells using a bioreactor with an external tangential-flow filtration device. Cytotechnology 14:61-66.

Kim BJ, Chang HN, Oh DJ. 2007. Application of a cell-once-through perfusion strategy for production of recombinant antibody from rCHO cells in a centritech lab II centrifuge system. Biotechnology Progress 23:1186-1197.

Klement T. 2013. Itaconic acid fermentation with *ustilago maydis* and its integration into a next gerneration bio-based process [Dissertation]. Aachen, Germany: RWTH Aachen.

Konstantinov K, Goudar C, Ng M, Meneses R, Thrift J, Chuppa S, Matanguihan C, Michaels J, Naveh D. 2006. The "push-to-low" approach for optimization of high-density perfusion cultures of animal cells. In: Hu WS, Scheper T, editors. Cell Culture Engineering. New York: Springer. p 75-98.

Korneli C, David F, Godard T, Franco-Lara E. 2011. Influence of fructose and oxygen gradients on fed-batch recombinant protein production using *Bacillus megaterium*. Engineering in Life Sciences 11:338-349.

Kuystermans D, Al-Rubeai M. 2011. Bioreactor systems for producing antibody from mammalian cells. In: Al-Rubeai M, editor. Antibody Expression and Production: Springer Netherlands. p 25-52.

Lara AR, Galindo E, Ramirez OT, Palomares LA. 2006. Living with heterogeneities in bioreactors. Molecular Biotechnology 34:355-381.

Lara AR, Taymaz-Nikerel H, Mashego MR, van Gulik WM, Heijnen JJ, Ramirez OT, van Winden WA. 2009. Fast dynamic response of the fermentative metabolism of *Escherichia coli* to aerobic and anaerobic glucose pulses. Biotechnology and Bioengineering 104:1153-1161.

Lejeune A, Delvigne F, Thonart P. 2013. Physiological response of yeast to process perturbations: A mini-bioreactor approach. Cerevisia 38:15-19.

Li H, Sethuraman N, Stadheim TA, Zha D, Prinz B, Ballew N, Bobrowicz P, Choi B-K, Cook WJ, Cukan M and others. 2006. Optimization of humanized IgGs in glycoengineered *Pichia pastoris*. Nature Biotechnology 24:210-215.

Liang M, Kim MH, He QP, Wang J. 2013. Impact of pseudo-continuous fermentation on the ethanol tolerance of *Scheffersomyces stipitis*. Journal of Bioscience and Bioengineering 116:319-326.

Lorantfy B, Jazini M, Herwig C. 2013. Investigation of the physiological response to oxygen limited process conditions of *Pichia pastoris Mut(+)* strain using a two-compartment scale-down system. Journal of Bioscience and Bioengineering 116:371-379.

Lottspeich F, Zorbas H, editors. 1998. Bioanalytik. Heidelberg: Spektrum Akademischer Verlag. 37 p.

Luedeking R, Piret EL. 1959. A kinetic study of the lactic acid fermentation - batch process at controlled pH. Journal of Biochemical and Microbiological Technology and Engineering 1:393-412.

McMillin CR. 1996. Mechanical breakdown in the biological environment. In: Ratner BD, Hoffmann AS, Schoen FJ, Lemons JE, editors. Biomaterials Science: An Introduction to Materials in Medicine: Elsevier Science. p 267 - 272.

Meier K, Carstensen F, Djeljadini S, Wessling M, Regestein L, Büchs J. June 2014. *In situ* cell retention of a perfusion CHO culture by a membrane bioreactor. Biotechnology Progress Submitted manuscript.

Meier K, Carstensen F, Scheeren C, Regestein L, Wessling M, Büchs J. 2014. *In situ* product recovery of single-chain antibodies in a membrane bioreactor. Biotechnology and Bioengineering 111:1566-1576.

Meier K, Carstensen F, Wessling M, Regestein L, Büchs J. May 2014. Quasi-continuous reverse-flow diafiltration. Biochemical Engineering Journal Submitted manuscript.

Meier K, Herweg E, Schmidt B, Klement T, Regestein L, Büchs J. 2013. Quantifying the release of polymer additives from single-use materials by respiration activity monitoring. Polymer Testing 32:1064-1071.

Melmer G, Hellwig S, Hehmann G, Dahlems U. 2011. Production of antibodies in *Hansenula polymorpha*. In: AlRubeai M, editor. Cell engineering, Vol 7: Antibody Expression and Production. Dordrecht, Netherlands: Springer. p 99-119.

Mernier G, Piacentini N, Tornay R, Buffi N, Renaud P. 2011. Cell viability assessment by flow cytometry using yeast as cell model. Sensors and Actuators B-Chemical 154:160-163.

Merseburger T, editor. 2011. An intorduction to the validation and qualification of disposables used in biomanufacture - a user`s perspective. Hoboken: John Wiley & Sons, Inc. 160 - 172 p.

Metropolis N, Ulam S. 1949. The Monte Carlo method. Journal of the American Statistical Association 44:335-341.

National Toxicology Program. 2010. Chemical Information Review Document for N-Butylbenzenesulfonamide.

NCI Yeast Anticancer Drug Screen. PubChem Compound Database. CID 283592, http://pubchem.ncbi.nlm.nih.gov/summary/summary.cgi?cid=283592, (accessed 26.03.2013).

Nienow AW. 2006. Reactor engineering in large scale animal cell culture. Cytotechnology 50:9-33.

Ott KD. 2011. Are single-use technologies changing the game? Bioprocess International 9:48-51.

Ozturk S. 1996. Engineering challenges in high density cell culture systems. Cytotechnology 22:3-16.

Paalme T, Kahru A, Elken R, Vanatalu K, Tiisma K, Vilu R. 1995. The computer-controlled continuous culture of *Escherichia coli* with smooth change of dilution rate (A-stat). Journal of Microbiological Methods 24:145-153.

Peuscher A, Gassler N, Schneider U, Thom P, Rasche S, Spiegel H, Schillberg S. 2014. An immunohistochemical assay on human tissue using a human primary antibody. Journal of immunoassay & immunochemistry 35:322-34.

Pharmaceutical Inspection Co-operation Scheme. 2007. Recommendations on validation master plan, installation and operational, nonsterile process validation, cleaning validation. PI 006-3. Geneva, Switzerland. .

Pohlscheidt M, Jacobs M, Wolf S, Thiele J, Jockwer A, Gabelsberger J, Jenzsch M, Tebbe H, Burg J. 2013. Optimizing capacity utilization by large scale 3000 L perfusion in seed train bioreactors. Biotechnology Progress 29:222-229.

Pollock J, Ho SV, Farid SS. 2013. Fed-batch and perfusion culture processes: Economic, environmental, and operational feasibility under uncertainty. Biotechnology and Bioengineering 110:206-219.

Regestein L, Giese H, Zavrel M, Büchs J. 2013. Comparison of two methods for designing calorimeters using stirred tank reactors. Biotechnology and Bioengineering 110:180-190.

Reijenga KA, Bakker BM, van der Weijden CC, Westerhoff HV. 2005. Training of yeast cell dynamics. FEBS Journal 272:1616-1624.

Rider CV, Janardhan KS, Rao D, Morrison JP, McPherson CA, Harry GJ. 2012. Evaluation of N-butylbenzenesulfonamide (NBBS) neurotoxicity in Sprague-Dawley male rats following 27-day oral exposure. Neurotoxicology 33:1528-35.

Rodrigues ME, Costa AR, Henriques M, Azeredo J, Oliveira R. 2010. Technological progresses in monoclonal antibody production systems. Biotechnology Progress 26:332-351.

Ryll T, Dutina G, Reyes A, Gunson J, Krummen L, Etcheverry T. 2000. Performance of small-scale CHO perfusion cultures using an acoustic cell filtration device for cell retention: Characterization of separation efficiency and impact of perfusion on product quality. Biotechnology and Bioengineering 69:440-449.

Scheeren C. 2012. Optimierung und Validierung der gepulsten Diafiltration zur *in situ* Produktabtrennung während der kontinuierlichen Fermentation des Modelorganismus *Hansenula polymorpha* [Master thesis]. Aachen: RWTH Aachen University.

Scheidle M, Klinger J, Büchs J. 2007. Combination of on-line pH and oxygen transfer rate measurement in shake flasks by fiber optical technique and Respiration Activity Monitoring System (RAMOS). Sensors 7:3472-3480.

Schrek R. 1963. A method for counting the viable cells in normal and in malignant cell suspensions. American Journal of Cancer 28:389-392.

Schroeter R, Hoffmann T, Voigt B, Meyer H, Bleisteiner M, Muntel J, Jurgen B, Albrecht D, Becher D, Lalk M and others. 2013. Stress responses of the industrial workhorse *Bacillus licheniformis* to osmotic challenges. PLoS ONE 8.

Searles JA, Todd P, Kompala DS. 1994. Viable cell recycle with an inclined settler in the perfusion culture of supsended recombinant chinese-hamster overy cells. Biotechnology Progress 10:198-206.

Sinclair A, Monge M. 2005. Concept facility based on single-use systems, Part 2. BioProcess International 3 Supplement:1-4.

Skjevrak I, Brede C, Steffensen IL, Mikalsen A, Alexander J, Fjeldal P, Herikstad H. 2005. Non-targeted multi-component analytical surveillance of plastic food contact materials: Identification of substances not included in EU positive lists and their risk assessment. Food Additives and Contaminants 22:1012-1022.

Stöckmann C, Maier U, Anderlei T, Knocke C, Gellissen G, Büchs J. 2003. The oxygen transfer rate as key parameter for the characterization of *Hansenula polymorpha* screening cultures. Journal of Industrial Microbiology & Biotechnology 30:613-622.

Su WW. 1995. *In situ* filtration of anchusa officinalis culture in a cell-retention stirred tank bioreactor. Biotechnology Techniques 9:259-264.

Su WW. 2010. Bioreactors, Perfusion. In: Flickinger MC, editor. Encyclopedia of Industrial Biotechnology, Bioprocess, Bioseparation, and Cell Technology: John Wiley & Sons. p 978 - 993.

Sunya S, Bideaux C, Molina-Jouve C, Gorret N. 2013. Short-term dynamic behavior of *Escherichia coli* in response to successive glucose pulses on glucose-limited chemostat cultures. Journal of Biotechnology 164:531-542.

Takamatsu H, Hamamoto K, Ishimaru K, Yokoyama S, Tokashiki M. 1996. Large-scale perfusion culture process for suspended mammalian cells that uses a centrifuge with multiple settling zones. Applied Microbiology and Biotechnology 45:454-457.

Tang YJ, Ohashi R, Hamel JFP. 2007. Perfusion culture of hybridoma cells for hyperproduction of IgG(2a) monoclonal antibody in a wave bioreactor-perfusion culture system. Biotechnology Progress 23:255-264.

Trampler F, Sonderhoff SA, Pui PWS, Kilburn DG, Piret JM. 1994. Acoustic cell filter for high-densitiy perfusion culture of hybridoma cells. Nature Biotechnology 12:281-284.

US Pharmacopeia. USP 87 Biological Reactivity Tests, In Vitro. In: US Pharmacopeia, editor. USP 87.

van der Marel P, Zwijnenburg A, Kemperman A, Wessling M, Temmink H, van der Meer W. 2009. An improved flux-step method to determine the critical flux and the critical flux for irreversibility in a membrane bioreactor. Journal of Membrane Science 332:24-29.

Verduyn C, Postma E, Scheffers WA, Vandijken JP. 1992. Effect of benzoic-acid on metabolic fluxes in yeasts - a continous-culture study on the regulation of respiration and alcoholic fermentation. Yeast 8:501-517.

Voisard D, Meuwly F, Ruffieux PA, Baer G, Kadouri A. 2003. Potential of cell retention techniques for large-scale high-density perfusion culture of suspended mammalian cells. Biotechnology and Bioengineering 82:751-765.

Walsh G. 2010. Biopharmaceutical benchmarks 2010. Nature Biotechnology 28:917-924.

Warikoo V, Godawat R, Brower K, Jain S, Cummings D, Simons E, Johnson T, Walther J, Yu M, Wright B and others. 2012. Integrated continuous production of recombinant therapeutic proteins. Biotechnology and Bioengineering 109:3018-3029.

Worsch A. 2013. Examination of the influence of reverse-flow diafiltration for continuous *in situ* product recovery on viability and productivity of the model organism *Hansenula polymorpha* [Master thesis]. Aachen: RWTH Aachen University.

Wurm FM. 2004. Production of recombinant protein therapeutics in cultivated mammalian cells. Nature Biotechnology 22:1393-1398.

Xing ZZ, Bishop N, Leister K, Li ZJ. 2010. Modeling Kinetics of a Large-Scale Fed-Batch CHO Cell Culture by Markov Chain Monte Carlo Method. Biotechnology Progress 26:208-219.

Xu B, Jahic M, Blomsten G, Enfors SO. 1999. Glucose overflow metabolism and mixed-acid fermentation in aerobic large-scale fed-batch processes with *Escherichia coli*. Applied Microbiology and Biotechnology 51:564-571.

Zeng A-P, Sun J. 2010. Continuous culture. In: Baltz RH, Davies JE, Demain AL, editors. Manual of Industrial Microbiology and Biotechnology 3rd ed. Washington DC: American Society for Microbiology (ASM).

Zha D, Linden T, Potgieter T. 2011. Production of monoclonal antibodies in glycoengineered *Pichia pastoris*. In: al-Rubeai M, editor. Cell engineering, Vol 7: Antibody Expression and Production. Dordrecht: Springer. p 77-98.

Zsirai T, Buzatu P, Aerts P, Judd S. 2012. Efficacy of relaxation, backflushing, chemical cleaning and clogging removal for an immersed hollow fibre membrane bioreactor. Water Research 46:4499-4507.